HETEROCYCLES, Vol. 94, No. 4, 2017, pp. 595 - 655. © 2017 The Japan Institute of Heterocyclic Chemistry
Received, 13th December, 2016, Accepted, 16th March, 2017, Published online, 22nd March, 2017
DOI: 10.3987/REV-16-854

SYNTHESIS OF HETEROCYCLES CATALYZED BY IRON OXIDE NANOPARTICLES

Ahmed H. M. Elwahy[a,*] **and Mohamed R. Shaaban**[a,b]

[a]Chemistry Department, Faculty of Science, Cairo University, Giza, Egypt
[b]Chemistry Department, Faculty of Applied Science, Umm Al-Qura University, Makkah Almukkarramah, Saudi Arabia

Abstract – Heterocycles constitute the largest diversity of organic molecules of chemical, biomedical, and industrial significance. They are also among the most frequently encountered scaffolds in numerous drugs and pharmaceuticals relevant substances. Development of efficient routes to many kinds of heterocycles is an attractive area of research. This review highlights some remarkable achievements made recently in the application of MNPs, magnetite (Fe_3O_4), maghemite (γ-Fe_2O_3), and spinel ferrites (MFe_2O_4) as heterogeneous catalysts in heterocyclic synthesis.

CONTENTS

1. INTRODUCTION

Heterocycles are an important class of compounds, which represent more than half of all known organic compounds. They are present in most vitamins, many natural products, biomolecules, and the majority of commercially available synthetic drugs has a heterocyclic structural component. Moreover, compounds containing heterocyclic moieties also exhibit a broad range of biological properties, including antitumor, antibiotic, anti-inflammatory, antidepressant, antimalarial, anti-HIV, antimicrobial, antibacterial, antifungal, antiviral, antidiabetic, herbicidal, fungicidal and insecticidal agents.[1-3]

The synthesis of heterocyclic compounds has always been among the most important research areas and the development of new ecofriendly sustainable procedures to synthesize these compounds has been the most important challenges in synthetic chemistry. Among different approaches in this respect, the application of non-traditional activation methods, such as microwave irradiation,[4] sonochemistry,[5] the use of environmentally benign solvents[6] as well as the application of catalysis[7] represent the most effective tools in green chemistry.

Catalysis can be broadly divided into homogeneous and heterogeneous catalysis,[8] although homogeneous catalysts often exhibit good catalytic activity, they do have some disadvantages, making many of them to have only limited applications, which is mainly that they are difficult to separate from the final products or reaction mixtures.

These disadvantages can be overcome by supporting the homogeneous catalytic species on solid support materials and producing their corresponding solid catalysts, known as heterogeneous catalysts.[9]

Heterogeneous catalysts often possess numerous advantages, such as their ease of handling, efficient recovery, enhanced stability, and reusability. However, because the reactants and the catalysts in heterogeneous catalysis must necessarily be in two different phases, the interaction between the reactant and the catalyst is reduced.

To overcome some of the limitations associated with both homogeneous and heterogeneous catalysts, new catalytic systems were needed that could have the advantages of both homogeneous and heterogeneous catalytic systems.[10]

Nano catalysts and nano-catalysis could meet the need of such new catalyst systems. Nanoparticles can serve as active and stable heterogeneous catalysts[11] or as support materials for various catalytic groups.[12] Due to their small sizes; catalytic-active nanoparticles have higher surface area and increased exposed active sites, and thereby improved contact areas with the reactants, like those of homogeneous catalytic systems. Nano catalysts with better activity, stability, and selectivity can be designed and synthesized merely by controlling the sizes, shapes, and morphologies of nanomaterials.[12–14]

The problems encountered in the use of nanoparticles are usually the unavoidable coagulation during the catalytic transformation.[15] It is necessary to stabilize the surface through the addition of capping agents or by immobilization or grafting on the surface of various supports such as porous materials (e.g. silicates, zeolites, alumina, carbons, etc.).[16-18]

Recently, the employment of nanocrystalline metal oxides as catalysts has attracted much attention in organic synthesis. It seems that these high reactivates are due to high surface areas combined with unusually reactive morphologies. Moreover, the use of magnetic nanoparticles allows their efficient removal from reaction mixtures with external magnets.[19]

Among these MNPs, magnetite (Fe_3O_4) has been identified as the ideal and most widely used support in catalysis[20,21] because of its low cost, ease of preparation, ease of handling, ease of recovery with an external magnetic field, high catalytic activities, and reactivity in various organic transformations.[22]

Other forms of iron oxide, hematite (α-Fe_2O_3), maghemite (γ-Fe_2O_3), and spinel ferrites (MFe_2O_4) have also received a lot of attention in the field of MNPs catalysis owing to their ferrimagnetism, environmental stability, and other properties.[23]

To solve the problem of aggregation, modification of MNPs by stabilizing with with suitable benign ligands such as dopamine or glutathione has been used. Also, coating with silica is the most popular inorganic material for MNPs. Encapsulation of MNPs in various solid supports such as mesoporous materials,[24,25] graphene,[26] carbon nanotubes,[27] and polymers was also efficient in stabilizing MNPs.

Graphene is a remarkable support for encapsulation of metal NPs, because of its two-dimensional plate-like structure and large specific surface area. Use of graphene not only avoids the aggregation of metal NPs, but also enhances their catalytic activity owing to the strong synergistic interaction between the two components.

Carbon nanotubes (CNTs) exhibit intriguing properties, such as nanoscale dimensions, high specific surface area, mechanical strength, and chemical stability.[28] The present review covers the synthesis of iron oxide nanoparticles and highlights their applications as effective catalysts in heterocyclic synthesis.

2. Fe_2O_3 NANOPARTICLES

2.1. SYNTHESIS OF 1,2,3-TRIAZOLE

Kamal and Swapna developed an interesting approach for the construction of 2,4,5-trisubstituted-1,2,3-triazoles **3** in good yields using a three-component reaction of chalcones **1**, sodium azide and aryl halides **2** catalyzed by Fe_2O_3 nanoparticles. The reaction involves an oxidative 1,3-dipolar cycloaddition of the chalcone and azide followed by a regioselective *N*-2-arylation (Scheme 1, Table 1).[29]

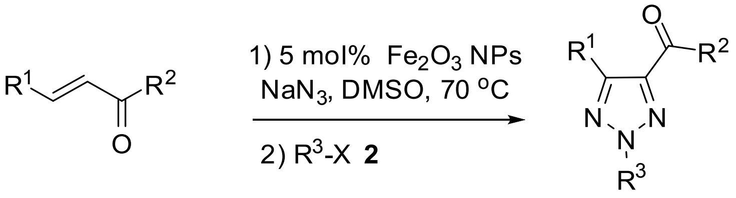

1 **3**

Scheme 1

Table 1. Synthesis of 2,4,5-trisubstituted-1,2,3-triazoles **3**

Entry	R^1	R^2	R^3	X	Yield of **3** (%)
1	$2\text{-}FC_6H_4$	$2\text{-}FC_6H_4$	$2\text{-}O_2NC_6H_4$	F	92
2	$4\text{-}FC_6H_4$	$3\text{-}CF_3C_6H_4$	$2\text{-}O_2NC_6H_4$	F	90
3	$4\text{-}O_2NC_6H_4$	C_6H_5	$2\text{-}O_2NC_6H_4$	F	89
4	$3\text{-}F\text{-}4\text{-}ClC_6H_3$	$4\text{-}FC_6H_4$	$2\text{-}O_2NC_6H_4$	F	80
5	$4\text{-}CF_3C_6H_4$	$4\text{-}FC_6H_4$	$2\text{-}O_2NC_6H_4$	F	80
6	$4\text{-}MeC_6H_4$	C_6H_5	$2\text{-}O_2NC_6H_4$	F	75
7	C_6H_5	$4\text{-}MeOC_6H_4$	$2\text{-}O_2NC_6H_4$	F	65
8	$4\text{-}MeC_6H_4$	$3\text{-}ClC_6H_4$	$2\text{-}O_2NC_6H_4$	F	70
9	$4\text{-}MeOC_6H_4$	$4\text{-}FC_6H_4$	$2\text{-}O_2NC_6H_4$	F	75
10	$3\text{-}MeO\text{-}4\text{-}FC_6H_3$	$4\text{-}FC_6H_4$	$2\text{-}O_2NC_6H_4$	F	72
11	$4\text{-}MeOC_6H_4$	$4\text{-}FC_6H_4$	$2\text{-}F\text{-}4\text{-}O_2NC_6H_3$	F	62
12	$4\text{-}MeC_6H_4$	$3\text{-}ClC_6H_4$	$2\text{-}F\text{-}4\text{-}O_2NC_6H_3$	F	59
13	$4\text{-}MeOC_6H_4$	$4\text{-}FC_6H_4$	$2,4\text{-}(O_2N)2C_6H_3$	Cl	70
14	$4\text{-}MeC_6H_4$	$3\text{-}ClC_6H_4$	$2\text{-}O_2NC_6H_4$	Cl	68
15	$4\text{-}^iPrC_6H_4$	C_6H_5	$2\text{-}O_2NC_6H_4$	F	62
16	$2\text{-}MeC_6H_4$	C_6H_5	$2\text{-}F\text{-}4\text{-}O_2NC_6H_3$	F	69
17	$2\text{-}MeC_6H_4$	C_6H_5	$2\text{-}F\text{-}4\text{-}O_2NC_6H_3$	F	65
18	$4\text{-}O_2NC_6H_4$	C_6H_5	$2\text{-}F\text{-}4\text{-}O_2NC_6H_3$	F	86
19	$4\text{-}FC_6H_4$	$4\text{-}FC_6H_4$	$2\text{-}F\text{-}2,4\text{-}(O_2N)_2C_6H_2$	F	93
20	2-thienyl	C_6H_5	$2\text{-}O_2NC_6H_4$	F	-
21	2-pyrrolyl	C_6H_5	$2\text{-}O_2NC_6H_4$	F	-
22	$2\text{-}MeC_6H_4$	C_6H_5	$2\text{-}O_2NC_6H_4$	Cl	-
23	$4\text{-}FC_6H_4$	$4\text{-}FC_6H_4$	$4\text{-}O_2N$pyridyl	Cl	-
24	$2\text{-}MeC_6H_4$	C_6H_5	$2\text{-}MeC_6H_4$	Cl	-

Among different sources of iron, such as Fe_2O_3 nanoparticles, $FeSO_4.7H_2O$, $FeCl_3$, $FeBr_2$, $Fe(acac)_2$ and bulk-Fe_2O_3, commercially available nano-Fe_2O_3 (50 nm) was found to afford the best yields of the target compounds.

The authors reported that five mol% of the catalyst were found to be optimal for this conversion. It was also observed that carrying out the reaction in DMSO at 70 °C afforded the best yield of the desired product. On the other hand, performing the reaction in solvents such as *N,N*-dimethylformamide (DMF), acetonitrile (MeCN), ethanol (EtOH), 1,4-dioxane and H_2O failed to produce the product in good yields. The low catalyst loading, ease of separation of the catalyst as well as its reuse without any significant loss in catalytic activity are advantages of the present method.

2.2. SYNTHESIS OF 4*H*-PYRAN

Commercially available nano-power magnetite or iron(III) oxide have been used as a catalyst in the construction of 4-substituted-4*H*-pyrans **6** from the reaction of *β*-keto esters or other 1,3-dicarbonyl compound **4** with the corresponding aldehyde **5** (Scheme 2, Table 2). The reaction implies a tandem process, involving an aldol condensation, a Michael-type addition, and a dehydrating annulation. The isolated yields of pyrans **6** were similar independently of the aromatic aldehyde used, with electron-withdrawing groups, unsubstituted rings, or electron-donating groups.[30]

Although the possible mechanism is still unknown, it should be pointed out that the formation of a catalytic species having an Fe(III)–Cl bond should play an important role as a Lewis acid, with the centers of iron(III) that could catalyze the final Michael addition.

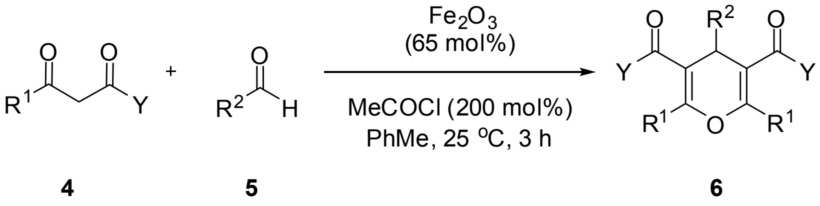

Scheme 2

Table 2. Synthesis of 4-substituted-4*H*-pyrans **6**

Entry	R^1	Y	R^2	Yield (%)[a]	Entry	R^1	Y	R^2	Yield (%)[a]
1	Me	OMe	4-BrC_6H_4	96 (94)	7	Me	OMe	$(CH_2)_5CH$	80 (79)
2	Me	OMe	4-NCC_6H_4	79	8	Me	OMe	*i*-Pr	72 (67)
3	Me	OMe	Ph	85 (82)	9	Me	OEt	4-BrC_6H_4	95
4	Me	OMe	4-$MeOC_6H_4$	83	10	Me	OEt	4-$MeOC_6H_4$	63
5	Me	OMe	4-HOC_6H_4	68	11	Me	Me	4-$MeOC_6H_4$	75 (64)
6	Me	OMe	2-naphthyl	57	12	Me	OMe	4-BrC_6H_4	91 (79)

[a] Reaction carried out using compound **4** (2.5 mmol), **5** (1 mmol), in 3 mL of toluene during 3 h, unless otherwise stated. Yields obtained by Fe_2O_3 catalysis appeared in paranthesis.

3. Fe_2O_3 NANOPARTICLE-SUPPORTED ANTIMONY

Ma *et al.* reported a facile approach to prepare magnetic nanoparticle-supported antimony catalyst (Fe_2O_3@SiO_2–Sb-IL) **11** in a three-step as shown in Scheme 3. Thus, 1-methyl-3-(trimethoxysilylpropyl)imidazolium chloride **9** was prepared by the reaction of *N*-methylimidazole **7** with 3-chloropropyltrimethoxysilane **8**. Subsequent treatment of **9** with anhydrous antimony(III) chloride ($SbCl_3$) afforded complex **10**. Immobilization of the latter complex in γ-Fe_2O_3@SiO_2 was carried out in ethanol under reflux for 48 h to give the catalyst **11**.[31]

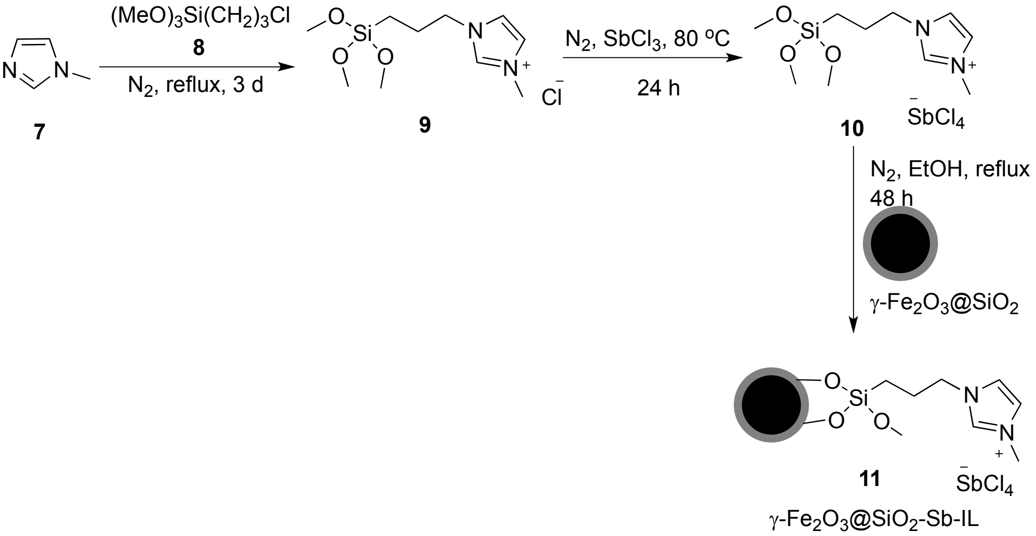

Scheme 3

3.1. SYNTHESIS OF PYRROLE

This catalyst exhibited an excellent catalytic efficiency in Clauson-Kaas reaction of amines **12** to 2,5-dimethoxytetrahydrofuran **13** in aqueous medium to afford the corresponding *N*-substituted pyrroles **14** (Scheme 4, Table 3).[31]

The authors used some commercially available catalysts, including trifluoroacetic acid, *p*-toluenesulfonic acid, silicotungstic acid, phosphotungstic acid, cerium ammonium nitrate, $NiCl_2$, $ZnBr_2$, *β*-cyclodextrin and I_2 but no satisfactory results were achieved. The efficiency of the supported catalyst was found to be affected by the nature of the solvent and the quantity of the catalyst used in the reaction. The results showed that the use of 5 mol% of the catalyst in water was the best choice for completing the reaction. Although the corresponding products have also been obtained in high yields using DMF and dimethyl sulfoxide (DMSO) as the solvents, but from the economic and environmental point of view, water was chosen as the reaction medium.

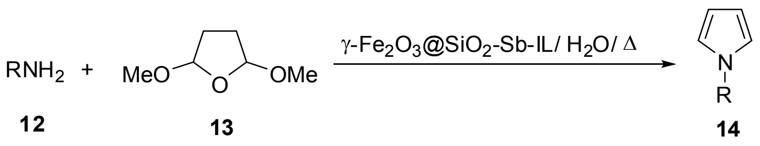

Scheme 4

Table 3. Preparation of *N*-substituted pyrroles **14**

Entry	R	Yield (%)	Entry	R	Yield (%)
1	C_6H_5	95	22	2-BrC_6H_4	82
2	3-HOC_6H_4	93	23	3-BrC_6H_4	85
3	2-$MeOC_6H_4$	85	24	4-BrC_6H_4	88
4	4-$MeOC_6H_4$	96	25	4-IC_6H_4	89
5	4-$EtOC_6H_4$	96	26	2-$O_2NC_6H_4$	80
6	2-MeC_6H_4	89	27	4-$O_2NC_6H_4$	85
7	4-MeC_6H_4	94	28	4-AcC_6H_4	89
8	3,4-$Me_2C_6H_3$	96	29	3-$F_3CC_6H_4$	84
9	2,5-$Me_2C_6H_3$	90	30	4-$F_3CC_6H_4$	83
10	2,6-$Me_2C_6H_3$	87	31	4-$EtO_2CC_6H_4$	90
11	2,6-$^iPr_2C_6H_3$	75	32	2-naphthyl	93
12	4-$^tBuC_6H_4$	92	33	2-(4-bromonaphthyl)	95
13	2-FC_6H_4	81	34	2-fluorenyl	93
14	4-FC_6H_4	82	35	2-pyridyl	71
15	2,4-$F_2C_6H_3$	85	36	6-picolyl	70
16	3,4-$F_2C_6H_3$	90	37	2-pyrimidyl	85
17	3-ClC_6H_4	86	38	2-(5-methylbenzothiazolyl)	80
18	4-ClC_6H_4	87	39	NH-COC_6H_4	90
19	3-Cl-4-MeC_6H_3	92	40	CO-4-$H_2NC_6H_4$	92
20	3-Cl-4-FC_6H_3	89	41	4-$NH_2C_6H_4$	94
21	2,4,5-$Cl_3C_6H_2$	88	42	2-(5-aminonaphthyl)	100

4. Fe_2O_3 NANOPARTICLE-SUPPORTED TRIS(TRIAZOLYL)–CuBr COMPLEXES

Wang *et al*. prepared nanoparticle-supported tris(triazolyl)–CuBr **21**, with a diameter of approximately 25 nm as outlined in Scheme 5. The first step was the synthesis of tris(1-benzyl-1*H*-1,2,3-triazol-4-yl)methanol **18** *via* the copper-catalyzed azide–alkyne cycloaddition (CuAAC) reactions between three equivalents of benzyl azide and a tris(alkynyl)carbinol intermediate **17** in the presence of copper sulfate and sodium ascorbate (a catalytic system developed by Sharpless et *al*.).[32] The intermediate **17** was readily prepared by the addition of trimethylsilylacetylide **15** to ethyl chloroformate to give **16**, followed by removal of the trimethylsilyl (TMS) groups. The 3-chloropropyltriethoxysilane-functionalized magnetic nanoparticles **19** were obtained through immobilization of 3-chloropropyltriethoxysilane on the surface of robust SiO_2/γ-Fe_2O_3[33] by means of heterogenization with the Si-OH binding sites of SiO_2/g-Fe_2O_3. Magnetic nanoparticle-supported tris(1-benzyl-1*H*-1,2,3-triazol-4-yl)methanol **20** was prepared by alkylation of **18** with **19**. Reaction of **20** with copper halide afforded **21** in good yield.[34]

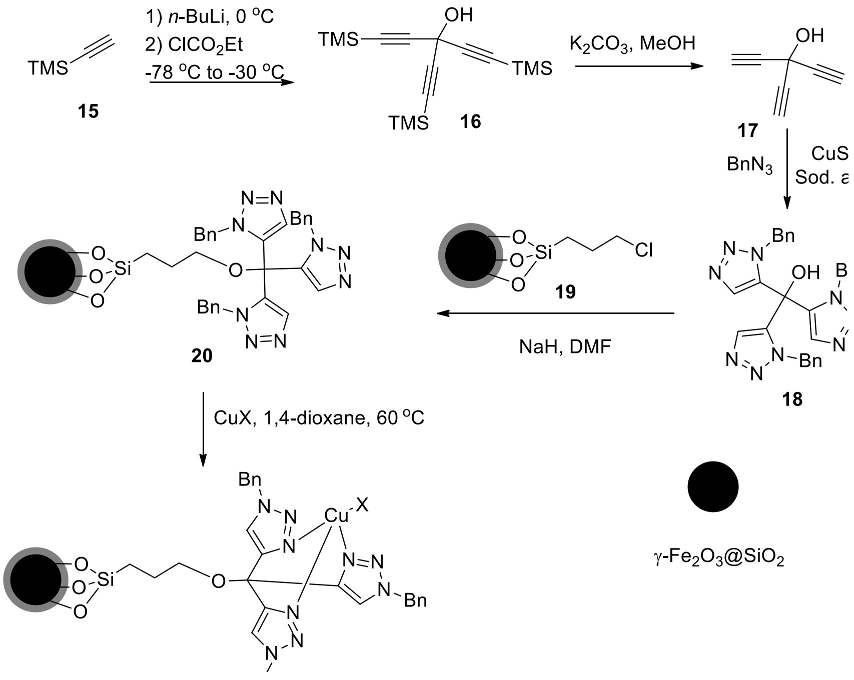

Scheme 5

4.1. SYNTHESIS OF 1*H*-1,2,3-TRIAZOLES

The reactivity of the catalyst was evaluated in the synthesis of 1*H*-1,2,3-triazoles **24** *via* copper-catalyzed azide-alkyne cycloaddition (CuAAC) reaction using various organic azides **23** and alkynes **22** (Scheme 6, Table 4).[35] The reaction proceeded well using 0.5 mol% [Cu] in water at room temperature, under a nitrogen atmosphere. After completion of the reactions, the catalyst was collected by using an external magnet. It could be reused six times without significant loss of its catalytic activity. The tris(triazolyl) fragment proved to be a stable chelating framework for the adsorption of the CuI salt, and a good linker for the SiO_2-coated γ-Fe_2O_3 nanoparticles through straightforward C-O bond formation. The catalyst also performed well in the presence of air, but became deactivated after the second run, probably caused by aerobic oxidation of the CuI species into a Cu(II) species.

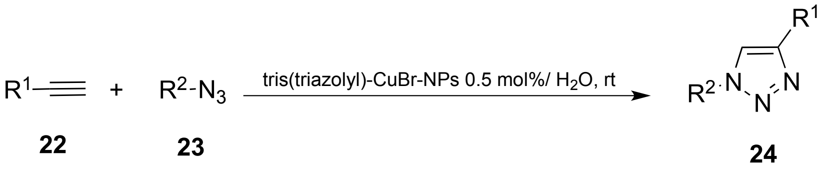

Scheme 6

Table 4. Synthesis of 2,4,5-trisubstituted-1,2,3-triazoles **24**

Entry	R^1	R^2	Yield (%)	Entry	R^1	R^2	Yield (%)
1	C_6H_5	C_6H_{13}	95	10	4-$NH_2OC_6H_4$	Bn	92
2	C_6H_5	C_8H_{17}	91	11	2-pyridyl	Bn	86
3	C_6H_5	$C_{18}H_{32}$	82	12	3-pyridyl	Bn	92
4	C_6H_5	C_6H_5	92	13	C_4H_9	Bn	99
5	C_6H_5	4-$MeOC_6H_4$	83	14	C_5H_{11}	Bn	93
6	C_6H_5	4-IC_6H_4	81	15	HO-C(Me)$_2$	Bn	89
7	C_6H_5	Bn	96	16	HO-C(C_6H_5)$_2$	Bn	93
8	4-$CHOC_6H_4$	Bn	96	17	ferrocenyl	Bn	96
9	4-$MeOC_6H_4$	Bn	94				

5. 2-HYDROXYETHYLAMMONIUM SULFONATE IMMOBILIZED ON-Fe_2O_3 NANOPARTICLES

2-Hydroxyethylammonium sulfonate immobilized on-Fe_2O_3 nanoparticles **27** (-Fe_2O_3-2-HEAS) was synthesized as a new supported ionic liquid by the reaction of *n*-butylsulfonated-Fe_2O_3 **26** with ethanolamine. *n*-Butylsulfonated-Fe_2O_3 was obtained by suspension of γ-Fe_2O_3 MNPs **25** in a refluxing toluene solution of 1,4-butanesultone (Scheme 7). [36]

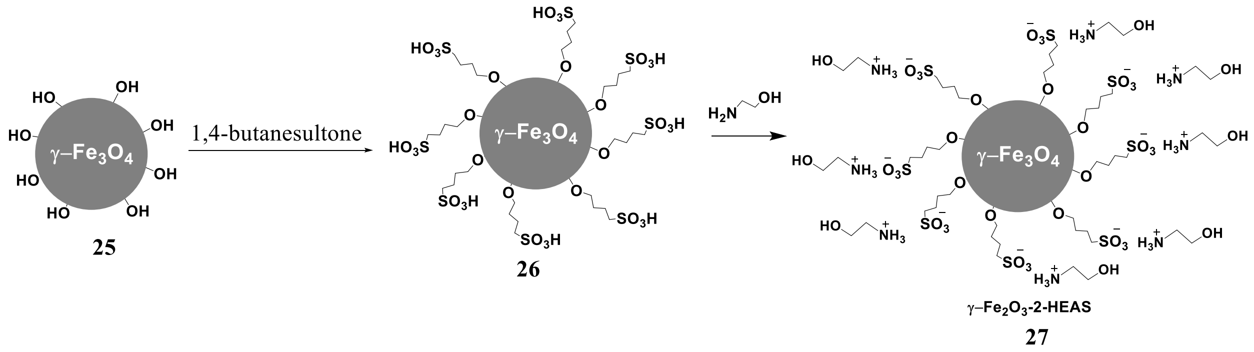

Scheme 7

5.1. SYNTHESIS OF PYRIDINE

This catalyst efficiently promoted the synthesis of 2-amino-3,5-dicarbonitrile-6-thiopyridines **30** in good to high yields *via* the reaction of the appropriate aldehyde **5**, malononitrile **28** and the corresponding thiol **29** under solvent-free conditions (Scheme 8, Table 5). The catalyst was easily isolated from the reaction mixture using an external magnet and reused at least five times without significant degradation in the activity.[36] The use of a small amount of the catalyst as well as the short reaction time (10 min), are also advantages of this method compared with other reported synthetic approaches.

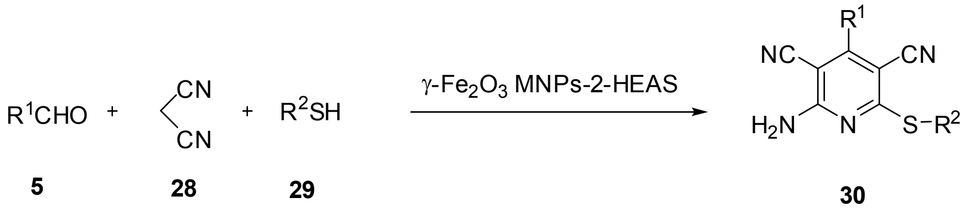

Scheme 8

Table 5. One-pot synthesis of pyridine-3,5- dicarbonitriles **30**

Entry	R^1	R^2	Yield^a (%)	Entry	R^1	R^2	Yield^a (%)
1	C_6H_5	C_6H_5	91	7	4-ClC_6H_4	4-MeC_6H_4	80
2	C_6H_5	4-ClC_6H_4	81	8	2-naphthyl	C_6H_5	79
3	C_6H_5	4-MeOC_6H_4	79	9	2-pyridinyl	C_6H_5	89
4	C_6H_5	4-MeC_6H_4	84	10	2-phenylpropanal	C_6H_5	88
5	4-MeC_6H_4	C_6H_5	81	11	Me	C_6H_5	90
6	4-ClC_6H_4	C_6H_5	87	12	C_6H_5	*n*-Bu	83

[a] Yields were analyzed by GC

A plausible mechanism for the formation of 2-amino-3,5-dicarbonitrile-6-thiopyridines using γ-Fe_2O_3-2-HEAS catalyst is shown in Scheme 9. The first step of the process involves the Knoevenagel condensation of aldehyde with malononitrile to form the corresponding *α,β*-unsaturated malonate A. The reaction then proceeds through the addition of thiolate to the nitrile of **A** followed by Michael addition of the second molecule of malononitrile to the adduct. Subsequent aromatization and oxidation of dihydropyridines by air under the reaction conditions gave pyridines **30**.

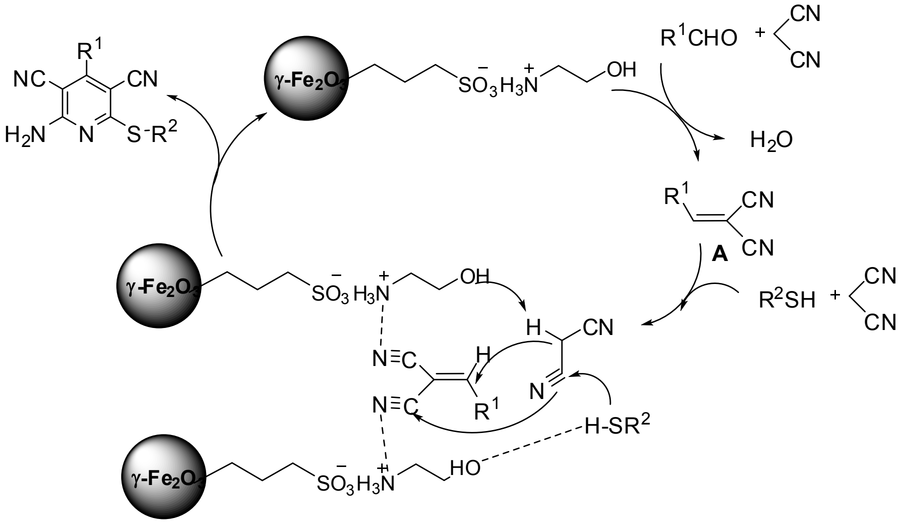

Scheme 9

It is supposed that dual activation of substrates by γ-Fe_2O_3-2-HEAS has been taken place in this three-component reaction. The hydroxyl group of the catalyst as a basic moiety has activated malononitrile and thiol. On the other hand, ammonium group acts as an acidic moiety that activate the nitrile of *α,β*-unsaturated malonates **A**.

When these reactions were carried out in the presence of 2-ethylammonium sulfonate immobilized on γ-Fe_2O_3 (γ-Fe_2O_3-2-EAS), it also proceeded to give the desired product in good yield, but in a longer reaction time (4 h). These results indicated that γ-Fe_2O_3-2-HEAS would take a part in the reaction as a functionalized ionic liquid.

6. A GRAPHENE BASED COMPOSITE MATERIAL WITH c-Fe_2O_3

A graphene based composite material with c-Fe_2O_3 nanoparticles has been synthesized *via* a simple chemical route as shown in the Scheme 1. At first iron oxide nanoparticles were prepared by high temperature decomposition of iron stearate. These hydrophobic nanoparticles were then transformed into water soluble nanoparticles by silica coating.[37] The resulting cationic charged amine terminated iron oxide nanoparticles have a hydrodynamic diameter of 10–12 nm. Graphene/Fe_2O_3 composite materials were synthesized by a reported method, in which water soluble graphene oxide GO was at first synthesized *via* a modified Hummers method.[38] Next, KOH was added to this solution in such a way that precipitation does not occur. Different amounts of amine terminated iron oxide nanoparticle solution were then added gradually to the GO solution under stirring conditions. At this stage iron oxide nanoparticles were attached to the GO surface *via* electrostatic interactions between positively charged silica coated iron oxide and negatively charged GO or *via* a nucleophilic reaction between the amine and the epoxide of the GO surface. GO was then reduced by chemical reduction using hydrazine as the reducing agent under heating conditions. The formed precipitate was separated from the solution using a magnet and was then washed and dried. The dry material was used for the characterization and catalytic application.

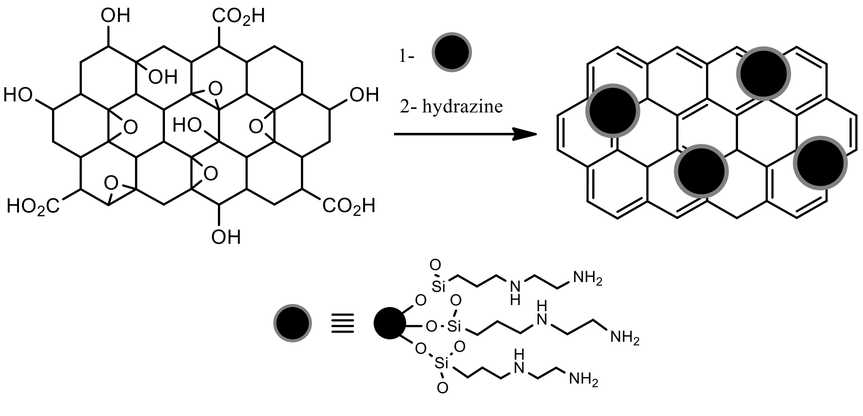

Scheme 10

6.1. SYNTHESIS OF 1,2,3-TRIAZOLES

The catalyst can serve as an efficient catalyst for one-pot synthesis of a series of 1,4-disubstituted-1,2,3-triazoles **24** *via* reaction of halides **2**, sodium azide and the corresponding alkynes **22** (Scheme 11, Table 6). The optimized conditions for this reaction include the use of 50 mg of the catalyst and water as a solvent at 60 °C. The increase of the electronic effect in both of the benzyl as well as the alkyne moieties increase the yield, whereas it decreases with electron deficient substrates.[39]

The superparamagnetic nature of c-Fe_2O_3 nanoparticles facilitated their separation from the reaction mixture just by applying an external magnet. The catalyst displayed an excellent catalytic activity even after five times recycling.

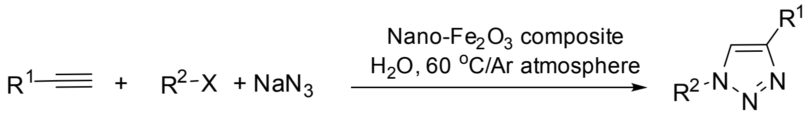

22 **2** **24**

Scheme 11

Table 6. One-pot synthesis of 1,2,3-triazoles **24**

Entry	R^1	R^2	X	Yield (%)	Entry	R^1	R^2	X	Yield (%)
1	C_6H_5	$C_6H_4CH_2$-	Br	92	8	4-MeOC_6H_4	$C_6H_4CH_2$-	Br	91
2	C_6H_5	4-$HOC_6H_4CH_2$-	Br	93	9	4-MeC_6H_4	$C_6H_4CH_2$-	Br	85
3	C_6H_5	4-Me$OC_6H_4CH_2$-	Br	91	10	4-BrC_6H_4	$C_6H_4CH_2$-	Br	78
4	C_6H_5	3-$O_2NC_6H_4$	Br	89	11	C_6H_5	^{c}hexyl	Br	70
5	C_6H_5	$C_6H_4CH_2CH_2$-	Br	81	12	C_6H_5	$C_6H_4CH_2$-	Cl	88
6	^{n}hexyl	$C_6H_4CH_2$-	Br	72	13	^{c}hexyl	4-Me$OC_6H_4CH_2$-	Cl	80
7	CO_2Et	$C_6H_4CH_2$-	Br	84					

Based on previous studies,[40-42] a plausible explanation regarding active sites and reaction mechanism can be proposed. First, the oxygen containing groups (–OH, –CO_2H etc.) on the GO provided the anchoring sites for the deposition of c-Fe_2O_3, which enable c-Fe_2O_3 to distribute on the surface of GO thus avoiding their aggregation. Second, reactants can be adsorbed onto graphene through π–π electronic interactions, which increased the effective contact between the reactant molecules and the c-Fe_2O_3. Oxygen can adsorb on the c-Fe_2O_3 sites and then spill over to the adjacent bridge sites of graphene. In this way, the adsorption of oxygen on the graphene/Fe_2O_3 composite is greatly promoted. The existence of mobile oxygen on the graphene support can promote the oxidation reactions. In 1,4-disubstituted-1,2,3-triazoles synthesis the GO acts as a base and removes the acetylenic proton to form a Fe-acetylide complex.[43,44] This complex undergoes cycloaddition with an in *situ* formed azide to form a triazole.

This reaction was studied using c-Fe_2O_3, graphene and graphene-c-Fe_2O_3. Among them, graphene was found to have a less catalytic activity. The graphene/Fe_2O_3 hybrids exhibited better catalytic activity than pure c-Fe_2O_3 which indicates that the catalytic activity of c-Fe_2O_3 can be remarkably improved by combining it with grapheme sheets. This implies the crucial role of interaction between c-Fe_2O_3 and graphene. The enhancement in catalytic activity can be attributed to three factors: (i) Graphene has conducting properties and provides high migration efficiency of electrons, which plays an important role in enhancing the catalytic activity for this reaction.[45,46] (ii) As compared with c-Fe_2O_3 and graphene, the graphene/Fe_2O_3 composite can offer an environment to prevent aggregation of c-Fe_2O_3 and grapheme and obstruct loss of activity. Graphene/Fe_2O_3 hybrids have a higher surface area which can provide more active sites for adsorption of reactants and catalytic oxidation and coupling reaction. (iii) Graphene is not only a support, but also as catalyst for the reaction.

7. *α*-Fe_2O_3–MCM-41

The integration of mesoporous silica with magnetic nanoparticles to form porous magnetic nanocomposite is of great interest in practical applications. MCM-41 (Mobil Composition of Matter No. 41) as a highly ordered mesoporous material was used as one of the best neutral coating layers to confine magnetic nanoparticles, due to its high chemical and thermal stability, large surface area and good compatibility.[47]

In this respect, (*α*-Fe_2O_3)–MCM-41 was prepared with 10 wt% of loaded iron oxide nanoparticles, by modification of a reported procedure (Scheme 12).[48] Thus, a solution of iron(III) chloride ($FeCl_3·6H_2O$) and iron(II) chloride ($FeCl_2·4H_2O$) was dissolved in distilled water under N_2 atmosphere and was then added to a cetyltrimethylammonium bromide (CTABr) to construct a colloidal suspension of iron oxide magnetic nanoparticles. Sodium silicate was then added, and the mixture was allowed to react at room temperature under stirring. The surfactant template was then removed from the synthesized material by calcination at 450 °C and the (Fe_3O_4)–MCM-41 converted to (*α*-Fe_2O_3)–MCM-41.

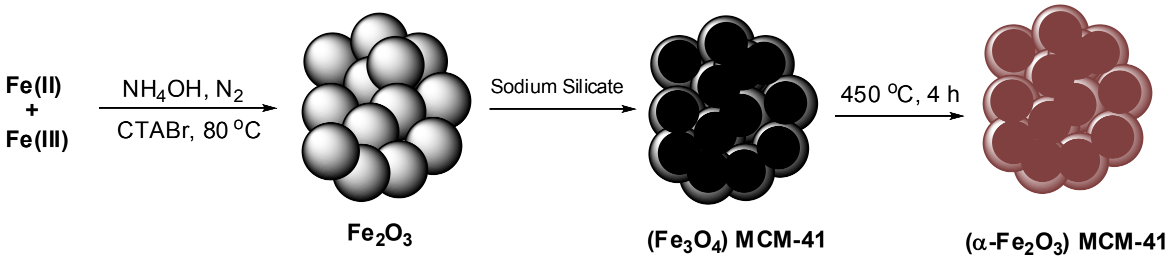

Scheme 12

7.1. SYNTHESIS OF PYRAZOLO[3,4-*c*]PYRIDINE

Rostamizadeh *et al.* used (α-Fe_2O_3)–MCM-41 as a catalyst for the synthesis of a new series of pyrazolo[3,4-*c*]pyridine derivatives **32**. The reaction proceeded at room temperature, by the reaction of 3,5-dibenzylidenepiperidin-4-one **31** with methylhydrazine, hydrazine hydrate or hydrazine hydrate and subsequent acylation of the bicyclic compounds with acetic anhydride (Scheme 13, Table 7).[49] The optimum amount of the catalyst was 0.015 g when (0.16 mmol) of the starting materials were used. It is worth mentioning that 3,5-dibenzylidenepiperidin-4-ones with electron-withdrawing groups on the phenyl rings facilitate the reaction by inducing a greater electronic positive charge on the corresponding *β*-atoms, this makes the reaction requires shorter reaction times. On the other hand, longer reaction times are needed when substrates with electron-rich groups on the phenyl rings are used.

It is important to note that the magnetic property of this catalyst facilitates its efficient recovery from the reaction mixture during the work-up procedure. The recovered catalyst was used in subsequent runs without observation of a significant decrease in activity even after 5 runs.

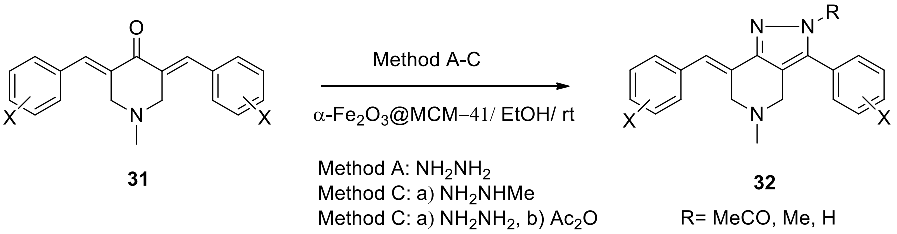

Scheme 13

Table 7. Synthesis of pyrazolo[3,4-*c*]pyridine derivatives **32**

Entry	X	R	Yield (%)	Entry	X	R	Yield (%)
1	4-Me	Me	97	9	4-Me	Me	98
2	2,4-Cl_2	Me	98	10	4-CN	Me	96
3	4-Br	Me	90	11	4-Cl	COMe	90
4	4-$PhCH_2O$	Me	95	12	4-$PhCH_2O$	COMe	90
5	2,3-Cl_2	Me	98	13	4-CN	COMe	95
6	4-Cl	Me	98	14	2,3-Cl_2	H	95
7	4-MeO	Me	90	15	3-O_2N	H	96
8	4-F	Me	98	16	2,4-Cl_2	H	98

A plausible mechanism for the formation of pyrazolo[4,3-*c*]pyridines **32** is shown in Scheme 14. The Lewis acidic property of the Fe^{3+} activates the reaction of hydrazine hydrate with activated C=C double bond in 3,5-dibenzylidenepiperidin-4-one **31** to form the intermediate **A**. The nucleophilic attack of the other NH_2 group on the carbonyl (C=O) moiety gives intermediate **B**. Finally, the expected product **32** is afforded by water elimination.

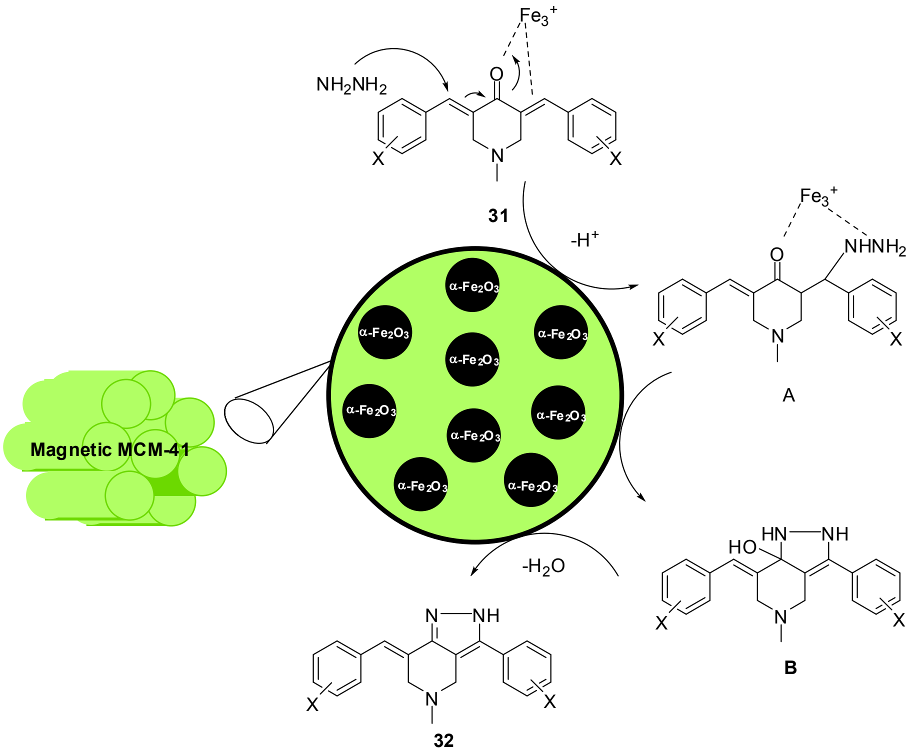

Scheme 14

8. BIMETALLIC MFe_2O_4 NANOPARTICLES

8.1. $ZnFe_2O_4$ NANOPOWDER

The bimetallic $ZnFe_2O_4$ nanopowder, a dual Lewis acid–base combined catalyst, was prepared by the coprecipitation method following a reported procedure.[50]

8.1.1. SYNTHESIS OF HEXAHYDROQUINOLINE

It was found to efficiently catalyze the synthesis of functionalized tetrahydrospiro[indoline-3,2'-quinoline] derivatives **36** in good yields *via* a four component reaction of arylamines **12**, cyclohexane-1,3-diones **33**, dialkyl acetylene dicarboxylates **34** and isatin derivatives **35** and in water (Scheme 15, Table 8).[51] Reduced reaction time, operational simplicity, elimination of hazardous solvent and more importantly, easy recoverability and reusability of the nanopowder make the present methodology economical, green and sustainable.

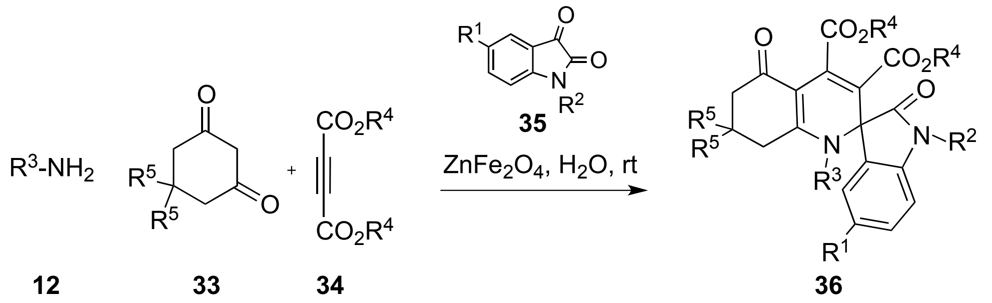

Scheme 15

Table 8. Synthesis of tetrahydrospiro[indoline-3,2'-quinoline] derivatives **36**

Entry	R^1	R^2	R^3	R^4	R^5	Yield (%)
1	H	H	$4\text{-MeC}_6\text{H}_4$	Me	Me	77
2	H	H	$4\text{-MeOC}_6\text{H}_4$	Et	Me	75
3	H	H	$4\text{-BrC}_6\text{H}_4$	Me	Me	72
4	H	H	$4\text{-BrC}_6\text{H}_4$	Et	Me	73
5	Et	H	$4\text{-MeOC}_6\text{H}_4$	Me	Me	80
6	Et	H	$4\text{-ClC}_6\text{H}_4$	Me	Me	78
7	H	Br	$4\text{-MeOC}_6\text{H}_4$	Me	Me	71
8	Et	Cl	$4\text{-MeOC}_6\text{H}_4$	Et	H	77
9	H	Cl	$4\text{-BrC}_6\text{H}_4$	Me	Me	69
10	Pr	H	$4\text{-MeOC}_6\text{H}_4$	Me	Me	72
11	H	Cl	$4\text{-ClC}_6\text{H}_4$	Et	Me	76
12	Pr	Cl	$4\text{-MeOC}_6\text{H}_4$	Me	Me	81
13	Pr	Cl	$4\text{-MeC}_6\text{H}_4$	Et	Me	72
14	Pr	H	$4\text{-ClC}_6\text{H}_4$	Me	H	70
15	H	H	$4\text{-MeOC}_6\text{H}_4$	Et	H	74
16	Pr	Cl	$4\text{-ClC}_6\text{H}_4$	Me	H	76
17	H	F	$4\text{-MeOC}_6\text{H}_4$	Et	H	78
18	H	Br	$4\text{-ClC}_6\text{H}_4$	Et	Me	73
19	Et	Cl	$4\text{-FC}_6\text{H}_4$	Et	H	79
20	H	Cl	$4\text{-MeC}_6\text{H}_4$	Et	Me	82
21	H	H	$3\text{-ClC}_6\text{H}_4$	Et	Me	67
22	H	H	$3\text{-MeOC}_6\text{H}_4$	Et	Me	70
23	H	Cl	$3\text{-ClC}_6\text{H}_4$	Et	Me	69
24	H	H	$4\text{-ClC}_6\text{H}_4$	Me	Me	77
25	H	Cl	$4\text{-MeOC}_6\text{H}_4$	Me	Me	73
26	H	Cl	C_6H_5	Me	Me	67
27	H	Cl	$4\text{-MeOC}_6\text{H}_4$	Et	Me	78
28	H	H	$4\text{-MeOC}_6\text{H}_4$	Me	Me	78
29	H	H	C_6H_5	Me	Me	73
30	H	H	$4\text{-ClC}_6\text{H}_4$	Et	Me	79
31	H	H	$4\text{-MeC}_6\text{H}_4$	Et	Me	82

A probable mechanism for the formation of **36** has been depicted in Scheme 16 which emphasizes the dual role of $ZnFe_2O_4$ as a Lewis acidic site, as well as basic site.[52] Normal spinel structure of $ZnFe_2O_4$ can be represented as (Zn^{2+}) $(Fe^{3+})_2$ $(O^{2-})_4$ where Fe^{3+} ions occupy the octahedral holes whereas diamagnetic Zn^{2+} remains in the tetrahedral holes. Both the octahedral and the tetrahedral holes in the spinel structure are well defined by the O^{2-} ions.[53-55] The Fe^{3+} ions in $ZnFe_2O_4$ act as a strong Lewis acid acceptor and the O^{2-} ions, which remain on the lattice site in the $ZnFe_2O_4$ spinel, act as a base in the reaction. The strong Lewis acidic site Fe^{3+} activates the carbonyl oxygen of isatin to facilitate the condensation between *p*-toluidine and isatin to form imine intermediate **A**. The enolization of dimedone is also catalyzed by Fe^{3+}, which is further assisted by the proton abstraction of basic O^{2-} ion. The nucleophilic attack of the enol form of dimedone on dimethyl acetylenedicarboxylate generates the intermediate **B**. This process is probably catalyzed by Zn^{2+} through the polarization of the π-electron cloud. The intermediate **B** is converted to **C** through the abduction of a proton from water. Intermediate **C** is then converted to intermediate **D** through the abstraction of proton by the O^{2-} ions of lattice sites which act as a base. The negative charge of the sp^2 hybridized carbon atom of **D** is stabilized by the strong Lewis acidic site Fe^{3+} which subsequently attacks the intermediate **A** leading to the formation of the intermediate **E**. In the conversion of **E** to **F**, Fe^{3+} plays a dual role by enhancing the electrophilicity of the carbonyl group of dimedone and also by bringing the nitrogen center of *p*-toluidine and carbonyl center of dimedone of **E** in close proximity for the ring-closure. Finally dehydration of **F** generates the product **36**.

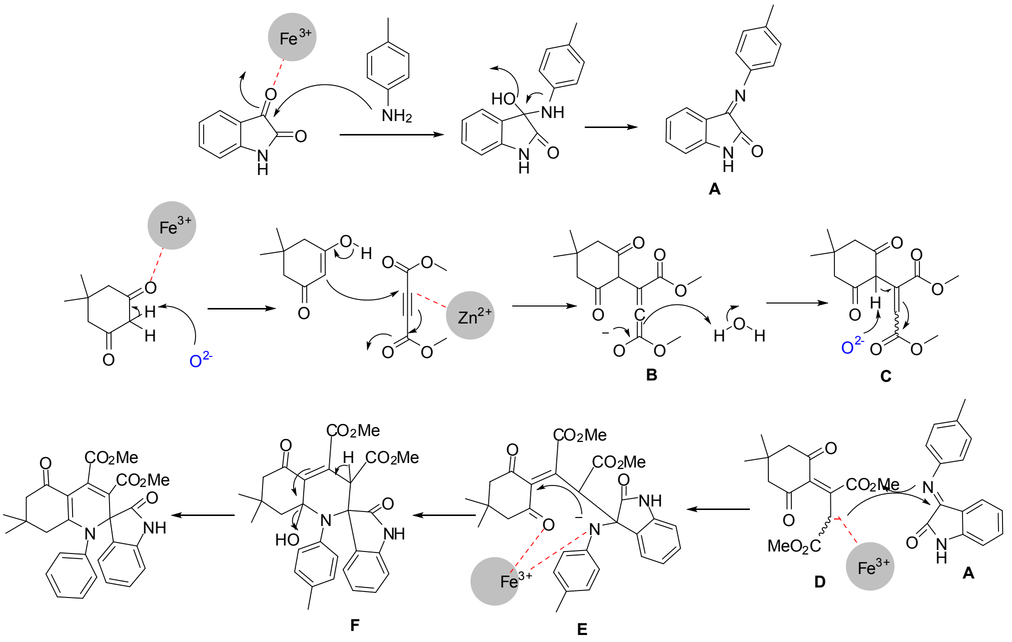

Scheme 16

8.2. $CuFe_2O_4$ MAGNETIC NANOPARTICLES

$CuFe_2O_4$ magnetic nanoparticles were synthesized by heating a solution of $Fe(NO_3)_3·9H_2O$, $Cu(NO_3)_2·3H_2O$ and citric acid in distilled water up to 90 °C to evaporate the water and the citric acid was then decomposed at 300 °C. The resultant powder was calcined at 500 °C to give the $CuFe_2O_4$ samples.[56]

8.2.1. SYNTHESIS OF TETRAHYDRO-4*H*-CHROMENE

The latter magnetic nanoparticles was used as an efficient catalyst for the one-pot synthesis of 4*H*-chromene derivatives **37** in aqueous medium at mild conditions and in excellent yields. The reaction proceeds *via* multi-component reaction (MCR's) of dimedone or cyclohexane-1,3-dione **33**, dialkyl acetylenedicarboxylates **34** and malononitrile or ethyl cyanoacetate **28** (Scheme 17, Table 9).[57]

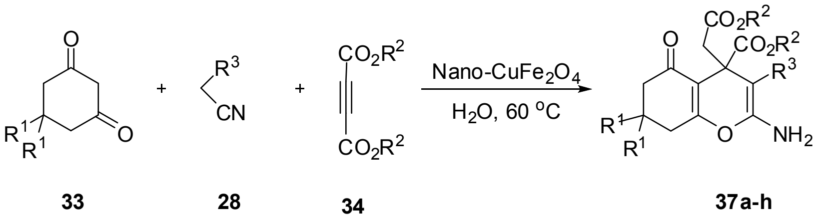

Scheme 17

Table 9. One-pot synthesis of 4*H*-chromene derivatives **37**

Entry	R^1	R^2	R^3	Time (h)	Yield (%)	Entry	R^1	R^2	R^3	Time (h)	Yield (%)
1	Me	Et	CN	2	92	5	H	Et	CN	2	94
2	Me	Et	CO$_2$Et	2.5	88	6	H	Et	CO$_2$Et	2.5	89
3	Me	Me	CN	2	91	7	H	Me	CN	2	92
4	Me	Me	CO$_2$Et	2.5	86	8	H	Me	CO$_2$Et	2.5	86

Pradhan *et al.* proposed a possible mechanism (Scheme 18) for this three CRs. Thus, Cu^{2+} of CuFe$_2$O$_4$ catalyzed the Michael addition reaction of dialkyl acetylenedicarboxylate with alkyl nitrile derivatives (malononitrile and ethyl cyanoacetate) during the formation of the intermediate **X**. The nucleophilic attack by the intermediate **Y** at the *β* position (with respect to nitrile group) of the intermediate **X** was enhanced by Cu^{2+} may be due to the polarization of the π-electron cloud. Finally, the Lewis acidic Fe^{3+} ions interacted with the enolate intermediate **Z** which in turn facilitates the intramolecular electrophilic cyclization with the formation of the six member ring in **37**.[57]

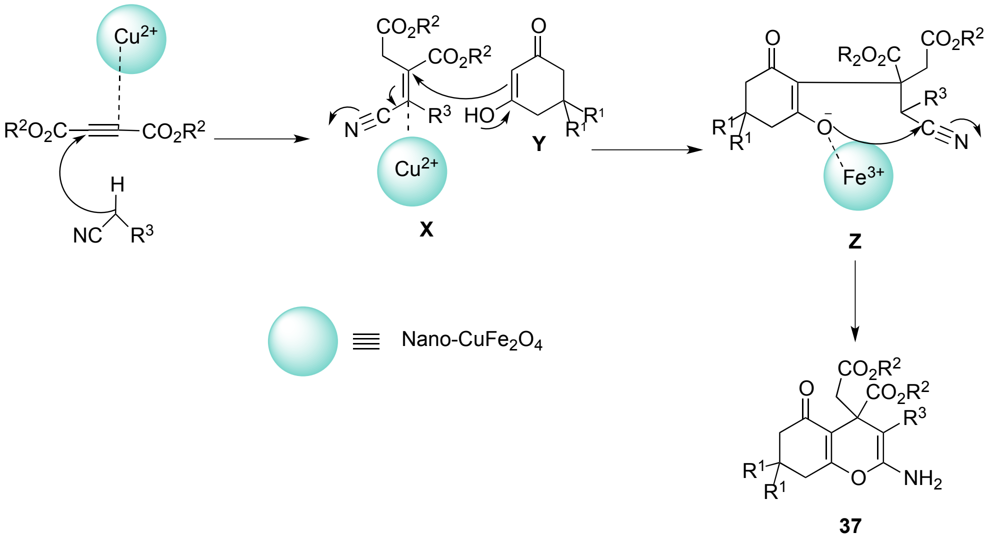

Scheme 18

8.2.2. SYNTHESIS OF BENZOXAZOLE

Sarode *et al.* reported a green and sustainable approach for the synthesis of 2-substituted benzoxazole **39** *via* a redox cascade condensation reaction of benzylamine derivatives **12** and 2-nitrophenols **38**, catalyzed by Cu Ferrite NPs (Scheme 19, Table 10).[58] Copper Ferrite NPs were prepared were prepared by thermal decomposition of $Cu(NO_3)_2$ and $Fe(NO_3)_3$ in water in the presence of 1*M* sodium hydroxide.[59-62]

Cu Ferrite NPs are magnetically separable, air stable and can be recycled up to fifth cycle without a significant loss in catalytic activity.

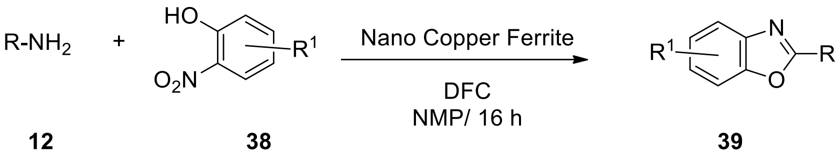

Scheme 19

Table 10. Synthesis of 2-substituted benzoxazoles **39**

Entry	R-NH$_2$	R^1	R	Yield (%)^b	Entry	R-NH$_2$	R^1	R	Yield (%)^b
1	$C_6H_5CH_2$-	H	C_6H_5	92	8	3,5-$(MeO)_2C_6H_3CH_2$-	H	3,5-$(MeO)_2C_6H_3$	81
2	3-$HOC_6H_4CH_2$-	H	3-HOC_6H_4	84	9	$C_6H_5CH_2$-	2-Me	C_6H_5	84
3	4-$MeOC_6H_4CH_2$-	H	4-$MeOC_6H_4$	89	10	$C_6H_5CH_2$-	3-Cl	C_6H_5	80
4	4-$FC_6H_4CH_2$-	H	4-FC_6H_4	85	11	$C_6H_5CH_2$-	3,4-Me$_2$	C_6H_5	90
5	4-$BrC_6H_4CH_2$-	H	4-BrC_6H_4	78	12	$C_6H_5CH_2$-	3-Cl	C_6H_5	86
6	2-naphthyl-CH_2-	H	2-naphthyl	90	13	$C_6H_5CH_2$-	2-Me-3-Cl	C_6H_5	83
7	3-pyridyl-CH_2-	H	3-pyridyl	87					

The plausible reaction mechanism depends on the basis that Cu Ferrite NPs provide the surface for the simultaneous oxidation and reduction of the reactants.[63] Benzylamine on autoxidation forms the corresponding aldehyde and releases ammonia, which acts as a hydrogen source for the reduction of the the *o*-nitrophenol to 2-aminophenol. The latter compound was then condensed with benzaldehyde to give the target 2-phenylbenzo[*d*]oxazole (Scheme 20).

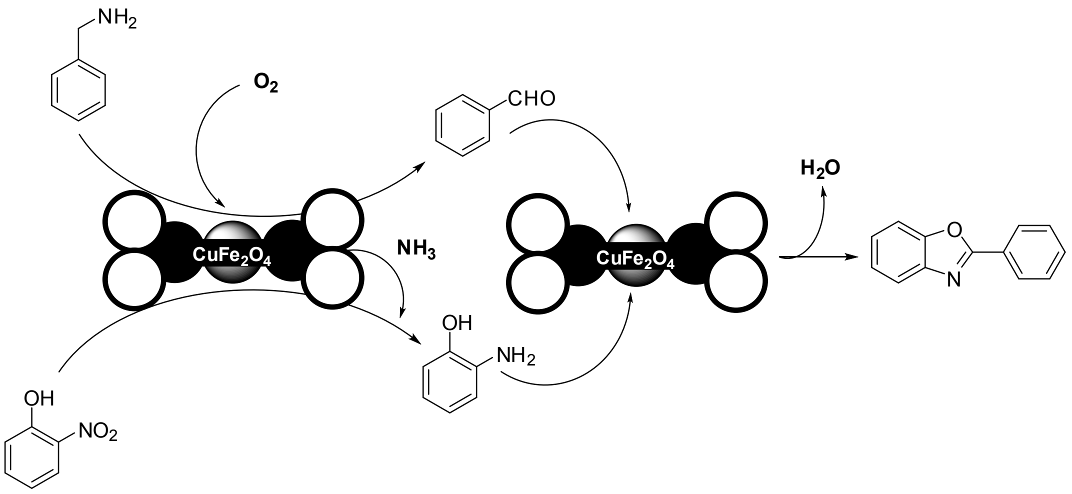

Scheme 20

8.2.3. SYNTHESIS OF PYRROLO[2,3-*d*]PYRIMIDINE

Paul *et al.* developed an efficient heteroannulation protocol for the synthesis of a library of uracil fused pyrrole derivatives **41** by a one-pot three-component domino coupling of 6-aminouracil **40**, aldehydes **5** and nitromethane catalyzed by $CuFe_2O_4$ nanoparticles (Scheme 21, Table 11).[64] It is evident that the reaction passes through the Knoevenagel condensation and the Michael reaction steps. The Fe^{3+} of the magnetic nanoparticles ($CuFe_2O_4$) has shown excellent catalytic activity in promoting the Knoevenagel condensation reaction by enhancing the electrophilicity of the aromatic aldehydes **5**. On the other hand, the Cu^{2+} catalyzes the subsequent Michael addition reaction of the 6-aminouracil **40** to the *α,β*-unsaturated nitroalkene. The easy recovery of the catalyst and high yield of the products makes the protocol attractive, sustainable and economical. The catalyst was recycled for six cycles with almost unaltered catalytic activity. The authors reported that no products were detected when the reactions were carried out using different Brønsted and Lewis acid catalysts for e.g., ZnO, alum, $InCl_3$, I_2, *p*-toluenesulfonic acid, CF_3CO_2H, $FeCl_3$ or CuO.

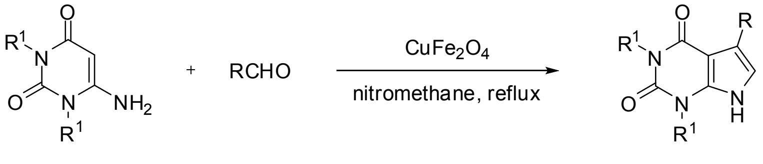

40 **5** **41**

Scheme 21

Table 11. Synthesis pyrrolo[2,3-*d*]pyrimidine **41**

Entry	R	R^1	Yield %	Entry	R	R^1	Yield %
1	C_6H_5	Me	89	6	$4\text{-}MeOC_6H_4$	H	91
2	$4\text{-}MeOC_6H_4$	Me	92	7	$4\text{-}FC_6H_4$	H	86
3	$4\text{-}FC_6H_4$	Me	88	8	$4\text{-}MeC_6H_4$	H	88
4	$4\text{-}MeC_6H_4$	Me	92	9	2-furyl	H	78
5	C_6H_5	H	91				

8.2.4. SYNTHESIS OF DIHYDROPYRANO[2,3-*c*]PYRAZOLE

Pradhan *et al.* synthesized $CuFe_2O_4$ magnetic nanoparticles and reported their use as an efficient catalyst for the one-pot synthesis of dihydropyrano[2,3-*c*]pyrazole derivatives **43**. Thus, a four component reaction (4CRs) of a wide variety of substituted hydrazine derivatives **42**, ethyl acetoacetate **4**, dialkyl acetylenedicarboxylates **34** and alkyl nitrile derivatives **28** (malononitrile and ethyl cyanoacetate) in water gave the target compounds **36** in good yield (Scheme 22, Table 12).[57]

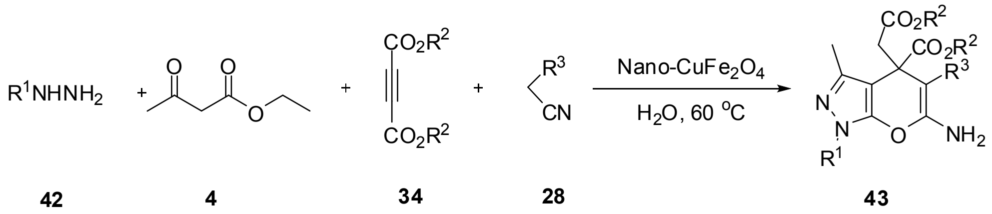

Scheme 22

Table 12. Synthesis of dihydropyrano[2,3-*c*]pyrazole derivatives **43**

Entry	R^1	R^2	R^3	Yield (%)	Entry	R^1	R^2	R^3	Yield (%)
1	C_6H_5	Et	CN	95	7	$4\text{-}O_2NC_6H_4$	Me	CO_2Et	98
2	$4\text{-}O_2NC_6H_4$	Et	CN	90	8	$4\text{-}BrC_6H_4$	Me	CO_2Et	92
3	$4\text{-}BrC_6H_4$	Et	CN	94	9	$4\text{-}NCC_6H_4$	Me	CO_2Et	92
4	$4\text{-}NCC_6H_4$	Et	CN	94	10	H	Me	CO_2Et	96
5	H	Et	CN	97	11	H	Et	CO_2Et	85
6	C_6H_5	Me	CO_2Et	93					

8.2.5. SYNTHESIS OF CHROMENO[4,3-*b*]PYRROLE

Paul *et al.* reported a practical heteroannulation protocol for the synthesis of a library of coumarin fused pyrrole derivatives **45** in good yields *via* a one-pot three-component domino coupling of 4-aminocoumarin **44**, aldehydes **5** and nitromethane catalyzed by $CuFe_2O_4$ magnetic nano particles (Scheme 23, Table 13).[64]

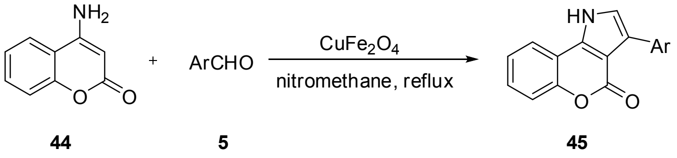

Scheme 23

Table 13. Synthesis of chromeno[4,3-*b*]pyrroles **45**

Entry	R	Yield (%)	Entry	R	Yield (%)
1	C_6H_5	87	7	3-HO-4-MeO	84
2	4-MeO	95	8	$4\text{-}O_2N$	85
3	4-F	85	9	$2,4\text{-}Cl_2$	90
4	4-Me	87	10	4-Br	87
5	$3\text{-}O_2N$	80	11	2-thienyl	81
6	4-Cl	85			

8.2.6. SYNTHESIS OF DIHYDROPYRANO[3,2-*c*]CHROMENE

$CuFe_2O_4$ magnetic nanoparticles were synthesized and recognized as an efficient catalyst for the one-pot synthesis of pyrano[3,2-*c*]coumarin derivatives **47** in excellent yields. The reaction proceeds *via* MCR's of 4-hydroxycoumarin **46**, dialkyl acetylenedicarboxylates **34** and malononitrile or ethyl cyanoacetate **28** in aqueous medium at mild conditions (Scheme 24, Table 14).[57]

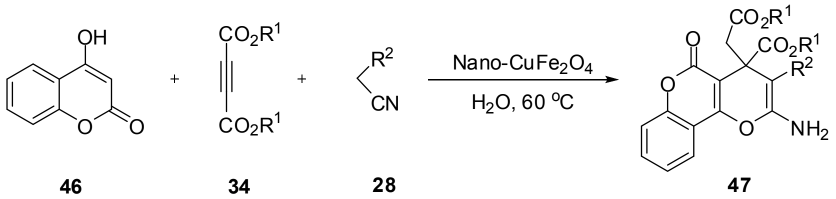

Scheme 24

Table 14. Synthesis of pyrano[3,2-*c*]coumarin derivatives **47**

Entry	R^1	R^2	Yield (%)
1	Et	CN	90
2	Et	CO_2Et	87
3	Me	CN	88
4	Me	CO_2Et	84

8.3. NANO-$CoFe_2O_4$ SUPPORTED Sb

Firstly, $CoFe_2O_4$ nanoparticles was prepared by a chemical co-precipitation technique using $FeCl_3·6H_2O$ and $CoCl_2·6H_2O$ as precursors.[65] $CoFe_2O_4$ nanoparticles were easily coated with a layer of SiO_2 though chemical bonds by sonication a suspension of $CoFe_2O_4$ in a 1 L solution with the molar composition of 292 NH_4OH : 1 CTABr : 2773 H_2O and tetraethyl orthosilicate (TEOS).[66] The obtained $CoFe_2O_4$@ SiO_2 was then treated with an excess amount of 3-chloropropyltrimethoxysilane and triethylamine in dry toluene at 110 °C to give $CoFe_2O_4$@SiO_2 bonded 3-propylchloride.[67] 3-Chloropropyl $CoFe_2O_4$@SiO_2 reacted then with 1,4-diazabicyclo[2.2.2]octane (DABCO) to afford $CoFe_2O_4$@SiO_2–DABCO. Finally, $CoFe_2O_4$@SiO_2–DABCO and antimony trichloride was added to acetone and heated under reflux conditions to yield MNPs supported Sb catalyst ([$CoFe_2O_4$@SiO_2–DABCO–Sb])[69] (Scheme 25).

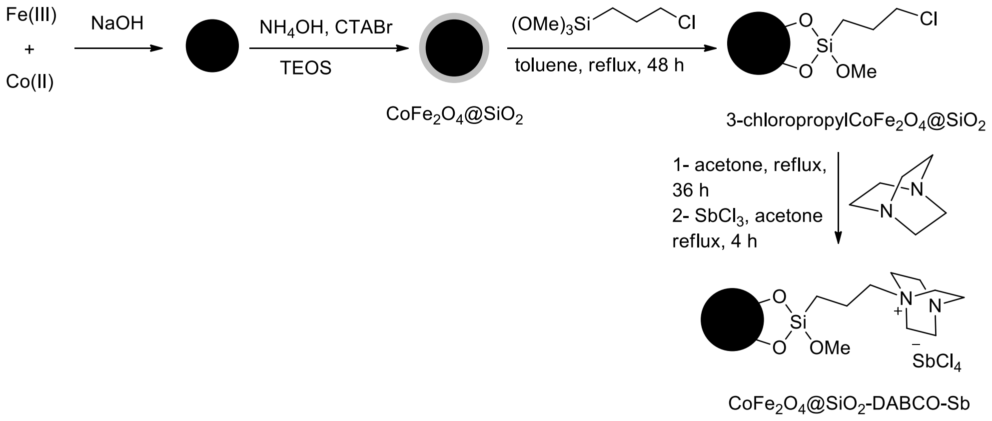

Scheme 25

8.3.1. SYNTHESIS OF PYRROLE

Li *et al.* reported a one-pot three-component synthesis of multisubstituted pyrroles **49** by the reaction of amines **12**, nitroolefins **48** and 1,3-dicarbonyl compounds **4** catalyzed by magnetic nano-$CoFe_2O_4$ supported Sb ([$CoFe_2O_4$@SiO_2–DABCO–Sb]), (Scheme 26, Table 15).[69]

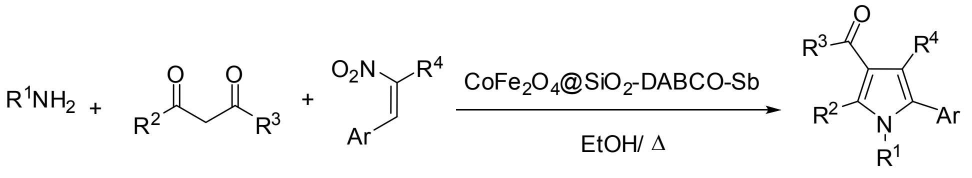

12 **4** **48** **49**

Scheme 26

Table 15. Synthesis of multisubstituted pyrroles **49**

Entry	R^1	R^2	R^3	R^4	Ar	Yield (%)	Entry	R^1	R^2	R^3	R^4	Ar	Yield (%)
1	C_6H_5	Me	Me	H	C_6H_5	93	25	4-BrC_6H_4	Me	Me	Me	C_6H_5	77
2	C_6H_5	Me	Me	Me	C_6H_5	80	26	4-$F_3CC_6H_4$	Me	Me	Me	C_6H_5	51
3	C_6H_5	Me	Me	Me	4-MeC_6H_4	87	27	4-$F_3COC_6H_4$	Me	Me	Me	C_6H_5	85
4	C_6H_5	Me	Me	Me	4-FC_6H_4	86	28	2-furyl-CH_2	Me	Me	Me	C_6H_5	90
5	C_6H_5	Me	Me	Me	2-ClC_6H_4	75	29	2-fluorenyl	Me	Me	Me	C_6H_5	73
6	C_6H_5	Me	Me	Me	3-ClC_6H_4	78	30	allyl	Me	Me	Me	C_6H_5	91
7	C_6H_5	Me	Me	Me	4-ClC_6H_4	85	31	Bn	Me	Me	Me	C_6H_5	90
8	C_6H_5	Me	Me	Me	4-$O_2NC_6H_4$	75	32	$C_6H_5CH_2CH_2$	Me	Me	Me	C_6H_5	92
9	C_6H_5	Me	Me	Me	2-furyl	88	33	$C_6H_5CHMe_2$	Me	Me	Me	C_6H_5	87
10	C_6H_5	Me	Me	Me	2-thienyl	82	34	^{c}Pr	Me	Me	Me	C_6H_5	89
11	C_6H_5	Me	Me	Me	2-naphthyl	47	35	^{c}Pn	Me	Me	Me	C_6H_5	72
12	C_6H_5	Me	Me	Et	C_6H_5	80	36	^{n}Pr	Me	Me	Me	C_6H_5	88
13	C_6H_5	Me	Me	Et	4-MeC_6H_4	80	37	^{n}Bu	Me	Me	Me	C_6H_5	86
14	C_6H_5	Me	Me	Et	2-furyl	76	38	C_6H_5	Me	OMe	Me	C_6H_5	82
15	C_6H_5	Me	Me	Et	2-thienyl	78	39	C_6H_5	Me	OEt	Me	C_6H_5	85
16	4-^{t}BuC_6H_4	Me	Me	H	C_6H_5	92	40	C_6H_5	Me	$O(CH_2)_2OMe$	Me	C_6H_5	80
17	2-naphthyl	Me	Me	H	C_6H_5	75	41	C_6H_5	Me	O-allyl	Me	C_6H_5	78
18	2-fluorenyl	Me	Me	H	C_6H_5	80	42	C_6H_5	Et	OMe	Me	C_6H_5	76
19	4-MeC_6H_4	Me	Me	Me	C_6H_5	82	43	C_6H_5	Me	$OCMe_3$	Me	C_6H_5	83
20	4-$MeOC_6H_4$	Me	Me	Me	C_6H_5	88	44	C_6H_5	Me	OCH_2CHMe_2	Me	C_6H_5	81
21	4-FC_6H_4	Me	Me	Me	C_6H_5	82	45	2-furyl-CH_2	Me	Me	Et	C_6H_5	89
22	4-ClC_6H_4	Me	Me	Me	C_6H_5	75	46	Bn	Me	Me	Et	C_6H_5	86
23	2-BrC_6H_4	Me	Me	Me	C_6H_5	70	47	^{c}Pr	Me	Me	Et	C_6H_5	82
24	3-BrC_6H_4	Me	Me	Me	C_6H_5	72	48	^{n}Pr	Me	Me	Et	C_6H_5	83

The magnetic heterogeneous catalyst could be easily recovered using an external magnet and reused many times without significant loss of catalytic activity. The results showed that the catalyst can be recycled for up to five times with essentially no loss of catalytic activity, which indicates that the prepared catalyst possessed excellent activity and reusability. Furthermore, the SEM image of the recovered catalysts after the fifth cycle does not show any significant change in the shape and size of the magnetic nanoparticles, which provides hard evidence to demonstrate that MNPs-supported Sb catalyst was highly chemically stable.

8.4. NANO-$CoFe_2O_4$ SUPPORTED MOLYBDENUM

A magnetic nanoparticle $CoFe_2O_4$ supported molybdenum catalyst ([$CoFe_2O_4$@SiO_2-$PrNH_2$-$Mo(acac)_2$]), was prepared according to the procedure shown in Scheme 27. At first, $CoFe_2O_4$ nanoparticles were prepared by a chemical co-precipitation technique using $FeCl_3 \cdot 6H_2O$ and $CoCl_2 \cdot 6H_2O$ as precursors according to a reported procedure.[70] The coating of a layer of silica on the surface of $CoFe_2O_4$ nanoparticles was achieved by sonication of a $CoFe_2O_4$ suspension in an alkaline ethanol–water solution of tetraethyl orthosilicate (TEOS). The surfaces of the particles were further functionalized with 3-aminopropyltriethoxysilane (APTES) to afford aminated-$CoFe_2O_4$@SiO_2 MNPs. The molybdenyl acetylacetonate complex was then anchored to aminated-$CoFe_2O_4$@SiO_2 to yield MNPs supported Mo catalyst ($CoFe_2O_4$@SiO_2-$PrNH_2$-Mo(acac)$_2$).

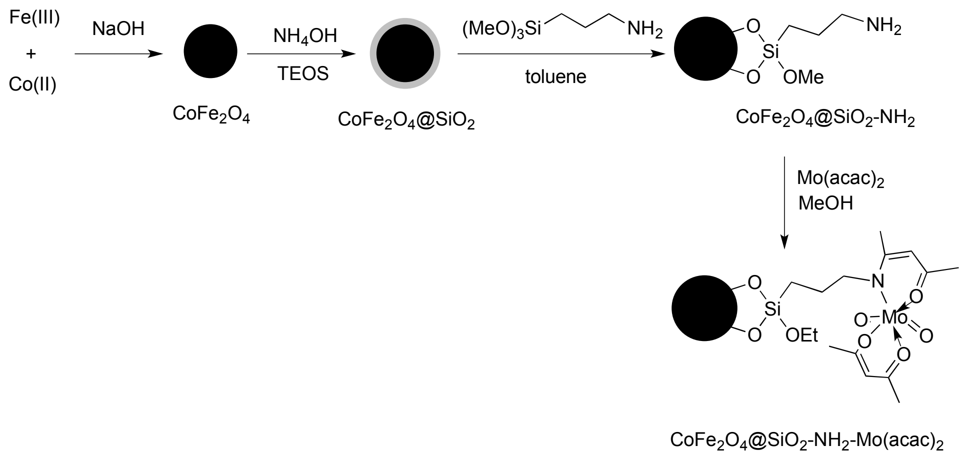

Scheme 27

8.4.1. SYNTHESIS OF PYRROLE

The catalyst was found to be a highly efficient catalyst for a one-pot synthesis of polysubstituted pyrroles **51** *via* a four-component reaction of aldehydes **5**, amines **12**, 1,3-dicarbonyl compounds **4** and nitromethane **50** (Scheme 28, Table 16). The catalyst could be easily separated by a simple magnet and can be reused five times without a significant loss of activity.[71]

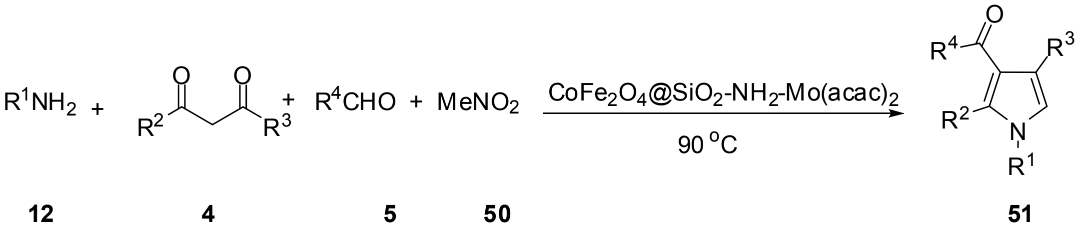

Scheme 28

Table 16. One-pot synthesis of polysubstituted pyrroles **51**

Entry	R^1	R^3	R^4	Yield (%)	Entry	R^1	R^3	R^4	Yield (%)
1	C_6H_5	Me	C_6H_5	90	22	C_6H_5	Me	4-ClC_6H_4	86
2	4-$MeOC_6H_4$	Me	C_6H_5	86	23	C_6H_5	Me	4-BrC_6H_4	85
3	4-MeC_6H_4	Me	C_6H_5	92	24	C_6H_5	Me	4-$O_2NC_6H_4$	83
4	4-FC_6H_4	Me	C_6H_5	90	25	C_6H_5	Me	4-$F_3CC_6H_4$	85
5	4-ClC_6H_4	Me	C_6H_5	80	26	C_6H_5	Me	2-furyl	60
6	4-BrC_6H_4	Me	C_6H_5	82	27	C_6H_5	Me	2-thienyl	71
7	4-$O_2NC_6H_4$	Me	C_6H_5	50	28	C_6H_5	Me	1-naphthyl	80
8	4-$F_3COC_6H_4$	Me	C_6H_5	80	29	4-MeC_6H_4-CH_2-	Me	2-thienyl	80
9	1-naphthyl	Me	C_6H_5	48	30	4-FC_6H_4	Me	2-thienyl	75
10	2-fluorenyl	Me	C_6H_5	83	31	4-FC_6H_4	Me	2-(5-methylthienyl)	78
11	allyl	Me	C_6H_5	88	32	4-ClC_6H_4	Me	2-(5-methylthienyl)	70
12	Bn	Me	C_6H_5	90	33	2-fluorenyl	Me	2-(5-methylthienyl)	80
13	4-MeC_6H_4-CH_2-	Me	C_6H_5	91	34	Bn	Me	2-thienyl	80
14	4-FC_6H_4-CH_2-	Me	C_6H_5	87	35	C_6H_4-CH_2-CH_2-	Me	4-MeC_6H_4	88
15	C_6H_4-CH_2-CH_2-	Me	C_6H_5	91	36	C_6H_4-CH_2-CH_2-	Me	4-FC_6H_4	89
16	4-HOC_6H_4-CH_2-CH_2-	Me	C_6H_5	90	37	C_6H_4-CH_2-CH_2-	Me	3-$F_3CC_6H_4$	85
17	^{c}Pr	Me	C_6H_5	90	38	^{c}Pr	Me	4-^{t}BuC_6H_4	88
18	^{c}Pn	Me	C_6H_5	86	39	C_6H_5	OMe	C_6H_5	80
19	^{n}Pr	Me	4-FC_6H_4	90	40	C_6H_5	OEt	C_6H_5	82
20	C_6H_5	Me	4-$(Me_2)CHOC_6H_4$	81	41	C_6H_5	$O(CH_2)_2OMe$	C_6H_5	80
21	C_6H_5	Me	4-FC_6H_4	87	42	C_6H_5	O-allyl	C_6H_5	78

The yield was greatly affected by the amount of catalyst loaded as well as the reaction temperature. The best results were achieved at 90 °C using 1.5 mol% of the catalyst. The reaction proceeded sluggishly in the absence of catalyst and offered only very low yield of the expected products.

9. Fe_3O_4 NANOPARTICLES

9.1. SYNTHESIS OF IMIDAZOLE

Montazeri *et al*. reported a four-component synthesis of 1,2,4,5-tetrasubstituted imidazoles **53** using nano Fe_3O_4 as a magnetically recyclable catalyst under solvent free conditions (Scheme 29, Table 17).[72] The yield of the products is affected by the catalyst amount and reaction temperature. No product was obtained in the absence of the catalyst or in the presence of the catalyst at room temperature. Increasing the amount of the catalyst up to 15 mol% and the reaction temperature to 140 °C, increased the yield of the product, but further increase in both catalyst amount and temperature did not increase the yield noticeably. After the completion of the reaction, the catalyst was recovered and could be reused at least five times with only slight reduction in the catalytic activity.

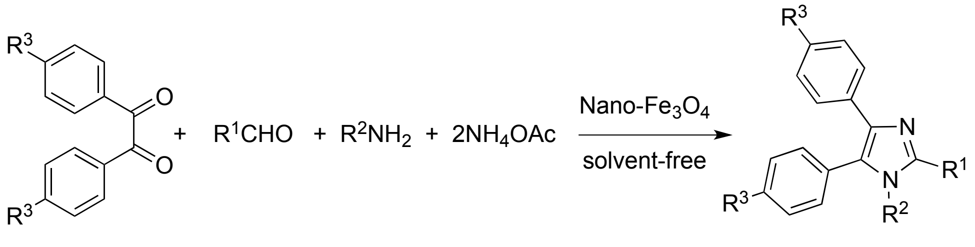

52 **5** **12** **53**

Scheme 29

Table 17. Synthesis of 1,2,4,5-tetrasubstituted imidazoles **53**

Entry	R^1	$^{a}R^2$	Yield (%)	Entry	R^1	$^{a}R^2$	Yield (%)
1	C_6H_5	C_6H_5	94	8	$4\text{-}O_2NC_6H_4$	Bn	81
2	C_6H_5	Bn	92	9	$4\text{-}MeC_6H_4$	Bn	87
3	$4\text{-}O_2NC_6H_4$	$4\text{-}MeC_6H_4$	80	10	$4\text{-}ClC_6H_4$	Bn	82
4	$4\text{-}ClC_6H_4$	C_6H_5	85	11	$4\text{-}MeOC_6H_4$	C_6H_5	92
5	$4\text{-}MeC_6H_4$	Bn	75	12	$4\text{-}MeOC_6H_4$	Bn	93
6	$4\text{-}MeC_6H_4$	C_6H_5	91	13	C_6H_5	Me	80
7	$4\text{-}ClC_6H_4$	$4\text{-}O_2NC_6H_4$	79				

[a] R^3 = H

9.2. SYNTHESIS OF 4*H*-PYRAN

Commercially available nano-power magnetite or iron(III) oxide have been used as a catalyst in the construction of 4-substituted-4*H*-pyrans **6** from reaction of *β*-keto esters or other 1,3-dicarbonyl compound **4** with the corresponding aldehyde **5** (Scheme 30, Table 18). The reaction implies a tandem process, involving an aldol condensation, a Michael-type addition, and a dehydrating annulation. A variety of several different aromatic aldehydes could be employed for the reaction and both electron-withdrawing and electron-donating groups were well tolerated, producing the pyrans **6** with a high efficiency.[30] Attempts to improve the obtained results by performing the reactions under similar conditions, using different impregnated metallic oxides, including (Co, Ni, Cu, Ru and Pd) on magnetite were unsuccessful.

Although the possible mechanism is still unknown, it should be pointed out that the formation of catalytic species having an Fe(III)–Cl bond should play an important role as a Lewis acid, with the centers of iron(III) being the only avail to catalyze the final Michael addition.

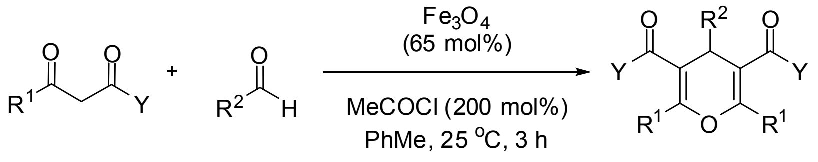

4 **5** **6**

Scheme 30

Table 18. Synthesis of 4-substituted-4*H*-pyrans **6**

Entry	R^1	Y	R^2	Yield (%)	Entry	R^1	Y	R^2	Yield (%)
1	Me	OMe	$4\text{-}BrC_6H_4$	96 (94)	7	Me	OMe	$(CH_2)_5CH$	80 (79)
2	Me	OMe	$4\text{-}NCC_6H_4$	79	8	Me	OMe	*i*-Pr	72 (67)
3	Me	OMe	Ph	85 (82)	9	Me	OEt	$4\text{-}BrC_6H_4$	95
4	Me	OMe	$4\text{-}MeOC_6H_4$	83	10	Me	OEt	$4\text{-}MeOC_6H_4$	63
5	Me	OMe	$4\text{-}HOC_6H_4$	68	11	Me	Me	$4\text{-}MeOC_6H_4$	75 (64)
6	Me	OMe	2-naphthyl	57	12	Me	OMe	$4\text{-}BrC_6H_4$	91 (79)

9.3. SYNTHESIS OF PYRIMIDINE

(4-Amino-6-aryl-2-phenyl)pyrimidine-5-carbonitrile derivatives **55** were synthesized through a one-pot, three-component reaction of an aldehydes **5**, malononitrile **28** and benzamidine hydrochloride **54**, in the presence of magnetic nano Fe_3O_4 particles as a catalyst under solvent-free conditions (Scheme 31, Table 19). The products **55** were prepared with excellent yields at 100 °C in 1–1.5 h. Both aromatic aldehydes with electron donating substituents and electron-withdrawing substituents showed a significant reactivity in this process.[73] The nano Fe_3O_4 was separated using an external magnet, and could be reused three times without any significant loss of activity.

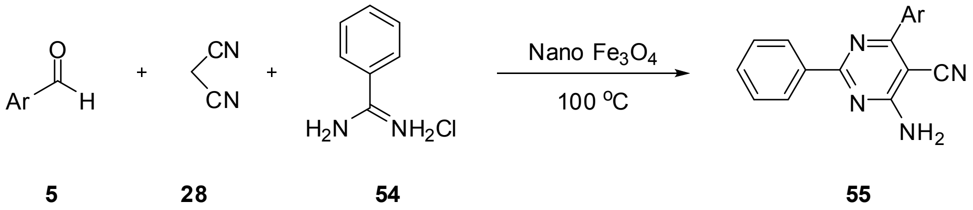

Scheme 31

Table 19. Synthesis of (4-amino-6-aryl-2-phenyl)pyrimidine-5-carbonitrile derivatives **55**

Entry	Ar	Yield^a (%)	Entry	Ar	Yield^a (%)
1	Ph	98	8	2,4-diClC_6H_3	96
2	4-ClC_6H_4	96	9	3-$O_2NC_6H_4$	96
3	4-BrC_6H_4	94	10	4-$O_2NC_6H_4$	96
4	2,3-diClC_6H_3	96	11	3-indolyl	90
5	2-ClC_6H_4	96	12	4-MeCONHC_6H_4	95
6	4-NCC_6H_4	98	13	4-MeOC_6H_4	95
7	4-MeC_6H_4	96			

[a] Isolated yields.

9.4. SYNTHESIS OF DECAHYDROACRIDINE

Fekri *et al*. reported an efficient, three component synthesis of a novel class of decahydroacridine derivatives **56** by the reaction of the appropriate aldehydes **5**, dimedone **33** and ammonium acetate in the presence of nano Fe_3O_4 as a recyclable catalyst under ultrasonic irradiation (Scheme 32, Table 20).[74] The higher yield, shorter reaction time and milder reaction condition gained under ultrasonic irradiation is a result of implosive collapse of the cavitations period of the sound waves.

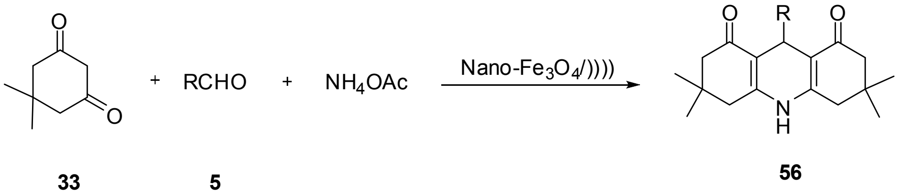

Scheme 32

Table 20. Synthesis of decahydroacridine derivatives **56**

Entry	R	Yield (%)	Entry	R	Yield (%)
1	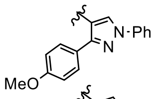	90	4	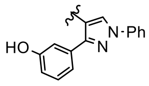	78
2	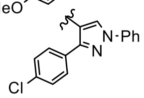	87	5	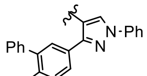	83
3	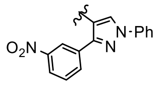	81	6	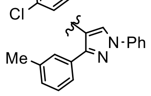	86

9.5. SYNTHESIS OF TETRAHYDROINDENO[1,2-*b*]PYRAZOLO[4,3-*e*]PYRIDINE

Mohammad *et al.* reported the synthesis of fused azo-linked pyrazolo[4,3-*e*]pyridines **52a-f** and **53a-c** from indan-1,3-dione **50** and 3-amino-5-methylpyrazole **51**, using nano-Fe_3O_4 in water as an effective and reusable catalyst (Scheme 33, Table 21).[75] The authors carried out the condensation reaction, (i) in a catalyst free reaction and (ii) in the presence of Fe_3O_4 and (iii) in the presence of nano-Fe_3O_4 and the results showed that nano-Fe_3O_4 proved to be a better catalyst than Fe_3O_4 for the synthesis of pyrazolopyridines. The authors studied the effect of the catalyst amount on the reaction and found that 50 mg of nano-Fe_3O_4 is sufficient to push the reaction forward completion while the less amount was not enough. On the other hand, higher amount of catalyst did not lead to significant change in the reaction yields. When indan-1,3-dione (**58**), 3-amino-5-methylpyrazole (**59**), and azo-linked benzaldehyde containing electron releasing substituents **57g-i** were refluxed for a required reaction time, the reaction leads to the formation of the aromatized pyrazolopyridine **61g-i**, but in the case of using azo-linked aldehydes containing electron withdrawing substituents **57a-f**, just pyrazolopyridines **60a-f** were observed. The simplicity of product isolation, replacement of the carcinogenic solvent with H_2O and the possibility to recycle nano-Fe_3O_4 offer a significant advantage. After the reaction was completed, the catalyst could be easily attracted by an efficient magnetic bar. The recovered catalyst could be successively recycled in subsequent reactions without any decrease of yields. The authors suggested a mechanism for the nano-Fe_3O_4 catalyzed synthesis of fused pyrazolopyridine *via* facilitating of the Knoevenagel condensation between aldehydes and indandione.

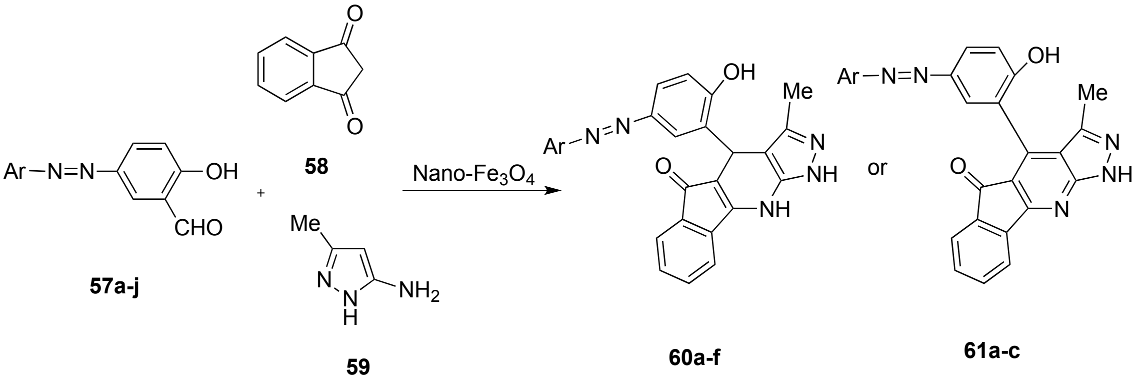

Scheme 33

Table 21. Synthesis of fused azo-linked pyrazolo[4,3-*e*]pyridines **60a-f** and **61a-c**

Entry	Ar	Product	Time (min)	Yield (%)	Entry	Ar	Product	Time (min)	Yield (%)
1	4-IC_6H_4	**60a**	5	75	6	4-ClC_6H_4	**60f**	5	84
2	4-$O_2NC_6H_4$	**60b**	8	83	7	Ph	**61a**	2	86
3	2-Me-4-$O_2NC_6H_4$	**60c**	8	75	8	4-MeC_6H_4	**61b**	1	79
4	2-ClC_6H_4	**60d**	5	83	9	4-$MeOC_6H_4$	**61c**	1	87
5	3-ClC_6H_4	**60e**	5	95					

10. IRIDIUM IMPREGNATED ON Fe_3O_4

10.1. SYNTHESIS OF FURAN

Cano *et al*. used commercially available nano-powder magnetite as an excellent catalyst for the addition of acid chlorides **62** to internal and terminal alkynes **63**, yielding the corresponding chlorovinyl ketones in good yields. Attempts to react the chlorovinyl ketone with nano-powder magnetite did not yield the expected furan even after 7 days at 130 °C. However, the same process, but using rhodium trichloride gave the product furan in a moderate yield. Other transition salts like, $PdCl_2$ and $IrCl_3$ give also excellent results. The use of the iridium impregnated on magnetite catalyst permit the integration of the chloroacylation process with a second dehydrochlorination annulation process to yield, in one-pot, 3-aryl-2,5-dialkylfurans **64** in good yields, independently of the nature of the starting reagents, and including the heteroaromatic ones (Scheme 34, Table 22).[76]

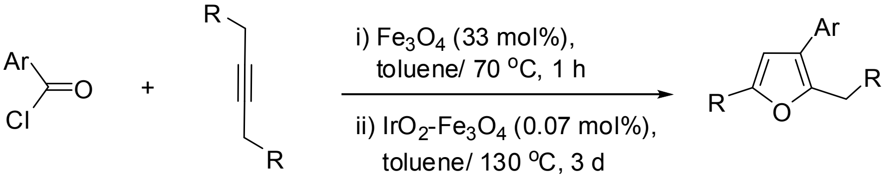

62 **63** **64**

Scheme 34

Table 22. One-pot synthesis of 3-aryl-2,5-dialkylfurans **64**

Entry	Ar	R	Yield (%)[a]
1	C_6H_5	^{n}Pr	88
2	C_6H_5	Me	91
3	4-ClC_6H_4	^{n}Pr	76
4	4-$MeOC_6H_4$	^{n}Pr	94
5	2-thienyl	^{n}Pr	74

[a] Isolated yield after column chromatography

11. MAGNETITE–SULFURIC ACID (Fe_3O_4·SO_3H)

Magnetite–sulfuric acid (Fe_3O_4·SO_3H) magnetic nanoparticles MSA-MNP 1 catalyst was obtained in a simple one-step procedure by the reaction of chlorosulfonic acid with bare magnetite (Fe_3O_4). For the synthesis of MSA-MNP 2, the surface of the nanoparticles was modified with negatively charged citrate groups before functionalization with chlorosulfonic acid (Scheme 35).

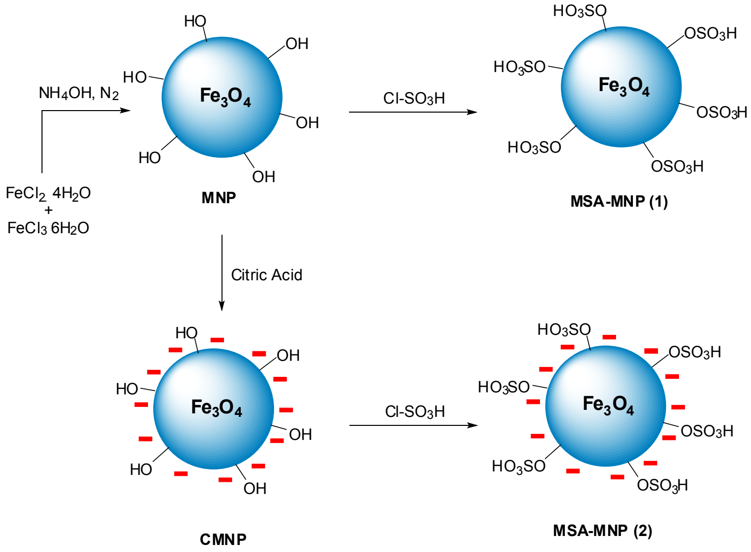

Scheme 35

11.1. SYNTHESIS OF 14*H*-DIBENZO[*a*,*j*]XANTHENE

MSA-MNP 1 and MSA-MNP 2 catalysts were shown to exhibit remarkable catalytic performance in the solvent-free synthesis of mono-, bis-, and tris-14*H*-dibenzo[*a*,*j*]xanthen-14-ylarenes **67a-g, 69, 70**, and **72a,b**. The reactions were performed by the reaction of 2-naphthol with benzaldehyde derivatives (Scheme 36), terephthalaldehyde, isophthalaldehyde (Scheme 37) or trialdehydes **66** and **71** (Scheme 38), respectively, in the presence of 0.1 g MSA-MNP 2 under solvent-free conditions.[77] The best reaction conditions involve the use of 0.1 grams of catalyst at 100 °C under solvent-free conditions. MSA-MNP 2 catalyzes the reaction better than do other catalysts; when MSA-MNP 2 is used, no by-products, such as noncyclized intermediates, are formed, and the time for the reaction is reduced to 10 min.

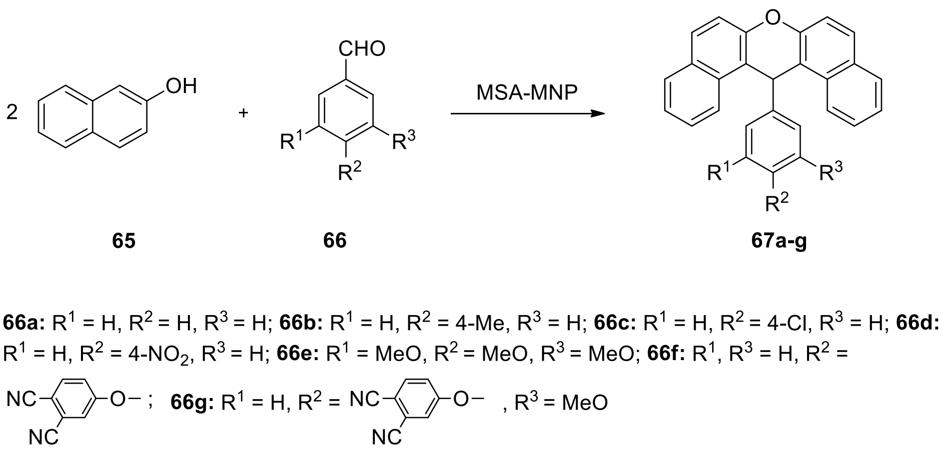

65 **66** **67a-g**

66a: R^1 = H, R^2 = H, R^3 = H; **66b:** R^1 = H, R^2 = 4-Me, R^3 = H; **66c:** R^1 = H, R^2 = 4-Cl, R^3 = H; **66d:** R^1 = H, R^2 = 4-NO_2, R^3 = H; **66e:** R^1 = MeO, R^2 = MeO, R^3 = MeO; **66f:** R^1, R^3 = H, R^2 = ; **66g:** R^1 = H, R^2 = , R^3 = MeO

Scheme 36

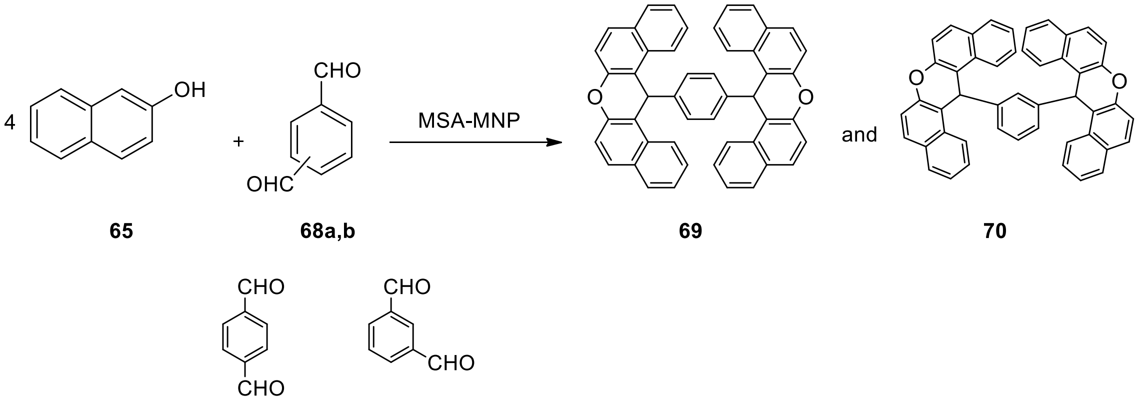

65 **68a,b** **69** **70**

68a **68b**

Scheme 37

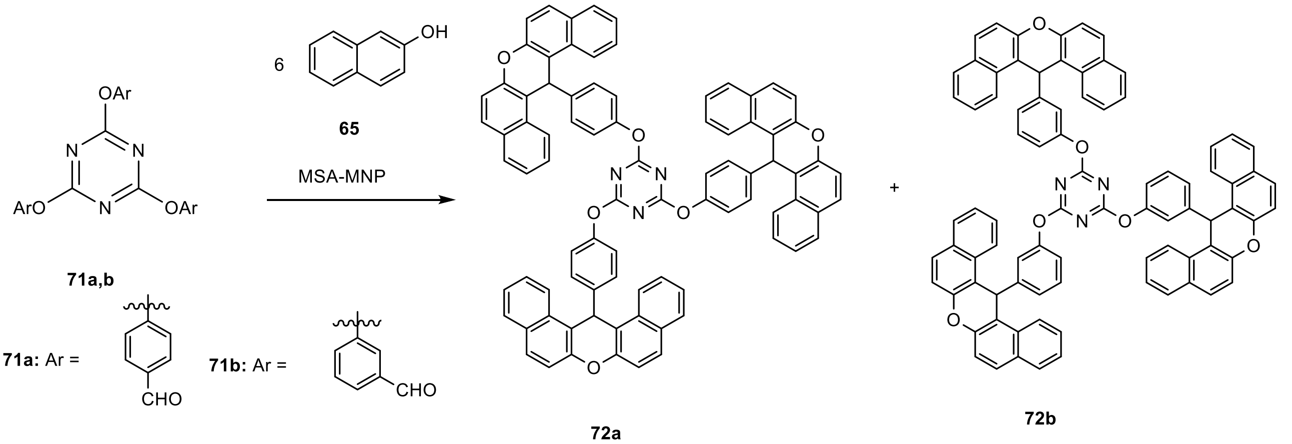

65

71a,b

71a: Ar = **71b:** Ar =

72a **72b**

Scheme 38

12. Fe_3O_4 NANOPARTICLE-SUPPORTED GLUTATHIONE

Polshettiwar and Varma prepared nano-organocatalyst by sonicating magnetic nanoparticles with glutathione in water (Scheme 39). Glutathione, have highly reactive thiol group, which can be used for anchoring to the nano-ferrite surfaces, keeping active sites free for catalysis.[78]

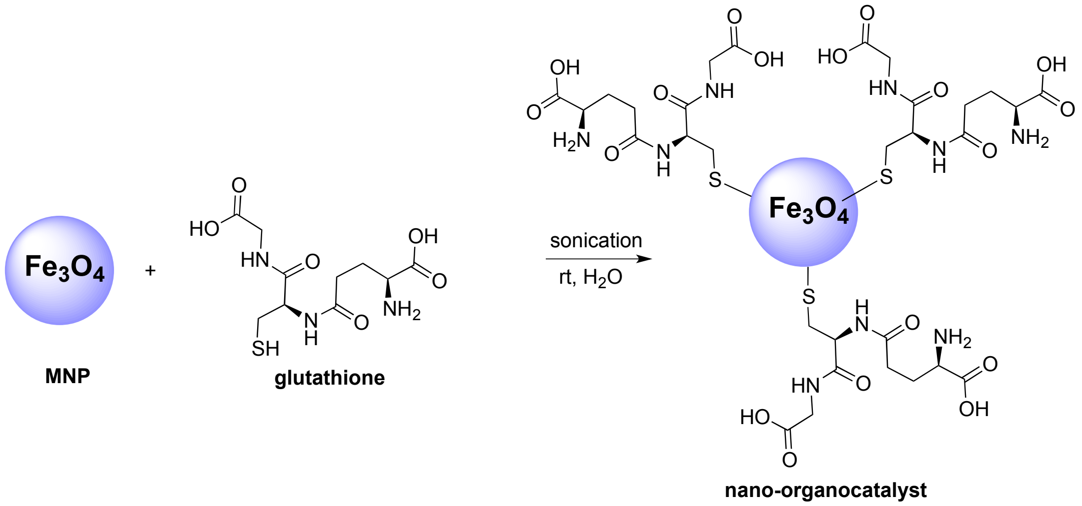

Scheme 39

12.1. SYNTHESIS OF PYRROLE

The catalyst showed excellent activity for microwave-assisted synthesis of *N*-substituted pyrroles **14** by the reaction of a variety of amines **12** with tetrahydro-2,5-dimethoxyfuran **13** (Scheme 40, Table 23). The rates were essentially the same for both of aliphatic or aromatic amines, showing the high activity of the catalyst.[78]

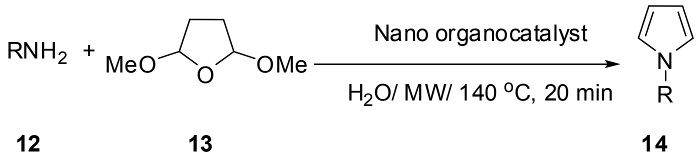

Scheme 40

Table 23. Preparation of *N*-substituted pyrroles **14**

Entry	R	Yield (%)	Entry	R	Yield (%)
1	$-CH_2C_6H_5$	92	9	$NHOCC_6H_5$	72
2	$-CH(Me)C_6H_5$ (*S*)	90	10	$-OCC_6H_5$	NR
3	$-CH(Me)C_6H_5$ (*R*)	90	11	$NH-4-O_2NC_6H_4$	NR
4	$-(CH_2)_3C_6H_5$	86	12	^{i}Bu	90
5	C_6H_5	88	13	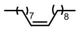	84
6	$3-EtO_2CC_6H_4$	85	14	$-(CH_2)_3OH$	86
7	$2-MeOCC_6H_4$	82	15	$-(CH_2)_3NH_2$	85
8	pyridyl-CH_2-	78	16	$-(CH_2)_3NH_2$	72

13. CHITOSAN-COATED Fe_3O_4 NANOPARTICLES

Zarnegar and Safari prepared chitosan-coated Fe_3O_4 nanoparticles (Fe_3O_4@CS) through in *situ* co-precipitation of Fe^{2+} and Fe^{3+} ions *via* NH_4OH in an aqueous solution of chitosan followed by the hydrothermal treatment (Scheme 41).[79]

Maleki and Kamalzare *et al*. prepared Fe_3O_4@chitosan composite nanocatalyst by adding water dispersed Fe_3O_4 nanoparticles into an acetic acid solution of chitosan and the obtained dispersion was stirred overnight at room temperature. The resulted gel separated from the reaction mixture was washed and vacuum dried to obtain the chitosan supported iron oxide nanoparticles nanocomposite (Fe_3O_4/chitosan).[80]

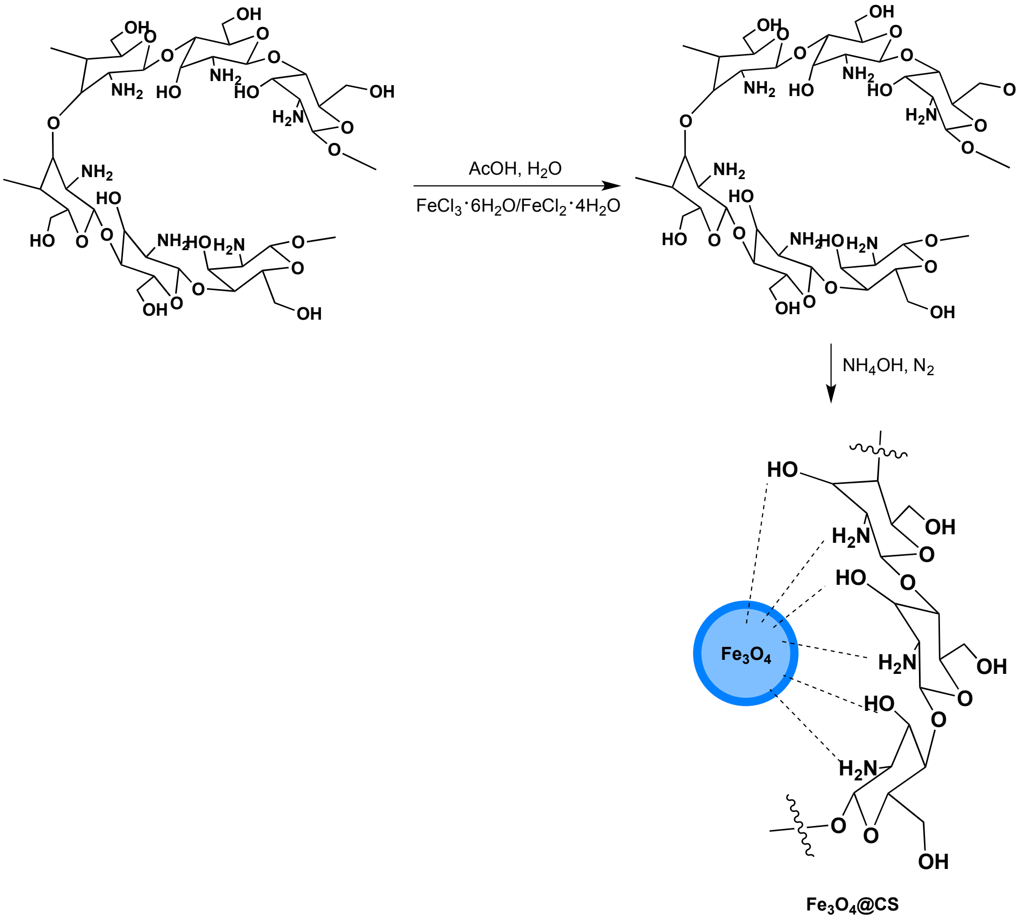

Scheme 41

13.1. SYNTHESIS OF IMIDAZOLE

They investigated the catalytic activity of Fe_3O_4@CS in the synthesis of 2,4,5-trisubstituted imidazoles **63** by a similar one-pot reaction (Scheme 42, Table 24).[79]

The catalyst exhibited highest catalytic activity as compared with Fe_3O_4 and chitosan. One of the advantages of this active, non-toxic, and environmentally benign heterogeneous bio-polymer catalyst is its easily and efficiently separation from the product by an external magnet. It could also be reused six times without great loss of catalytic activity.

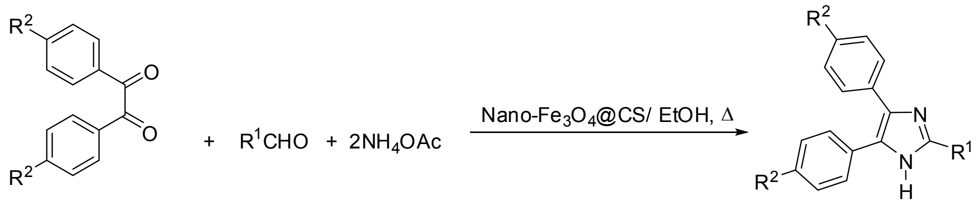

52 **5** **53**

Scheme 42

Table 24. Preparation of 2,4,5-trisubstituted imidazoles **53**

Entry	R1	R2	Yield (%)	Entry	R1	R2	Yield (%)
1	C_6H_5	H	95	7	3-$MeOC_6H_4$	H	98
2	4-$MeOC_6H_4$	H	90	8	C_6H_5	OMe	95
3	3-$MeOC_6H_4$	H	92	9	4-$MeOC_6H_4$	OMe	90
4	4-ClC_6H_4	H	96	10	2-naphthyl	OMe	95
5	3-$MeOC_6H_4$	H	98	11	3-$MeOC_6H_4$	F	98
6	2-naphthyl	H	98	12	2-naphthyl	F	98

13.2. SYNTHESIS OF TETRAHYDRO-1*H*-DIBENZO[*b*,*e*][1,4]DIAZEPINE

The synthetic utility of the catalyst was also investigated in the synthesis of benzodiazepine derivatives **74** *via* a one-pot, three-component reaction of *o*-phenylenediamine **73**, dimedone **33**, and different aldehydes **5** at room temperature (Scheme 43, Table 25).[81]

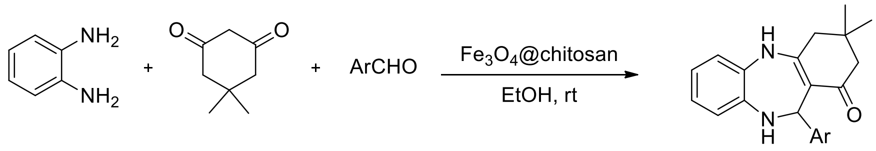

73 **33** **5** **74**

Scheme 43

Table 25. Synthesis of benzodiazepine derivatives **74**

Entry	Ar	Yield (%)	Entry	Ar	Yield (%)
1	4-$O_2NC_6H_4$	94	7	2-HOC_6H_4	85
2	3-$O_2NC_6H_4$	89	8	4-MeC_6H_4	91
3	4-ClC_6H_4	91	9	4-$Me_2NC_6H_4$	94
4	2-ClC_6H_4	90	10	2-thienyl	85
5	2,4-$Cl_2C_6H_3$	96	11	2-furyl	87
6	4-HOC_6H_4	88	12	2-pyridyl	84

Different catalytic amounts of Fe_3O_4@chitosan were applied at ambient temperature in EtOH as a green solvent. It was found that 0.03 g of the catalyst catalyzed efficiently the reaction and the corresponding product was obtained in high yield and in a short reaction time and increasing or reducing the amount of the catalyst did not improve the reaction yield. After completion of the reaction, the nanocatalyst was separated from the reaction mixture by using an external magnet, washed with acetone or ethanol, dried, and then used in subsequent reactions at least five times without any significant loss in its catalytic efficiency.

The proposed mechanism for the reaction is shown in Scheme 44. Initially, the intermolecular imine formation from *o*-phenylenediamine (OPDA) and dimedone promoted by the Fe_3O_4@chitosan catalyst occurs. The oxygen atoms of dimedone interact *via* lone pairs of electrons with the active sites of the catalyst surface, and the amino groups of OPDA attack the carbonyl group of dimedone with elimination of H_2O leading to imine intermediate. A 1,3-hydrogen shift, then results in isomeric (tautomerized) enamine. After this step, the other amino group of the OPDA part of enamine attacks the carbonyl group of aldehyde, which is itself activated by the catalyst to form enamine intermediate. Finally, the seven-membered ring products are afforded *via* intramolecular cyclization of enamine intermediate.

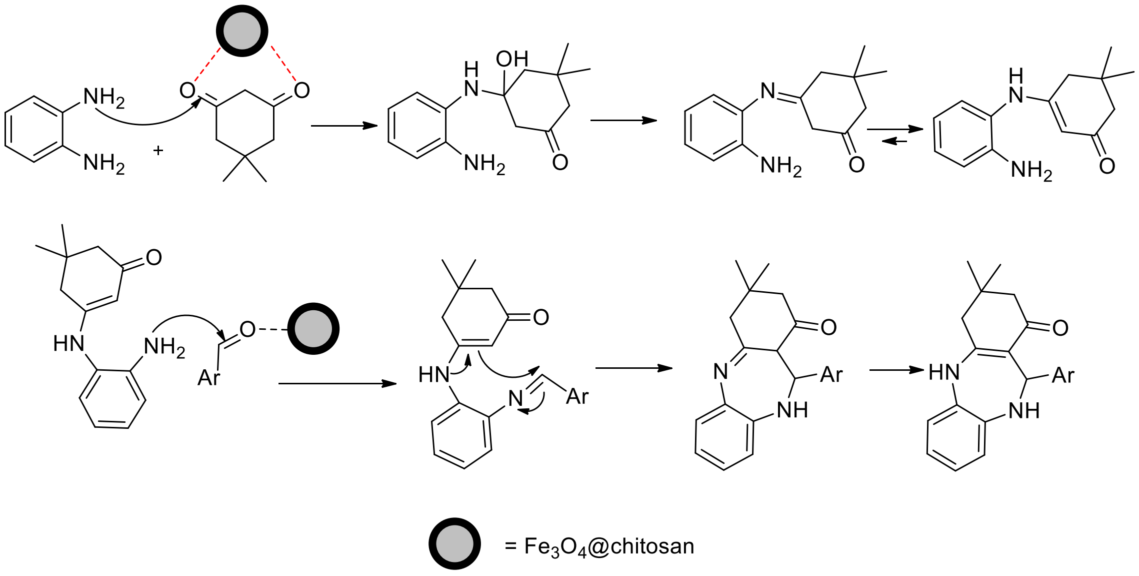

Scheme 44

14. Fe_3O_4@CS-SO_3H NPs

Mohammad and Kassaee reported the synthesis of sulfochitosan-coated Fe_3O_4 magnetic nanoparticles (Fe_3O_4@CS-SO_3H NPs) as outlined in Scheme 45. Thus, Fe_3O_4 nanoparticles were firstly prepared by a chemical co-precipitation of Fe^{3+} and Fe^{2+} ions with molar ratio of 2:1, in the presence of chitosan, followed by the hydrothermal treatment. Consequently, NH_4OH is injected dropwise into the reaction mixture with constant stirring. After 30 min, the mixture is cooled to room temperature and chitosan coated over magnetic nanoparticles are separated by an external magnet. Fe_3O_4@CS NPs is dispersed in dry CH_2Cl_2 in an ultrasonic bath, then chlorosulfonic acid is added. Finally, functionalized magnetic Fe_3O_4@CS-SO_3H NPs are separated by an external magnet.

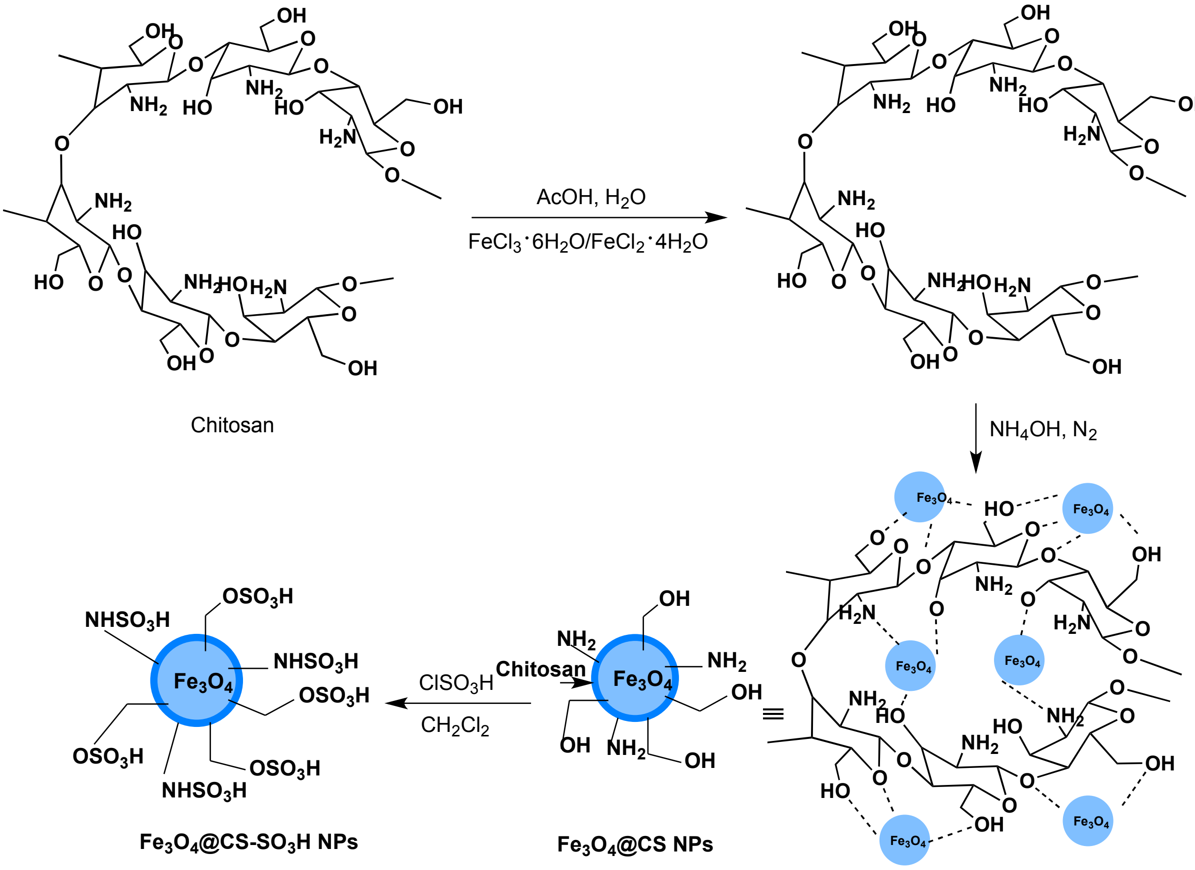

Scheme 45

14.1. SYNTHESIS OF 4*H*-CHROMENE

The catalyst was successfully used for preparation of 2-amino-4*H*-chromen-4-yl phosphonates **76** through one-pot, three-component reactions of salicylaldehydes **75**, malononitrile **28**, and triethyl phosphite in water at room temperature (Scheme 46, Table 26).[82]

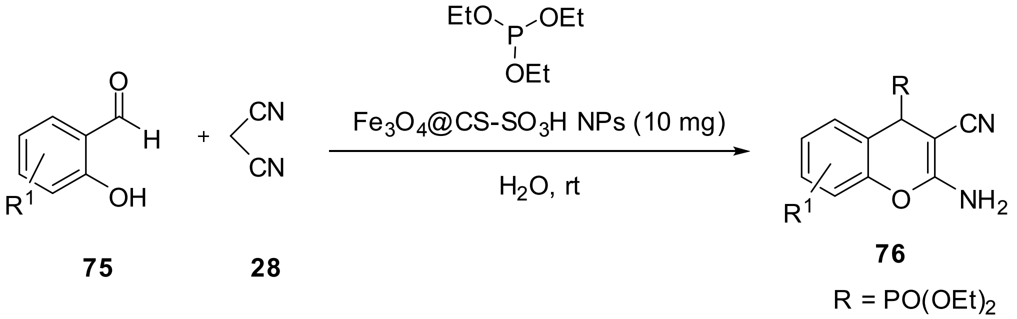

Scheme 46

Table 26. Preparation of 2-amino-4*H*-chromen-4-yl phosphonates **76**

Entry	R^1	Yield (%)	Entry	R^1	Yield (%)
1	H	93	6	7-MeO	93
2	6-Cl	96	7	6,8-Br_2	97
3	6-O_2N	92	8	6,8-Br_2	94
4	6-Me	95	9	6-MeO	88
5	6-Br	97			

The authors reported that in the absence of the catalyst no product was produced and the use of just 10 mg of Fe_3O_4@CS-SO_3H NPs was found to be sufficient to push the reaction forward. Moreover, the recovered catalyst is recycled in subsequent runs without any significant loss of its activity.

15. Fe_3O_4@SiO_2 NANOPARTICLES

Wang *et al*. prepared Fe_3O_4@SiO_2 nanoparticle which consists of Fe_3O_4 spheres as the core and SiO_2 as an outer shell, by a simple, low cost, and convenient method.[83] Fe_3O_4 nanoparticles were synthesized by the co-precipitation of ferric nitrate and ferrous sulphate in ammonia solution. To improve the chemical stability of Fe_3O_4 nanoparticles, their surface modification was successfully performed by the suitable deposition of silica on to the Fe_3O_4 nanoparticles by the ammonia-catalyzed hydrolysis of tetraethylorthosilicate (TEOS) (Scheme 47).

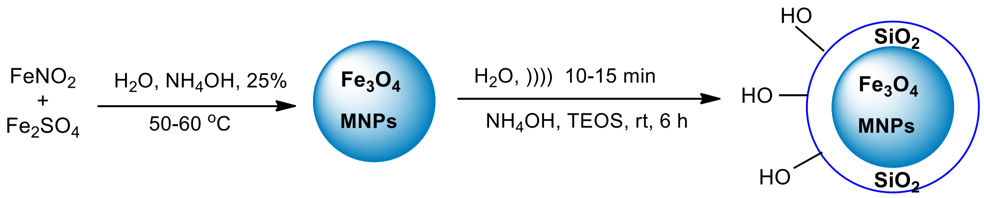

Scheme 47

15.1. SYNTHESIS OF DECAHYDROACRIDINE

Dam *et al*. used Fe_3O_4@SiO_2 nanoparticles as a recyclable heterogeneous catalyst for the synthesis of decahydroacridine derivatives **56** *via* a one-pot multi-component condensation of dimedone **33**, aldehydes **5**, and ammonium acetate in water (Scheme 48, Table 27).[84]

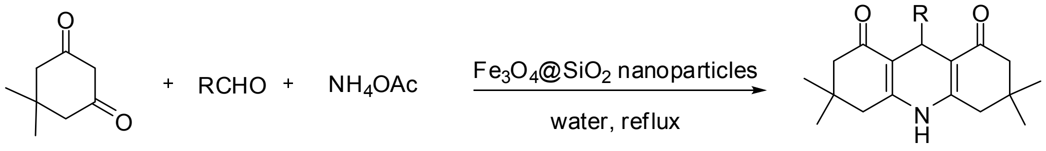

33 **5** **56**

Scheme 48

Table 27. Synthesis of decahydroacridine derivatives **56**

Entry	R	Yield (%)	Entry	R	Yield (%)
1	4-ClC_6H_4	92	5	2-$O_2NC_6H_4$	94
2	4-BrC_6H_4	89	6	2-ClC_6H_4	90
3	4-NCC_6H_4	93	7	4-$MeOC_6H_4$	85
4	4-$O_2NC_6H_4$	95	8	4-MeC_6H_4	82

In addition to the advantage of using water as a green solvent, the nanoparticles were separated by using an external magnet and can be reused for five times and give the products in good yields. It was observed that 10 mol% was chosen as the optimum catalyst concentration. No desired product was formed even after 5 h of stirring at room temperature. The desired product, proportionally increased with temperature and maximum yield was obtained under refluxing conditions. The nature and position of substitution in the aromatic ring did not affect the reactions much. The reaction was tried with aliphatic aldehydes, ketones, and furfuraldehyde but no desired products were formed even after 5 h of refluxing.

A plausible mechanism for the synthesis of 1,4-dihydropyridines (1,4-DHPs) by using Fe_3O_4@SiO_2 is shown in Scheme 49. First, the nanoparticles bind with oxygen of carbonyl group, hence it increases the carbonyl activity which in turn makes alpha hydrogen very acidic thereby facilitating the enolization and nucleophilic attack to the aromatic aldehydes leading to the formation of Knoevenagel product. The Knoevenagel product reacts then in Michael fashion with another molecule of C–H activated molecule to furnish the corresponding bis-intermediate. Ammonia then induced cyclization to offer the desired product.

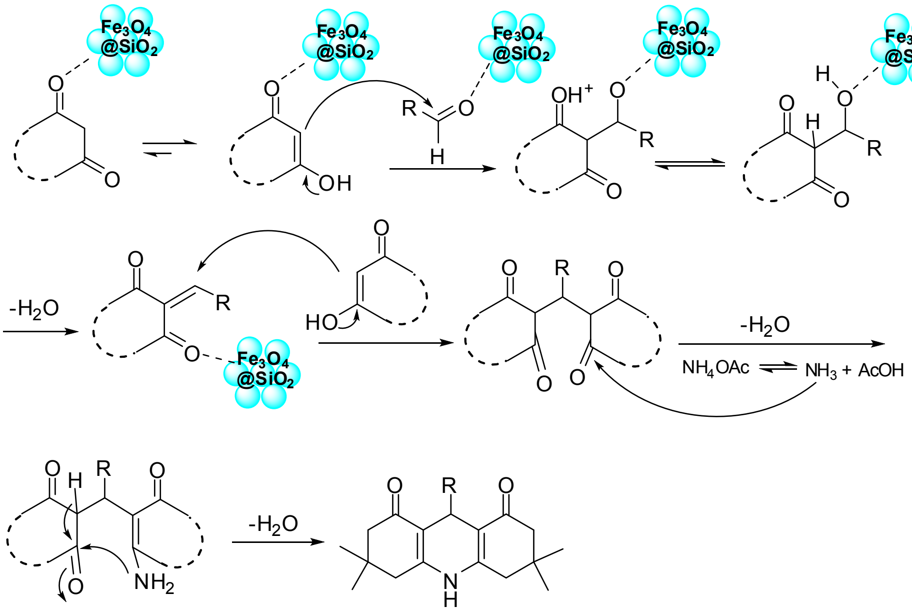

Scheme 49

15.2. SYNTHESIS OF DICHROMENO[4,3-*b*:3',4'-*e*]PYRIDINE

Dam *et al.* reported an efficient, high yielding method for the synthesis of dichromeno[4,3-*b*:3',4'-*e*]pyridine derivatives **77** *via* a one-pot multi-component condensation of 4-hydroxycoumarine **46**, aldehydes **5**, and ammonium acetate in water using Fe_3O_4@SiO_2 nanoparticles as a recyclable heterogeneous catalyst (Scheme 50, Table 28).[84]

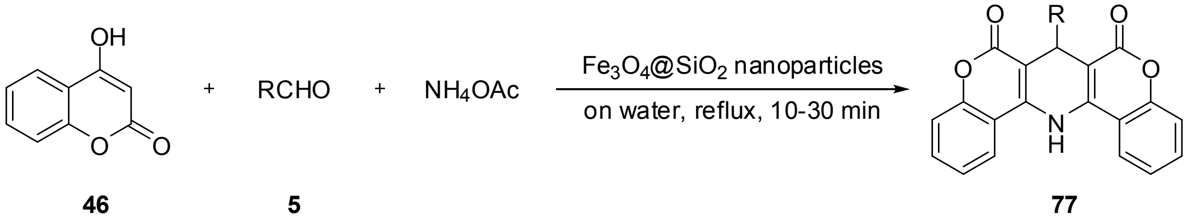

Scheme 50

Table 28. Synthesis of dichromeno[4,3-*b*:3',4'-*e*]pyridine derivatives **77**

Entry	Ar	Yield (%)	Entry	Ar	Yield (%)
1	4-ClC$_6$H$_4$	88	5	2-ClC$_6$H$_4$	88
2	4-BrC$_6$H$_4$	86	6	2-BrC$_6$H$_4$	88
3	4-NCC$_6$H$_4$	90	7	4-MeC$_6$H$_4$	82
4	4-FC$_6$H$_4$	87			

16. NANO-Fe_3O_4–$KHSO_4 \cdot SiO_2$

Magnetic nano-Fe_3O_4–$KHSO_4 \cdot SiO_2$ was prepared by soaking a saturated solution of $KHSO_4$ in distilled water in silica gel. The soaked mixture was thoroughly mixed and dried at 150 °C.[85]

16.1. SYNTHESIS OF IMIDAZO[1,2-*a*]PYRIDINE

Guntreddi *et al.* demonstrated the use of magnetic nano-Fe_3O_4–$KHSO_4 \cdot SiO_2$ as an efficient catalyst for the synthesis of imidazo[1,2-*a*]pyridines **79** through a one pot three-component reaction of 2-aminopyridine **78**, aldehyde **5**, and alkyne **22** (Scheme 51, Table 29).[86]

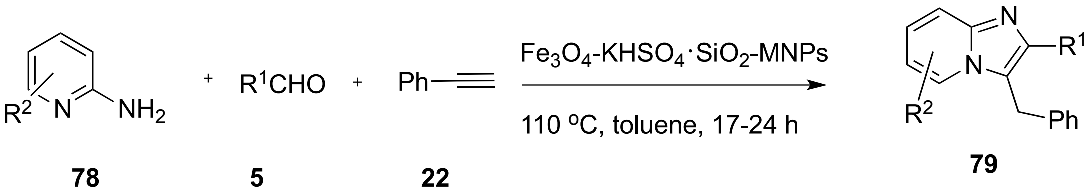

Scheme 51

Table 29. Synthesis of imidazo[1,2-*a*]pyridines **79**

Entry	R^1	R^2	Yield (%)	Entry	R^1	R^2	Yield (%)
1	H	C_6H_5	89	8	H	4-$Me_2NC_6H_4$	-
2	H	4-ClC_6H_4	86	9	H	4-MeC_6H_4	79
3	H	3-ClC_6H_4	84	10	H	4-$O_2NC_6H_4$	69
4	H	4-BrC_6H_4	83	11	H	2-$O_2NC_6H_4$	65
5	H	3-BrC_6H_4	82	12	H	Et	70
6	H	2-BrC_6H_4	83	13	H	2-furyl	72
7	H	4-$MeOC_6H_4$	75	14	H	3-MeO-4-OHC_6H_4	55

Nano-Fe_3O_4 (10 mol%) notably gave the product in moderate yield. A further increase in the catalyst mol% did not improve the yield. The amino–imino tautomerism in 2-aminopyridine and the soft acidic centers of nano-iron did not appear to favor formation of imine, which may be the reason for low yields obtained in the presence of nano-Fe_3O_4 alone. The use of additives and solvents, which conclusively provided Fe_3O_4–$KHSO_4 \cdot SiO_2$ in toluene as the best combination improved the yield. The $KHSO_4 \cdot SiO_2$ additive is assumed to promote the formation of imine considerably to facilitate a nucleophilic attack of the C–H activated phenylacetylene to the intermediate imine. The propargylamine, thus formed, subsequently underwent nano-Fe_3O_4 catalyzed 5-*exo*-dig cyclization. Other additives such as *L*-proline, K-10, and P_2O_8 did not improve the yield.

17. NANO-Fe_3O_4 SUPPORTED SILICA SULFURIC ACID

The magnetic nanoparticles supported silica sulfuric acid ($Fe_3O_4@SiO_2$–SO_3H) was prepared by addition of chlorosulfonic acid to a cooled solution of $Fe_3O_4@SiO_2$. Subsequent separation of the resulted MNPs by an external magnet, washing with methanol and drying give $Fe_3O_4@SiO_2$-SO_3H as a brown powder (Scheme 52).[88] Nano-$Fe_3O_4@SiO_2$ was synthesized according to a previously published literature method.[89]

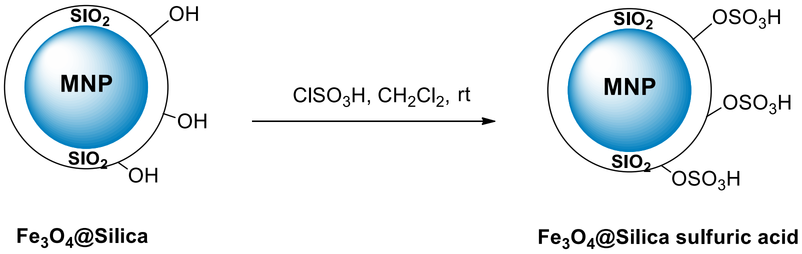

Scheme 52

17.1. SYNTHESIS OF PYRIDO[2,3-*d*]PYRIMIDINE

$Fe_3O_4@SiO_2$-SO_3H nanoparticles were used as an efficient catalyst for the synthesis of pyrido[2,3-*d*]pyrimidines **80a,b**. The reaction of 6-amino-1,3-dimethyluracil **40** with ethyl acetoacetate **4** and various substituent benzaldehydes **5** in water in the presence of 0.02 g of the catalyst afforded the target compounds **80a,b** in excellent yields irrespective of the presence of an electron withdrawing or releasing substituent (Scheme 53). The catalyst was readily recovered using an external magnet and could be reused several times without significant loss of reactivity.[87] The proficient catalytic activity of Fe_3O_4@SiO_2–SO_3H was related to the –SO_3H groups of the catalyst, which could provide efficient acidic sites. Although various solvents were also screened, product yields were found to be improved with water.

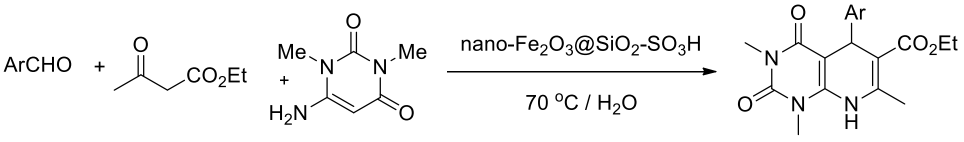

5 **4** **40** **80a,b**

Product	Ar	Yield (%)
80a	Ph	92
80b	4-$MeOC_6H_4$	87

Scheme 53

17.2. SYNTHESIS OF PYRAZOLO[2,1-*b*]PHTHALAZINE

The Fe_3O_4@silica sulfuric acid was also proved to be an effective catalyst in the synthesis of 1*H*-pyrazolo[1,2-*b*]phthalazine-5,10-dione derivatives **82**. The reaction proceeded *via* a one-pot three-components condensation reaction of phthalhydrazide **81**, aromatic aldehydes **5** and cyclic or acyclic 1,3-diketones **4** under solvent free conditions (Scheme 54, Table 30).[90] The catalyst was easily separated from the product by an external magnet and can be reused in subsequent reactions for six consecutive runs.

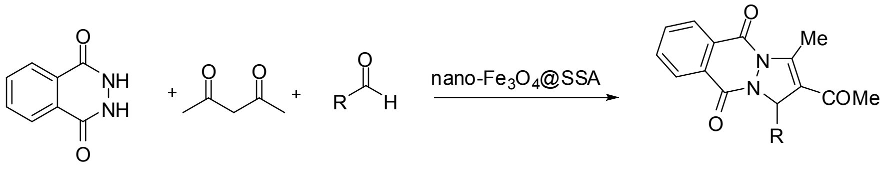

81 **4** **5** **82**

Scheme 54

Table 30. Synthesis of 2*H*-pyrazolo[2,1-*b*]phthalazinedione derivatives **82**

Entry	R	Yield (%)
1	C_6H_5	85
2	4-$O_2NC_6H_4$	88
3	4-NCC_6H_4	87
4	4-ClC_6H_4	84

17.3. SYNTHESIS OF TETRAHYDROPYRIMIDO[4,5-*b*]QUINOLINE

Nemati and Saeedirad reported the synthesis of pyrimido[4,5-*b*]quinolines **83** by using magnetic nanoparticles supported silica sulfuric acid (Fe_3O_4@SiO_2–SO_3H) as an efficient catalyst for the three-component reaction of 6-amino-1,3-dimethyluracil **40** with dimedone **33** and various substituent benzaldehydes **5** in water (Scheme 55, Table 31).[87] The desired products were obtained in excellent yields irrespective of the electron-releasing or electron-withdrawing nature of the substituent of the phenyl ring. The catalyst was readily recovered using an external magnet and could be reused several times without significant loss of reactivity.

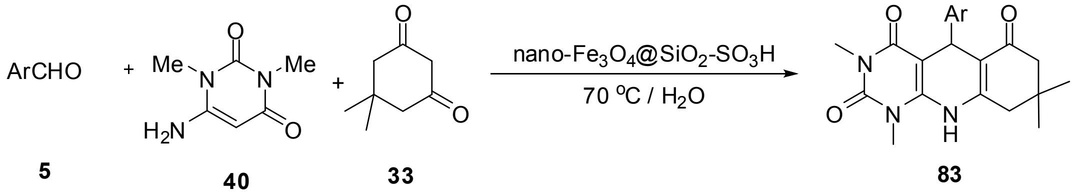

Scheme 55

Table 31. Synthesis of pyrimido[4,5-*b*]quinolines **83**

Entry	Ar	Time (min)	Yield (%)	Entry	Ar	Time (min)	Yield (%)
1	Ph	30	92	6	2-ClC_6H_4	35	81
2	4-$MeOC_6H_4$	40	86	7	4-ClC_6H_4	25	92
3	3-BrC_6H_4	35	90	8	4-FC_6H_4	30	89
4	4-$O_2NC_6H_4$	25	92	9	2-thiophene	35	87
5	3-$O_2NC_6H_4$	30	90				

17.4. SYNTHESIS OF PYRIMIDO[5',4':5,6]PYRIDO[2,3-*d*]PYRIMIDINE

The magnetic nanoparticles supported silica sulfuric acid (Fe_3O_4@SiO_2–SO_3H) was also successfully used as an efficient catalyst for the synthesis of pyrimido[5',4':5,6]pyrido[2,3-*d*]pyrimidine **84** by reacting 6-amino-1,3-dimethyl uracil **40** with 4-methylbenzaldehyde **5** in water (Scheme 56).[87]

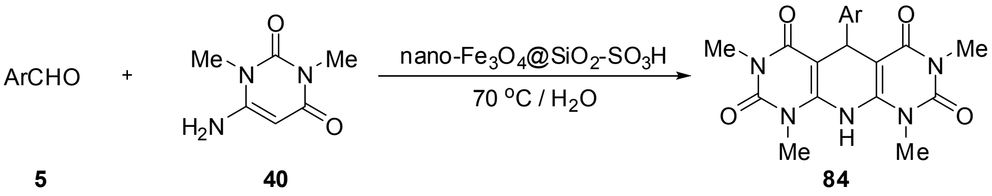

Ar = 4-MeC_6H_4, Yield = 95%

Scheme 56

17.5. SYNTHESIS OF DIHYDRO-2*H*-INDAZOLO[2,1-*b*]PHTHALAZINE

Kiasat and Davarpanah reported also the use of Fe_3O_4@silica sulfuric acid as a catalyst for the synthesis of 2*H*-indazolo[2,1-*b*]phthalazine-1,6,11-trione derivatives **85** *via* a one-pot three component reaction of phthalazine **81**, cyclic diketones **33** and the appropriate aromatic aldehydes **5**. (Scheme 57, Table 32).[90]

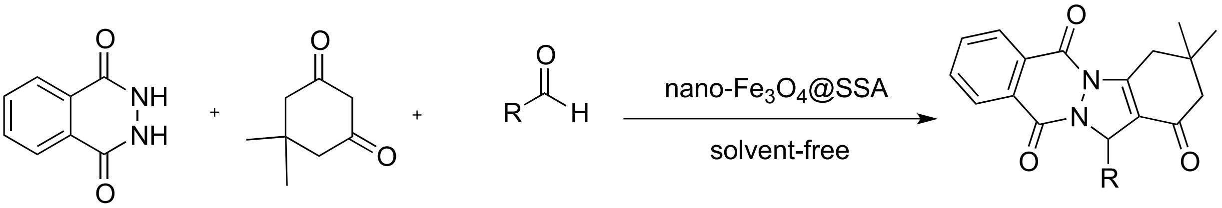

81 **33** **5** **85**

Scheme 57

Table 32. Synthesis of 2*H*-indazolo[2,1-*b*]phthalazine-1,6,11-trione derivatives **73**

Entry	R	Yield (%)	Entry	R	Yield (%)
1	C_6H_5	88	7	3-ClC_6H_4	90
2	4-ClC_6H_4	90	8	3-MeC_6H_4	88
3	4-$O_2NC_6H_4$	94	9	4-MeC_6H_4	86
4	4-HOC_6H_4	85	10	4-$MeOC_6H_4$	85
5	4-NCC_6H_4	92	11	2-$O_2NC_6H_4$	90
6	3-FC_6H_4	90			

17.6. SYNTHESIS OF INDENO[2',1':5,6]PYRIDO[2,3-*d*]PYRIMIDINE

Nemati and Saeedirad also used $Fe_3O_4@SiO_2–SO_3H$) as an efficient catalyst for the synthesis of indeno[2',1':5,6]pyrido[2,3-*d*]pyrimidine **86a,b**. The reaction proceeded by the reaction of 6-amino-1,3-dimethyluracil **40** with 1,3-indandione **58** and various substituted benzaldehydes **5** in water (Scheme 58).[87]

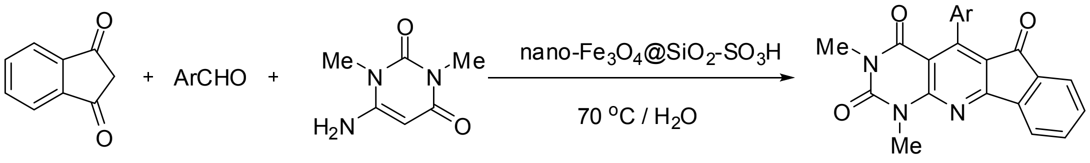

58 **5** **40** **86a-b**

Ar = C_6H_5, yield = 90%

Ar = 4-$O_2NC_6H_4$, yield = 94%

Scheme 58

18. Fe_3O_4 NANOPARTICLES COATED BY (3-AMINOPROPYL)-TRIETHOXYSILANE

Fe_3O_4–MNPs were firstly prepared through chemical coprecipitation method, and were subsequently coated with (3-aminopropyl)triethoxysilane (APTES) to achieve aminofunctionalized magnetic nanoparticles (Scheme 59).[91]

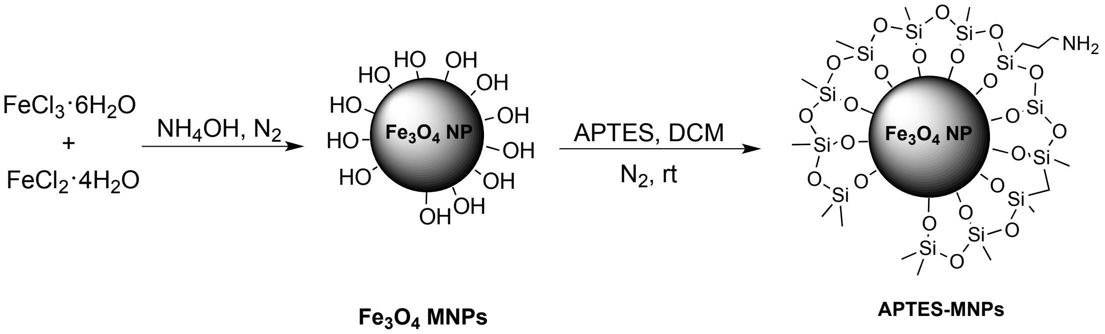

Scheme 59

18.1. SYNTHESIS OF PYRAZOLO[1,2-*a*][1,2,4]TRIAZOLE

Shaterian and Moradi reported the synthesis of 7-amino-1,3-dioxo-1,2,3,5-tetrahydropyrazolo[1,2-*a*][1,2,4]triazole derivatives **88** by employing magnetic Fe_3O_4 nanoparticles coated by (3-aminopropyl)triethoxysilane (APTES–MNPs) as a catalyst for the three-component reaction of aromatic aldehydes **5**, malononitrile **28**, and 4-aryltriazoles **87** under solvent-free conditions (Scheme 60, Table 33).[92]

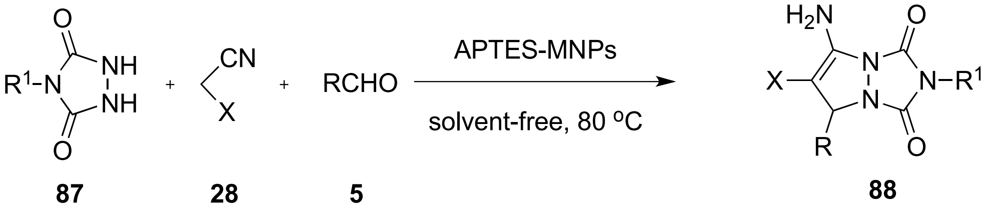

Scheme 60

Table 33. Synthesis of pyrazolo[1,2-*a*][1,2,4]triazole-1,3-dione derivatives **88**

Entry	R	X	R^1	Yield (%)	Entry	R	X	R^1	Yield (%)
1	C_6H_5	CN	C_6H_5	92	8	$2,4\text{-}Cl_2C_6H_3$	CN	C_6H_5	90
2	$4\text{-}ClC_6H_4$	CN	C_6H_5	90	9	$3\text{-}O_2NC_6H_4$	CN	C_6H_5	90
3	$4\text{-}FC_6H_4$	CN	C_6H_5	92	10	$4\text{-}MeC_6H_4$	CN	C_6H_5	89
4	$2\text{-}ClC_6H_4$	CN	C_6H_5	88	11	$3\text{-}BrC_6H_4$	CN	C_6H_5	93
5	$3\text{-}ClC_6H_4$	CN	C_6H_5	94	12	$2\text{-}BrC_6H_4$	CN	C_6H_5	92
6	$2\text{-}O_2NC_6H_4$	CN	C_6H_5	88	13	$4\text{-}BrC_6H_4$	CN	C_6H_5	89
7	$4\text{-}O_2NC_6H_4$	CN	C_6H_5	89	14	*n*-heptanal	CN	C_6H_5	-

The reaction was carried out with different amounts of APTES–MNPs (5, 7, 10, 20, 25 mol%) and at various temperatures (25, 50, 80 °C). The results showed that 7 mol% of APTES–MNPs at 80 °C achieved the best results. The catalyst was separated by an external magnet and can be reused several times without significant loss of its catalytic activity

18.2. SYNTHESIS OF 1*H*-PYRAZOLO[1,2-*b*]PHTHALAZINE

Shaterian and Mohammadnia reported an efficient procedure for the preparation of 1*H*-pyrazolo[1,2-*b*]phthalazine-5,10-dione derivatives **90** by a four-component condensation reaction of hydrazine monohydrate **42**, phthalic anhydride **89**, malononitrile or ethyl cyanoacetate **28** and aromatic aldehydes **5** in the presence of magnetic Fe_3O_4 nanoparticles coated by (3-aminopropyl)triethoxysilane[22] as a catalyst under mild, ambient, and solvent-free conditions (Scheme 61, Table 34).[93] APTES-MNPs are a stable catalyst in reaction media and can be reused several times without significant loss of catalytic activity. Due to the high magnetization of the Fe_3O_4 core in the catalyst, it can be recovered by a simple external magnet. The Brønsted basic (–NH_2) functionalized Fe_3O_4 core plays a crucial catalytic role in the described transformation. The reaction was carried out with different amounts of APTES-MNPs and 10 mol% of APTES-MNPs was found to achieve the best results. The results showed that APTES-MNPs are the most efficient catalyst with respect to reaction times and in terms of yields in comparison with results reported in the literature in which *p*-toluenesulfonic acid (*p*-TSA) or triethylamine were used as a catalyst under ultrasound conditions or in the presence of 1-butyl-3-methylimidazolium hydroxide ([Bmim]OH).[94-96]

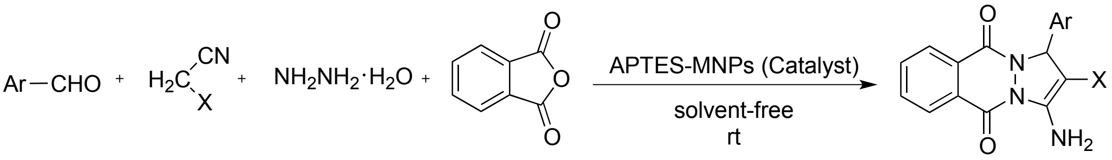

5 **28** **42** **89** **90**

Scheme 61

Table 34. Synthesis of 1*H*-pyrazolo[1,2-*b*]phthalazine-5,10-dione derivatives **90**

Entry	ArCHO	X	Time (min)	Yield (%)	Entry	ArCHO	X	Time (min)	Yield (%)
1	C_6H_5CHO	CN	19	92	15	2,4-$Cl_2C_6H_3CHO$	CN	15	91
2	2-ClC_6H_4CHO	CN	15	93	16	2,3-$Cl_2C_6H_3CHO$	CN	16	93
3	3-ClC_6H_4CHO	CN	16	90	17	2-$MeOC_6H_4CHO$	CN	14	90
4	4-ClC_6H_4CHO	CN	15	93	18	3-$MeOC_6H_4CHO$	CN	16	92
5	4-FC_6H_4CHO	CN	17	89	19	2,4,6-$(MeO)_3C_6H_2CHO$	CN	17	91
6	2-$O_2NC_6H_4CHO$	CN	14	91	20	2,6-$(MeO)_2C_6H_3CHO$	CN	16	93
7	4-BrC_6H_4CHO	CN	15	92	21	5-MeC_6H_4CHO	CN	16	92
8	3-BrC_6H_4CHO	CN	16	89	22	4-$F_3CC_6H_4CHO$	CN	16	90
9	3-ClC_6H_4CHO	CO_2Et	23	88	23	2,6-$Cl_2C_6H_3CHO$	CO_2Et	22	89
10	2-$O_2NC_6H_4CHO$	CO_2Et	21	89	24	2,4-$Cl_2C_6H_3CHO$	CO_2Et	21	88
11	3-$O_2NC_6H_4CHO$	CO_2Et	22	91	25	2,3-$Cl_2C_6H_3CHO$	CO_2Et	23	89
12	4-$O_2NC_6H_4CHO$	CO_2Et	21	89	26	2-$MeOC_6H_4CHO$	CO_2Et	22	90
13	4-BrC_6H_4CHO	CO_2Et	22	90	27	4-$F_3CC_6H_4CHO$	CO_2Et	22	89
14	2,6-$Cl_2C_6H_3CHO$	CN	14	92	28	*n*-heptanal	CN	10 h	Trace

19. Fe_3O_4 NANOPARTICLES COATED BY *N*-PROPYLSULFAMIC ACID

Magnetite nanoparticles (SA–MNPs) of 18–20 nm were prepared firstly by coprecipitation of iron(II) and iron(III) ions in basic solution using literature methods[97,98] and subsequently were coated with 3-aminopropyltriethoxysilane (APTES) to give aminofunctionalized magnetic nanoparticles. Finally, the reaction of amino groups with chlorosulfuric acid led to sulfamic acid-functionalized magnetic Fe_3O_4 nanoparticles (SA-MNPs).

19.1. SYNTHESIS OF IMIDAZOLE

Safari and Zarnegar synthesized trisubstituted imidazoles **56** in high yield in the presence of sulphamic acid functionalized magnetic Fe_3O_4 nanoparticles (SA–MNPs) as a solid acid catalyst.[99] The reaction proceeds *via* a three component reaction of benzil **52**, aromatic aldehyde **5** and ammonium acetate under solvent-free classical heating conditions or under microwave irradiation (Scheme 62, Table 35). Aldehydes carrying either electron-withdrawing or electron-donating groups perform equally well in the reaction and all imidazoles were obtained in high yields. Also, microwave irradiation achieved better yields in shorter reaction times. The efficiency of the reaction is mainly affected by the amount of catalyst and temperature. The best results have been obtained at 100 °C with an amount of 0.01 g SA–MNPs (equal to 0.012 mmol H^+), and the yield of reaction was not affected by an increase in the amount of SA–MNPs or temperature. The catalyst could be recovered easily and reused many times without significant loss of catalytic activity.[99]

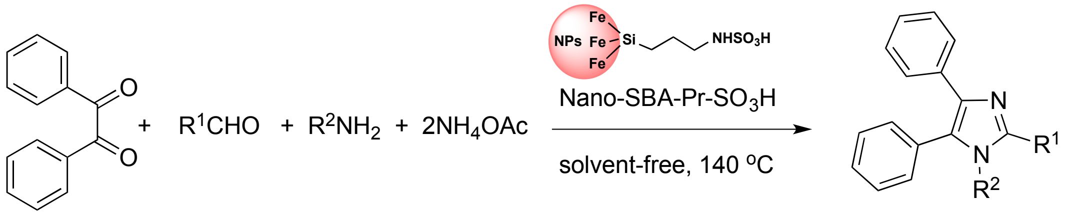

52 **5** **12** **53**

Scheme 62

Table 35. Synthesis of trisubstituted imidazoles **53**

Entry	R^1	R^2	Yield (%)	Entry	R^1	R^2	Yield (%)
1	C_6H_5	H	85 (96)	9	2-naphthyl	H	77(94)
2	4-MeC_6H_4	H	87 (99)	10	2,4-$Cl_2C_6H_3$	H	79(94)
3	3-MeC_6H_4	H	76(95)	11	2-thienyl	H	75(95)
4	4-MeC_6H_4	H	82(98)	12	3-$O_2NC_6H_4$	H	85(93)
5	4-ClC_6H_4	H	78(95)	13	4-$Me_2NC_6H_4$	H	77(96)
6	3-ClC_6H_4	H	83(95)	14	2-HOC_6H_4	H	85(93)
7	4-BrC_6H_4	H	88(93)	15	3-HOC_6H_4	H	90(93)
8	3-BrC_6H_4	H	78(95)				

*MW yields % were indicated between paranthes

19.2. SYNTHESIS OF DIHYDRO-2*H*-INDAZOLO[2,1-*b*]PHTHALAZINE

Rostami *et al.* also applied (MNPs-PSA) as an efficient and magnetically recoverable catalyst for the synthesis of 2*H*-Indazolo[2,1-*b*]phthalazine-1,6,11(13*H*)-triones **85** from a one-pot three-component reaction of phthalhydrazide **81**, cyclic diketones **33** and the appropriate aromatic aldehydes **5** (Scheme 63, Table 36).[100] The reaction was catalyzed by MNPs-SA or SA under solvent-free conditions at 100 °C. The effect of different amounts of MNPs-PSA or SA on the three-component reaction was studied and 30 mg of MNPs-SA or 10 mol% of SA was chosen for the desired reaction. Although both catalysts can catalyze the synthesis of 2*H*-indazolo[1,2-*b*]phthalazinetriones, the product separation and catalyst recycling are easier and simpler in the case of (MNPs-SA). The catalyst can be recycled and reused for 7 times with little loss of activity.

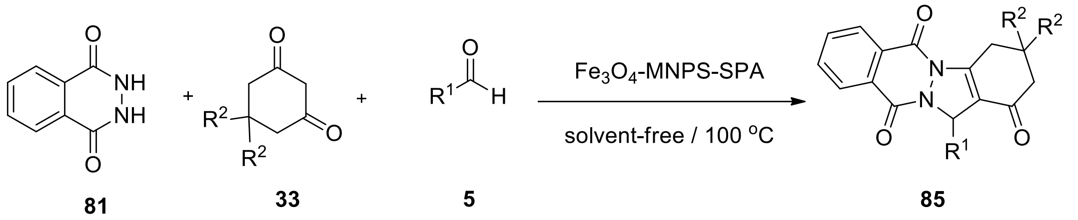

Scheme 63

Table 36. One-pot synthesis of 2*H*-indazolo[2,1-*b*]phthalazinetrione derivatives **85**

Entry	R^1	R^2	Yield (%)	Entry	R^1	R^2	Yield (%)
1	C_6H_5	Me	93	12	2-$O_2NC_6H_4$	Me	82
2	2-MeC_6H_4	Me	91	13	3-$O_2NC_6H_4$	Me	86
3	4-MeC_6H_4	Me	90	14	4-$O_2NC_6H_4$	Me	83
4	3-$MeOC_6H_4$	Me	87	15	2-naphthyl	Me	84
5	4-$MeOC_6H_4$	Me	89	16	C_6H_5	H	86
6	3,4-$(MeO)_2C_6H_3$	Me	88	17	4-Me	H	88
7	3-BrC_6H_4	Me	85	18	4-$MeOC_6H_4$	H	90
8	2-ClC_6H_4	Me	87	19	4-$O_2NC_6H_4$	H	83
9	4-ClC_6H_4	Me	93	20	4-FC_6H_4	H	89
10	2,4-$(Cl)_2C_6H_3$	Me	91	21	3-$HOCC_6H_4$	Me	80*
11	4-FC_6H_4	Me	90				

* the product was:

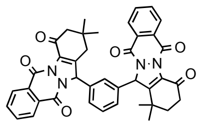

20. IONIC LIQUID SUPPORTED ON Fe_3O_4@SiO_2 NANOPARTICLES

A magnetically ionic liquid supported on Fe_3O_4@SiO_2 nanoparticles (MNPs@SiO_2-IL) was synthesized following the procedure shown in Scheme 2. These nanoparticles were easily prepared *via* the chemical co-precipitation of Fe^{2+} and Fe^{3+} ions in basic solution. These were subsequently coated with silica (Fe_3O_4@SiO_2) through the well-known Stober method.[101] 1-Methyl-3-(3-trimethoxysilylpropyl)-

imidazolium chloride (IL), was then prepared from the reaction of *N*-methylimidazole with (3-chloropropyl)trimethoxysilane.[102] Finally, the external surface of MNPs was coated with IL to give MNPs@SiO2-IL (Scheme 64).

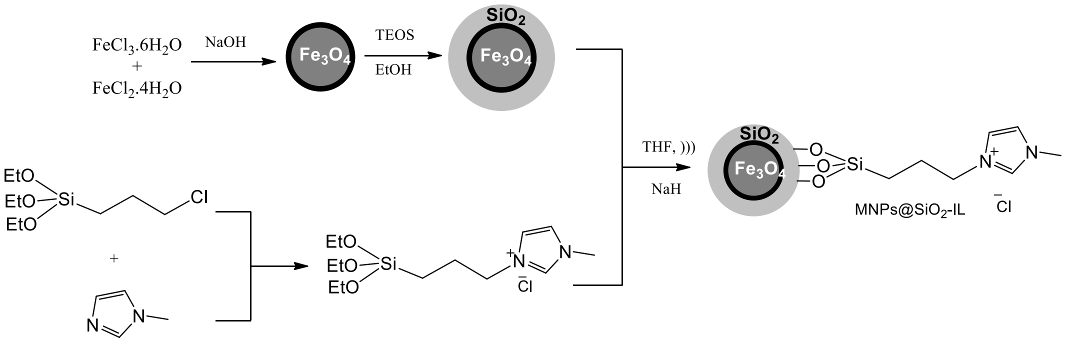

Scheme 64

20.1. SYNTHESIS OF THIAZOLE

The catalyst was evaluated as a recoverable catalyst for the one-pot synthesis of 1,3-thiazolidin-4-ones **92** in high to excellent yield by the three-component condensation of arylaldehydes **5**, anilines **12** and thioglycolic acid **91** under solvent-free conditions (Scheme 65, Table 37).[103]

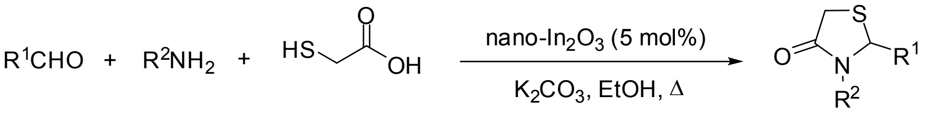

5 **12** **91** **92**

Scheme 65

Table 37. One-pot synthesis of 1,3-thiazolidin-4-ones **92**

Entry	R^1	R^2	Yield (%)	Entry	R^1	R^2	Yield (%)
1	C_6H_5	C_6H_5	94	6	4-MeC_6H_4	C_6H_5	88
2	C_6H_5	4-MeC_6H_4	90	7	4-ClC_6H_4	C_6H_5	95
3	C_6H_5	4-ClC_6H_4	90	8	4-$O_2NC_6H_4$	C_6H_5	92
4	C_6H_5	4-$O_2NC_6H_4$	86	9	4-$O_2NC_6H_4$	4-MeC_6H_4	90
5	4-MeC_6H_4	4-MeC_6H_4	93	10	3-$O_2NC_6H_4$	C_6H_5	89

A plausible mechanism for the formation of 1,3-thiazolidin-4-ones catalyzed by MNPs@SiO2-IL, is shown in Scheme 66. It can be speculated that the methylimidazolium cation [MIM]$^+$ in the MNPs@SiO2-IL interacts with the oxygen atom of the carbonyl group of the aldehyde and facilitates the formation of imine intermediate I. The free chloride ions interact then with thioglycolic acid proton and facilitate the attack of sulfur atom of thioglycolic acid to the activated imine group of intermediate I to afford intermediate II. Finally, the MNPs@SiO2-IL again activates the removal of water from intermediate II to give 1,3-thiazolidin-4-ones.

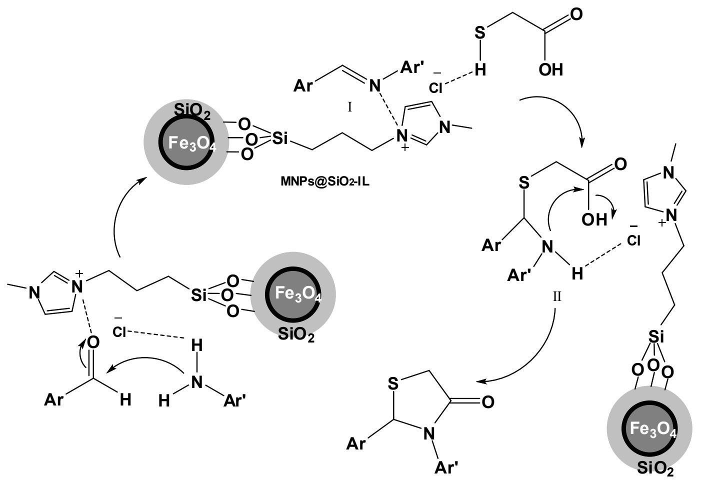

Scheme 66

21. MNPs–IIL–OAc AND MNPs–IIL–HSO$_4$

Fe$_3$O$_4$–MNPs were prepared as described in the literature using chemical coprecipitation technique.[104] Thus, 1-methyl-3-(3-trimethoxysilylpropyl)imidazolium chloride (IIL-Cl) was prepared from the reaction of *N*-methylimidazole with (3-chloropropyl)trimethoxysilane.[102] Chloride IL was then immobilized on MNPs (MNP–IIL–Cl) in deionized water and an excess amount of NaOAc (or KHSO$_4$) were added. NaCl, which was formed during the exchange of chloride anion, was removed by washing with deionized water. MNPs–IIL–OAc and MNPs–IIL–HSO$_4$ were obtained as a brownish black powder (Scheme 67).

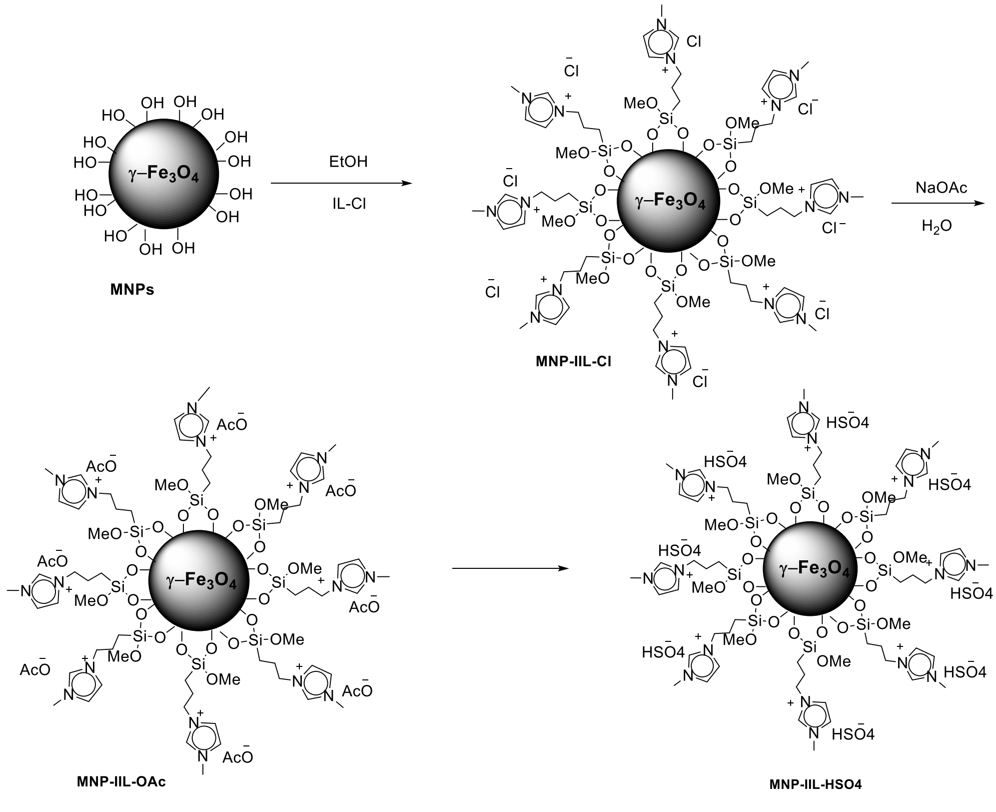

Scheme 67

21.1. SYNTHESIS OF DIHYDROPYRIMIDINE

Zarnegar and Safari used the magnetic Fe_3O_4 nanoparticles supported imidazolium-based ionic liquids (MNPs–IILs) as an efficient catalyst for the one-pot synthesis of 3,4-dihydropyrimidin-2(1*H*)-ones(thiones) **94**. The reaction proceeded *via* a Biginelli reaction of an aromatic aldehydes **5**, *β*-dicarbonyl compound **4**, urea or thiourea **93** in the presence of the magnetic nanocatalysts under microwave irradiation and solvent-free conditions (Scheme 68, Table 38).[105]

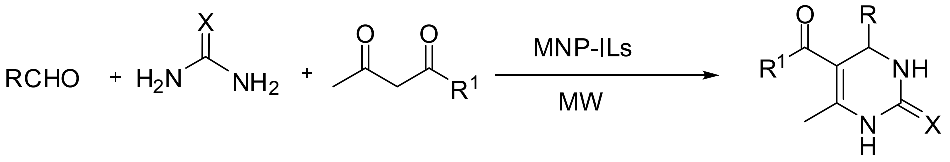

5 **93** **4** **94a-l**

Scheme 68

Table 38. One-pot synthesis of 3,4-dihydropyrimidin-2(1*H*)-ones(thiones) **94**

Entry	R	X	R^1	Time /Yield (%)		Entry	R	X	R^1	Time /Yield (%)	
				MW[a]	Δ [b]					MW[a]	Δ [b]
1	Ph	O	OEt	4/97	30/95	7	4-MeC_6H_4	S	OEt	4/95	40/90
2	3-ClC_6H_4	O	OEt	4/98	25/97	8	Ph	S	OEt	4/97	35/96
3	4-$O_2NC_6H_4$	O	OEt	4/98	30/97	9	2-thienyl	S	OEt	4/95	25/95
4	2-thienyl	O	OEt	4/98	25/98	10	Ph	O	Me	4/97	30/95
5	2-FC_6H_4	O	OEt	4/97	35/92	11	Ph	S	Me	4/96	30/93
6	3,4-$(OMe)_2C_6H_3$	O	OEt	4/99	20/98	12	4-MeC_6H_4	S	Me	4/95	35/92

[a] Using microwave irradiation
[b] Under classical heating conditions

MNPs–IILs as a Brønsted acidic catalyst can participate in the reaction by activating the aldehyde for the nucleophilic addition of urea or thiourea. The reaction was evaluated by using various amounts of catalyst and temperature and the best result was obtained with an amount of 0.02 g MNP–IIL–HSO4 at 90 °C. Among other employed catalysts, the MNPs–IIL–HSO_4 was found to exhibit the highest catalytic activity with respect to reaction times and yields of the products. This may be attributed to the strength of anion–cation interaction inside the IILs by the less electrostatic interaction between the hydrogen sulfate anion and the cation.[106,107] The catalyst was found to be easily separated from the reaction mixture using a normal magnet. Moreover, it can be recycled in subsequent experiments (up to six cycles) under similar reaction conditions without any further treatment.

22. NANO Fe_3O_4 BASED ON A BIIMIDAZOLE Cu(I) COMPLEX

Tajbakhsh *et al.* synthesized a magnetically recoverable nano-catalyst based on a biimidazole Cu(I) complex by covalent grafting of biimidazole on chloride-functionalized silica@magnetite nanoparticles, followed by metalation with CuI.[108] At first, magnetite nanoparticles were synthesized by a typical chemical co-precipitation of $FeCl_3$ and $FeCl_2$ in an ammonia solution. The surface of the magnetite NPs was successfully coated by silica. Next, MNP@SiO_2 was functionalized with (3-chloropropyl)triethoxysilane (CPTES), afterward, biimidazole, was immobilized on MNP@CPS, then CuI was anchored on the functionalized beads to obtain a final heterogenous catalyst (Scheme 69).

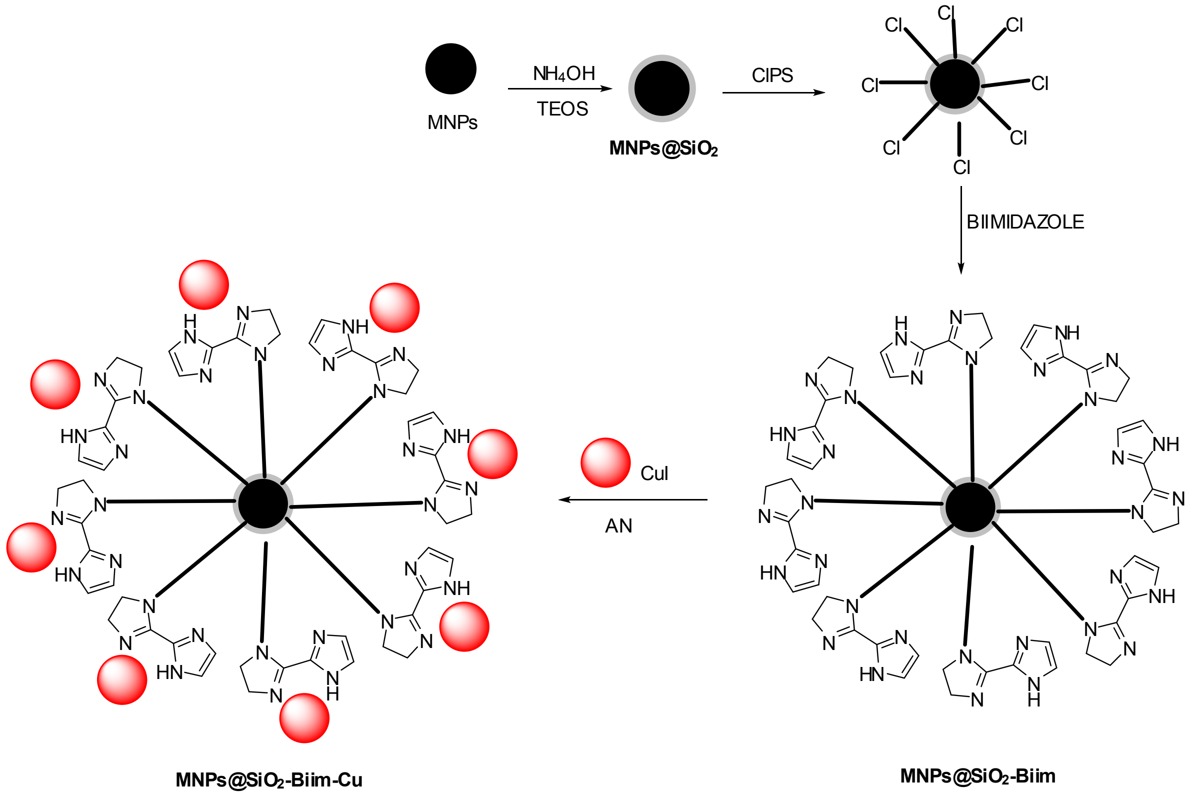

Scheme 69

22.1. SYNTHESIS OF IMIDAZO[1,2-*a*]PYRIDINE

The prepared nanocatalyst was also shown to have excellent and green catalytic activity in the synthesis of imidazo[1,2-*a*]pyridines **79** *via* a one-pot reaction of 2-aminopyridines **12**, aldehydes **5** and phenylacetylene **22** in aqueous media (Scheme 70, Table 39).[108] Aromatic and hetero aromatic aldehydes tolerated well in this reaction. Appreciable lower yields were obtained for aliphatic aldehydes which might be due to their low boiling-point.[109] It is worth that the catalyst is stable and is easily recovered by magnet. In addition, it can be reused without any significant loss of its activity after at least 10 successive runs.

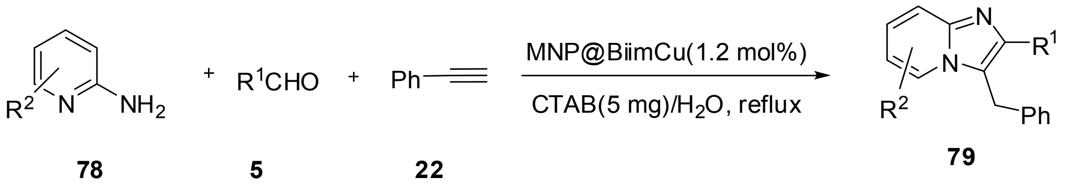

Scheme 70

Table 39. Synthesis of imidazo[1,2-*a*]pyridines **79**

Entry	R^1	R^2	Yield (%)	Entry	R^1	R^2	Yield (%)
1	H	4-ClC$_6$H$_4$	90	10	H	2-ClC$_6$H$_4$	87
2	H	C$_6$H$_5$	92	11	H	3-BrC$_6$H$_4$	82
3	H	4-MeOC$_6$H$_4$	85	12	H	3-ClC$_6$H$_4$	85
4	H	4-BrC$_6$H$_4$	90	13	H	1-naphthyl	78
5	H	4-MeC$_6$H$_4$	78	14	H	2-furyl	90
6	H	4-NCC$_6$H$_4$	95	15	H	^{n}Pr	65
7	H	4-F$_3$CC$_6$H$_4$	90	16	H	^{i}Pr	76
8	H	4-FC$_6$H$_4$	95	17	3-Me	C$_6$H$_5$	82
9	H	2-MeC$_6$H$_4$	80	18	3-Me	C$_6$H$_5$	78

23. NANOMAGNETIC ORGANIC-INORGANIC HYBRID PREYSSLER HPA (Fe@Si-Gu-Prs)

Eshghi *et al*. prepared a nanomagnetic organic-inorganic hybrid catalyst (Fe@Si-Gu-Prs) by the concise route outlined in Scheme 71.[110] Thus, Fe_3O_4 magnetic nanoparticles were prepared *via* a chemical method, and subsequently were modified with (3-chloropropyl)trimethoxysilane and guanidine hydrochloride to achieve functionalized silica Fe_3O_4 nanoparticles (Fe@Si-Gu). Ultimately, the Preyssler heteropoly acid HPA ($H_{14}[NaP_5W_{30}O_{110}]$) was immobilized onto the modified silica MNPs *via* non-covalent interactions, leading to the formation of the nanomagnetic organic-inorganic hybrid catalyst (Fe@Si-Gu-Prs).

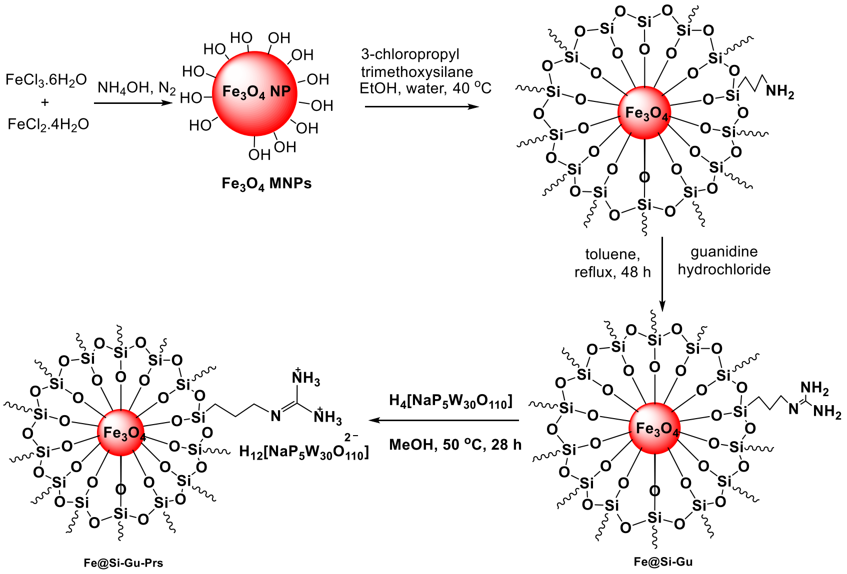

Scheme 71

23.1. SYNTHESIS OF TETRAHYDROPYRIDINE

The catalytic activity of this catalyst in the synthesis of tetrahydropyridine **95** was investigated. Thus, the reaction of aldehydes **5**, amines **12**, and ethyl acetoacetate **4** using 0.025 g Fe@Si-GuPrs at room temperature and under solvent-free conditions afforded **95** in high yield (Scheme 72, Table 40). The results shown in Table 40 confirmed that aldehyde **5** and amine **12** with substituents carrying either electron donating or electron-withdrawing groups reacted successfully and gave the expected products in excellent yields in short reaction times.[110] The Fe@Si-Gu-Prs was separated from the reaction mixture by employing an external magnet and could be reused in a subsequent reaction to give excellent yields of the target products.

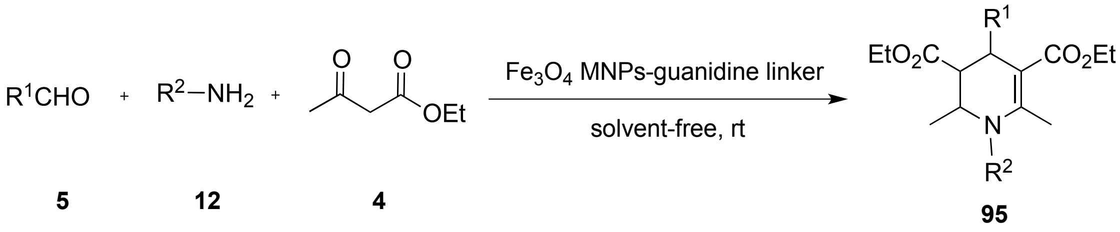

Scheme 72

Table 40. Synthesis of tetrahydropyridines **95**

Entry	R^1	R^2	Yield (%)	Entry	R^1	R^2	Yield (%)
1	C_6H_5	C_6H_5	96	12	4-$MeOC_6H_4$	4-ClC_6H_4	93
2	C_6H_5	4-BrC_6H_4	94	13	4-ClC_6H_4	4-BrC_6H_4	90
3	C_6H_5	4-ClC_6H_4	91	14	4-ClC_6H_4	4-MeC_6H_4	93
4	4-NCC_6H_4	C_6H_5	92	15	4-ClC_6H_4	C_6H_5	91
5	4-NCC_6H_4	4-ClC_6H_4	95	16	4-$MeOC_6H_4$	4-MeC_6H_4	92
6	4-MeC_6H_4	4-MeC_6H_4	95	17	4-$MeOC_6H_4$	C_6H_5	90
7	4-MeC_6H_4	C_6H_5	91	18	4-$MeOC_6H_4$	4-BrC_6H_4	94
8	4-MeC_6H_4	4-BrC_6H_4	92	19	C_6H_5	4-IC_6H_4	91
9	4-MeC_6H_4	4-$O_2NC_6H_4$	95	20	4-ClC_6H_4	4-BrC_6H_4	92
10	4-MeC_6H_4	4-MeC_6H_4	92	21	4-NCC_6H_4	4-BrC_6H_4	91
11	3-$O_2NC_6H_4$	C_6H_5	90				

24. BACTERIOGENIC IRON OXIDE (*L*-BIOX)

L-BIOX was obtained as an ocher precipitate either from an experimental fresh water purifying tank in Joyo, Japan (47 wt% of Fe) or an experimental water purifying tank in Okayama, Japan (48 wt% of Fe) and purified by following the reported procedure.[111] *L*-BIOX is an amorphous iron oxide in micro-tubular form that contains specific amounts of silicon, phosphorous (Fe:Si:P = 73:22:5, except oxygen), and additional organic compounds such as polysaccharides and proteins. L-BIOX was dried under reduced pressure at 100 °C before using as a catalyst.

24.1. SYNTHESIS OF 2*H*-PYRAN-2-ONE AND OXEPAN-2-ONE

L-BIOX could be used as an effective catalyst for Baeyer-Villiger oxidation with molecular oxygen in the presence of benzaldehyde at 25 °C (Scheme 73).[112] The catalyst showed superior catalytic activity compared to other iron compounds including commercially available α-Fe_2O_3, γ-Fe_2O_3,Fe_3O_4, and α-Fe. The *L*-BIOX-catalyzed oxidation proceeded efficiently even at ambient temperature and can be applied to a variety of substrates (Table 41).

The catalytic activity might depend on the presence of silicon and its amount in the amorphous oxide structure of *L*-BIOX. Thus, *L*-BIOX bearing an elemental composition of Fe: Si: P = 73: 22: 5 gave the best results compared with *L*-BIOX with Fe: Si: P = 78: 10: 12.

The used aldehydes also influence the reactivity of this reaction. While the reaction proceeded more efficiently with 3 equivalents of benzaldehyde, aliphatic aldehydes were found to be less effective.

Although the reaction was carried out in different solvents including, benzene, dichloromthane, 1,2-dichloroethane, toluene, tetrahydrofuran or *N,N*-dimethylformamide, the reaction was found to proceed more efficiently with benzene under milder conditions.

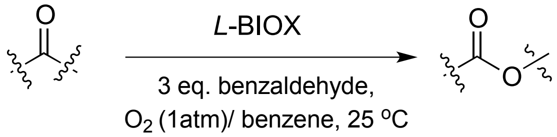

96 **97**

Scheme 73

Table 41. Baeyer-Villiger oxidation of various ketones with *L*-BIOX

Entry	**96**	**97**	Yield %	Entry	**96**	**97**	Yield %
1	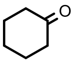	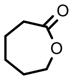	>98	4	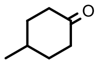	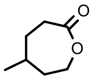	>98
2	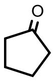	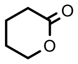	84	5	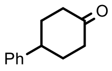	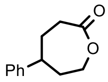	>98
3	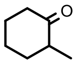	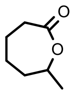	96	6	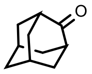	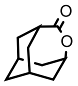	96

ACKNOWLEDGEMENTS

Prof. Dr. Ahmed H. M. Elwahy thanks the Alexander von Humboldt Foundation for a research fellowship. He is also greatly indebted to Prof. K. Hafner, University of Darmstadt for his continuous help and generous support.

REFERENCES

1. T. Eicher and S. Hauptmann, The Chemistry of Heterocycles: Structure, Reactions, Syntheses, and Applications. 2nd ed; Wiley-VCH, Verlag gmbh: Weinheim, 2003.

2. K. Nylund, P. Johansson, Z. Puterova, and A. Krutosikova, Heterocyclic Compounds: Synthesis, Properties and Applications, Nova Science Publishers, Hauppauge: New York, 2010.
3. A. R. Katritzky and C. W. Rees, Comprehensive Heterocyclic Chemistry I, Pergamon Press, Oxford, 1984; ed. by A. R. Katritzky, C. W. Rees, and F. V. Scriven; Comprehensive Heterocyclic Chemistry II, Pergamon Press, Oxford, 1996; A. R. Katritzky, C. A. Ramsden, E. F. V. Scriven, and R. J. K. Taylor, Comprehensive Heterocyclic Chemistry III, Elsevier, Amsterdam, 2008; A. R. Katritzky, C. A. Ramsden, J. A. Joule, and V. V. Zhdankin, Handbook of Heterocyclic Chemistry, 3rd ed, Elsevier: Amsterdam, 2010; ed. by A. R. Katritzky, Advances in Heterocyclic Chemistry, Elsevier, Amsterdam, 2010; A. T. Balaban, D. C. Oniciu, and A. R. Katritzky, *Chem. Rev.*, 2004, **104**, 2777.
4. A. Loupy, Microwaves in Organic Synthesis, 2002, Wiley-VCH, Weinheim; C. O. Kappe, *Angew. Chem. Int. Ed.*, 2004, **43**, 6250; C. O. Kappe and A. Stadler, Microwaves in Organic and Medicinal Chemistry, 2005, Wiley-VCH,Weinheim; J. P. Tierney and P. Lidström, Microwave-Assisted Organic Synthesis, 2005, Blackwell, Oxford; C. O. Kappe, D. Dallinger, and S. S. Murphree, Practical Microwave Synthesis for Organic Chemists-Stategies, Instruments, and Protocols, 2008, Wiley-VCH, Weinheim; C. O. Kappe, *Chem. Soc. Rev.*, 2008, **37**, 1127; W. Santagada, F. Frecentese, E. Perisutti, F. Fiorino, B. Severino, and G. Caliendo, *Mini Rev. Med. Chem.*, 2009, **9**, 340; C. O. Kappe and D. Dalinger, *Mol. Diversity*, 2009, **13**, 71; Microwave Heating as a Tool for Sustainable Chemistry, ed. by N. Leadbeater; 2010, CRC Press, Boca Raton, FL.
5. T. J. Mason and J. P. Lorimer, Sonochemistry, 1988 Ellis Horwood, Chichester; Synthetic Organic Sonochemistry, ed. by J. L. Luche, 1998, Plenum Press, New York. K. S. Suslick, in Handbook of Heterogeneous Catalysis, ed. by G. Ertl, H. Knozinger, and J. Weitkamp, 1997, Wiley-VCH,Weinheim,Vol. 3, p 1350; B. Török, K. Balázsik, K. Felföldi, and M. Bartók, *Ultrason. Sonochem.*, 2001, **8**, 191; R. S. Varma, *Green Chem. Lett. Rev.*, 2007, **1**, 37.
6. K. Mikami, Green Reaction Media in Organic Synthesis, 2005, Blackwell, Oxford; D. Dallinger and C. O. Kappe, *Chem. Rev.*, 2007, **107**, 2563; V. Polshettiwar and R. S. Varma, Aqueous Microwave Assisted Chemistry, 2010, 91; V. Polshettiwar and R. S. Varma, *Chem. Soc. Rev.*, 2008, **37**, 1546.
7. G. A. Somorjai, Introduction to Surface Chemistry and Catalysis, 1994, Wiley, New York; J. M. Thomas and W. J. Thomas, Principles and Practice of Heterogeneous Catalysis, 1996, Wiley-VCH, New York, Weinheim; Encyclopedia of Catalysis, ed. by I. Horvath; Wiley, New York, 2003; Handbook of Heterogeneous Catalysis, ed. by G. Ertl, 2nd Ed. 2008, Wiley-VCH, Weinheim-New York.
8. Five Thousand Years of Glass, ed. by H. Tait, London: The British Museum Press, 1991.
9. S. Carboni, Glass from Islamic Lands. London: Thames & Hudson, Ltd, 2001, p 51.

10. H.-J. Freund and H. J. Knozinger, *Phys. Chem. B*, 2004, **108**, 14183; B. R. Cuenya, *Thin Solid Films*, 2010, **518**, 3127; G. Ertl, *Angew. Chem. Int. Ed.*, 2008, **47**, 3524; C. Beta, M. G. Moula, A. S. Mikhailov, H. H. Rotermund, and G. Ertl, *Phys. Rev. Lett.*, 2004, **93**, 188302; M. Kim, M. Bertram, M. Pollmann, A. von Oertzen, A. S. Mikhailov, H. H. Rotermund, and G. Ertl, *Science*, 2001, **292**, 1357.
11. Nanochemistry: A Chemical Approach to Nanomaterials, 2nd edn., ed. by G. A. Ozin, A. C. Arsenault, and L. Cademartiri, Royal Society of Chemistry, 2008.
12. Nanoparticles and Catalysis, ed. by D. Astruc, Weinheim: Wiley-VCH Verlag GmbH, 2008.
13. T. Ishida and M. Haruta, *Angew. Chem. Int. Ed.*, 2007, **46**, 7154.
14. A. S. K. Hashmi and G. J. Hutchings, *Angew. Chem. Int. Ed.*, 2006, **47**, 7896.
15. C. N. R. Rao, A. Müller, and A. K. Cheetham, The Chemistry of Nanomaterials: Synthesis and Applications, Vol. 1, Wiley-VCH, Weinheim, 2004; P. T. Anastas and M. M. Kirchkoff, *Acc. Chem. Res.*, 2002, **35**, 686; G. Schmid, V. Maihack, F. Lantermann, and S. Peschel, *J. Chem. Soc., Dalton Trans.*, 1996, 589; W. Yan, S. Mahurin, S. Overbury, and S. Dai, *Top. Catal.*, 2006, **39**, 199; R. M. Rioux, H. Song, J. D. Hofelmeyer, P. Yang, and G. A. Somorjai, *J. Phys. Chem. B*, 2005, **109**, 2192; G. Budroni and A. Corma, *Angew. Chem.*, 2006, **118**, 3406; *Angew. Chem. Int. Ed.*, 2006, **45**, 3328.
16. J. M. Campelo, D. Luna, R. Luque, J. M. Marinas, and A. A. Romero, *ChemSusChem*, 2009, **2**, 18; G. Glaspell, H. M. A. Hassan, A. Elzatahry, V. Abdalsayed, and M. S. El-Shall, *Top. Catal.*, 2008, **47**, 22; P. Claus, A. Bruckner, C. Mohr, and H. Hofmeister, *J. Am. Chem. Soc.*, 2000, **122**, 11430; A. Martino, S. A. Yamanaka, J. S. Kawola, and D. A. Ly, *Chem. Mater.*, 1997, **9**, 423; X. D. Mu, D. G. Evans, and Y. Kou, *Catal. Lett.*, 2004, **97**, 151; C. B. Hwang, Y. S. Fu, Y.-L. Lu, S.-W. Jang, P.-T. Chou, C.-R. Wang, and S.-J. Yu, *J. Catal.*, 2000, **195**, 336; J. A. Dahl, B. L. S. Maddux, and J. E. Hutchinson, *Chem. Rev.*, 2007, **107**, 2228.
17. A. H. Lu, E. L. Salabas, and F. Schth, *Angew. Chem.*, 2007, **119**, 1242; *Angew. Chem. Int. Ed.*, 2007, **46**, 1222; U. Jeong, X. Teng, Y.Wang, H. Yang, and Y. Xia, *Adv. Mater.*, 2007, **19**, 33; Y. W. Jun, J. W. Seo, and J. Cheon, *Acc. Chem. Res.*, 2008, **41**, 179.
18. Y. Borodko, S. E. Habas, M. Koebel, P. Yang, H. Frei, and G. A. Somorjai, *J. Phys. Chem. B*, 2006, **110**, 23052; I. Washio, Y. Xiong, Y. Yin, and Y. Xia, *Adv. Mater.*, 2006, **18**, 1745.
19. W. Wu, Z. Wu, T. Yu, C. Jiang, and W.-S. Kim, *Sci. Technol. Adv. Mater.*, 2015, **16**, 023501.
20. M. B. Gawande, P. S. Brancoa, and R. S. Varma, *Chem. Soc. Rev.*, 2013, **42**, 3371.
21. S. Roy and M. A. Pericas, *Org. Biomol. Chem.*, 2009, **7**, 2669.
22. W. I. Gilbert, J. Turkevich, and E. S. Wallis, *J. Org. Chem.*, 1938, **3**, 611; L. S. Glebov, G. A. Kliger, T. P. Popova, V. E. Shiryaeva, V. P. Ryzhikov, E. V. Marchevskaya, O. A. Lesik, S. M. Loktev, and V. G. Beryezkin, *J. Mol. Catal. A: Chem.*, 1986, **35**, 335; Q. Liu, W. Ma, R. He, and Z. Mu, *Catal. Today*, 2005, **106**, 52; A. SchPle, U. Nieken, O. Shekhah, W. Ranke, R. Schlçgl, and G. Kolios, *Phys. Chem.*

Chem. Phys., 2007, **9**, 3619; J. Liang, Q. Zhang, H. Wu, G. Meng, Q. Tang, and Y. Wang, *Catal. Commun.*, 2004, **5**, 665; D. Guin, B. Baruwati, and S. V. Manorama, *J. Mol. Catal. A: Chem.*, 2005, **242**, 26; M. M. Mojtahedi, M. S. Abaee, and T. Alishiri, *Tetrahedron Lett.*, 2009, **50**, 2322; T. Q. Zeng, W.-W. Chen, C. M. Cirtiu, A. Moores, G. Song, and C.-J. Li, *Green Chem.*, 2010, **12**, 570; Z.-H. Zhang, H.-Y. Lu, S.-H. Yang, and J.-W. Gao, *J. Comb. Chem.*, 2010, **12**, 643; L. Lartigue, K. Oumzil, Y. Guari, J. Larionova, C. Guerin, J. L. Montero, V. Barragan-Montero, C. Sangregorio, A. Caneschi, C. Innocenti, T. Kalaivani, P. Arosio, and A. Lascialfari, *Org. Lett.*, 2009, **11**, 2992; M. M. Mojtahedi, M. S. Abaee, and M. Eghtedari, *Appl. Organomet. Chem.*, 2008, **22**, 529; V. Polshettiwar, R. Luque, A. Fihri, H. Zhu, M. Bouhrara, and J. M. Basset, *Chem. Rev.*, 2011, **111**, 3036; H. Firouzabadi, N. Iranpoor, M. Gholinejad, and S. J. Hoseini, *Adv. Synth. Catal.*, 2011, **353**, 125; R. Martinez, D. J. Ramon, and M. Yus, *Adv. Synth. Catal.*, 2008, **350**, 1235; F. Shirini and M. Abedini, *J. Nanosci. Nanotechnol.*, 2013, **13**, 4838.

23. D. Wang and D. Astruc, Chem. Rev., 2014, **114** , 6949.
24. A.-H. Lu, W. Schmidt, N. Matoussevitch, H. Böennemann, B. Spliethoff, B. Tesche, E. Bill, W. Kiefer, and F. Schüth, *Angew. Chem. Int. Ed.*, 2004, **43**, 4303.
25. J. Liu, S. Z. Qiao, Q. H. Hu, and G. Q. Lu, *Small*, 2011, **7**, 425.
26. T. Zeng, X.-L. Zhang, Y.-R. Ma, H.-Y. Niu, and Y.-Q. J. Cai, *Mater. Chem.*, 2012, **22**, 18658.
27. S. Ko and J. Jang, *Angew. Chem. Int. Ed.*, 2006, **45**, 7564.
28. J. Deng, X. Wen, and Q. Wang, *Mater. Res. Bull.*, 2012, **47**, 3369.
29. A. Kamal and P. Swapna, *RSC Adv.*, 2013, **3**, 7419.
30. R. Cano, D. J. Ramón, and M. Yus, *Synlett*, 2011, 2017.
31. F. P. Ma, P. H. Li, B. L. Li, L. P. Mo, N. Liu, H. J. Kang, Y. N. Liu, and Z. H. Zhang, *Appl. Catal.*, *A*, 2013, **457**, 34.
32. V. V. Rostovtsev, L. G. Green, V. V. Fokin, and K. B. Sharpless, *Angew. Chem.*, 2002, **114**, 2708; *Angew. Chem. Int. Ed.*, 2002, **41**, 2596.
33. E. Ozkal, S. Özçubukçu, C. Jimeno, and M. A. Pericàs, *Catal. Sci. Technol.*, 2012, **2**, 195.
34. S. Shylesh, L. Wang, and W. R. Thiel, *Adv. Synth. Catal.*, 2010, **352**, 425.
35. D. Wang, L. Etienne, M. Echeverria, S. Moya, and D. Astruc, *Chem. Eur. J.*, 2014, **20**, 4047.
36. S. Sobhani and M. Honarmand, *Appl. Catal., A*, 2013, **467**, 456.
37. N. R. Jana, C. Earhart, and J. Y. Ying, *Chem. Mater.*, 2007, **19**, 5074.
38. A. Sinha and N. R. Jana, *Chem. Asian J.*, 2013, **8**, 786.
39. N. Salam, A. Sinha, P. Mondal, A. S. Roy, N. R. Jana, and S. M. Islam, *RSC Adv.*, 2013, **3**, 18087.
40. G. He, W. Liu, X. Sun, Q. Chen, X. Wang, and H. Chen, *Mater. Res. Bull.*, 2013, **48**, 1885.
41. G. Wu, X. Wang, N. Guan, and L. Li, *Appl. Catal., B*, 2013, **136**, 177.

42. S. R. Kale, S. S. Kahandal, M. B. Gawande, and R. V. Jayaram, *RSC Adv.*, 2013, **3**, 8184.
43. L. D. Field, A. V. George, F. Laschi, E. Y. Malouf, and P. Zanello, *J. Organomet. Chem.*, 1992, **435**, 347.
44. G. Albertin, P. Agnoletto, and S. Antoniutti, *Polyhedron*, 2002, **21**, 1755.
45. Z. Ji, X. Shen, G. Zhu, H. Zhou, and A. Yuan, *J. Mater. Chem.*, 2012, **22**, 3471.
46. T. Wu, L. Zhang, J. Gao, Y. Liu, C. Gao, and J. Yan, *Mater. J. Chem. A*, 2013, **1**, 7384.
47. Z. Y. Lu, J. Dai, X. N. Song, G. Wang, and W. S. Yang, *Colloids Surf. A*, 2008, **317**, 450.
48. X. Chen, K. F. Lam, Q. Zhang, B. Pan, M. Arruebo, and K. L. Yeung, *J. Phys. Chem. C*, 2009, **113**, 9804.
49. S. Rostamizadeh, N. Shadjou, M. Azad, and N. Jalali, *Catal. Commun.*, 2012, **26**, 218.
50. T. Sato, K. Haneda, N. Seki, and T. Iijima, *Appl. Phys. A*, 1990, **50**, 13.
51. K. Debnath and A. Pramanik, *Tetrahedron Lett.*, 2015, **56**, 1654.
52. P. Das, A. Dutta, A. Bhaumik, and C. Mukhopadhyay, *Green Chem.*, 2014, **16**, 1426.
53. M. R. Anantharaman, S. Jagatheesan, K. A. Malini, S. Sindhu, A. Narayanasamy, C. N. Chinnasamy, J. P. Jacobs, S. Reijne, K. Seshan, R. H. H. Smits, and H. H. Brongersma, *J. Magn. Magn. Mater.*, 1998, **189**, 83.
54. M. Thomas and K. C. George, *Indian J. Pure Appl. Phys.*, 2009, **47**, 81.
55. I. Mohai, J. Szépvölgyi, I. Bertóti, M. Mohai, J. Gubicza, and T. Ungár, *Solid State Ionics*, 2001, **141**, 163.
56. K. Faungnawakj, R. Kikuchi, N. Shimoda, T. Fukunaga, and K. Eguchi, *Angew. Chem.*, 2008, **120**, 9454; *Angew. Chem. Int. Ed.*, 2008, **47**, 9314; C. Liu, B. Zou, A. J. Rondinone, and Z. J. Zhang, *J. Am. Chem. Soc.*, 2000, **122**, 6263.
57. K. Pradhan, S. Paul, and A. R. Das, *Catal. Sci. Technol.*, 2014, **4**, 822.
58. S. A. Sarode, J. M. Bhojane, and J. M. Nagarkar, *Tetrahedron Lett.*, 2015, **56**, 206.
59. A. Dandia, A. K. Jain, and S. Sharma, *RSC Adv.*, 2013, **3**, 2924.
60. N. Panda, A. K. Jena, S. Mohapatra, and S. R. Rout, *Tetrahedron Lett.*, 2011, **52**, 1924.
61. A. Bazgir, G. Hosseini, and R. Ghahremanzadeh, *ACS Comb. Sci.*, 2013, **15**, 530.
62. J. E. Tasca, A. Ponzinibbio, G. Diaz, R. D. Bravo, A. Lavat, and M. G. Gonzàlez, *Top Catal.*, 2010, **53**, 1087.
63. A. Hari, C. Karan, W. C. Rodrigues, and B. L. Miller, *J. Org. Chem.*, 2001, **66**, 991; J. Lee, J. Kim, Y. M. Jun, B. H. Kim, and B. M. Lee, *Tetrahedron*, 2009, **65**, 8821; H. Nishioka, Y. Ohmori, Y. Iba, E. Tsuda, and T. Harayama, *Heterocycles*, 2004, **64**, 193; M. Wu, X. Hu, J. Liu, Y. Liao, and G.-J. Deng, *Org. Lett.*, 2012, **14**, 2722; L. Tang, X. Guo, Y. Yang, Z. Zha, and Z. Wang, *Chem. Commun.*, 2014, 6145; J. M. Kim, I. S. Cho, and P. S. Mariano, *J. Org. Chem.*, 1991, **56**, 4943; K. Ohkubo, T. Nanjo,

and S. Fukuzumi, *Bull. Chem. Soc. Jpn.*, 2006, **79**, 1489; T. B. Nguyen, L. Ermolenko, and A. Al-Mourabit, *Green Chem.*, 2013, **15**, 2713; H. K. Chaudhari and V. N. Telvekar, *Synth. Commun.*, 2013, **43**, 1155; Z. Duan, G. Ma, and W. Zhang, *Bull. Korean Chem. Soc.*, 2012, **33**, 4003.

64. S. Paul, G. Pal, and A. R. Das, *RSC Adv.*, 2013, **3**, 8637.
65. P.-H. Li, B.-L. Li, Z.-M. An, L.-P. Mo, Z.-S. Cui, and Z.-H. Zhang, *Adv. Synth. Catal.*, 2013, **355**, 2952.
66. X. Chen, K. F. Lam, Q. Zhang, B. Pan, M. Arruebo, and K. L. Yeung, *J. Phys. Chem. C*, 2009, **113**, 9804.
67. A. Hasaninejad, M. Shekouhy, N. Golzar, A. Zare, and M. M. Doroodmand, *Appl. Catal., A*, 2011, **402**, 11.
68. A. R. Hajipour, N. Najafi, and F. Rafiee, *Appl. Organomet. Chem.*, 2013, **27**, 228.
69. B. L. Li, H. C. Hu, L. P. Mo, and Z. H. Zhang, *RSC Adv.*, 2014, **4**, 12929.
70. H. Wang, J. Huang, L. Y. Ding, D. P. Li, and Y. Han, *Appl. Surf. Sci.*, 2011, **257**, 7107.
71. B. L. Li, M. Zhang, H. C. Hu, X. Du, and Z. H. Zhang, *New J. Chem.*, 2014, **38**, 2435.
72. N. Montazeri, K. Pourshamsian, H. Rezaei, M. Fouladi, and S. Rahbar, *Asian J. Chem.*, 2013, **25**, 3463.
73. S. Rostamizadeh, M. Nojavan, R. Aryan, H. Sadeghian, and M. Davoodnejad, *Chinese Chem. Lett.*, 2013, **24**, 629.
74. L. Z. Fekri, M. Nikpassand, and K. H. Pour, *Curr. Org. Synth.*, 2015, **12**, 76.
75. M. Nikpassand, L. Zare, T. Shafaati, and S. Shariati, *Chin. J. Chem.*, 2012, **30**, 604.
76. R. Cano, M. Yus, and D. J. Ramón, *Tetrahedron*, 2013, **69**, 7056.
77. A. R. Karimi, Z. Dalirnasab, and M. Karimi, *Synthesis*, 2014, **46**, 917.
78. V. Polshettiwar and R. S. Varma, *Tetrahedron*, 2010, **66**, 1091.
79. Z. Zarnegar and J. Safari, *RSC Adv.*, 2014, **4**, 20932.
80. A. Maleki, N. Ghamari, and M. Kamalzare, *RSC Adv.*, 2014, **4**, 9416.
81. A. Maleki and M. Kamalzare, *Tetrahedron Lett.*, 2014, **55**, 6931.
82. R. Mohammadi and M. Z. Kassaee, *J. Mol. Catal. A: Chem.*, 2013, **380**, 152.
83. C. Wang, L. Yin, L. Zhang, L. Kang, X. Wang, and R. Gao, *J. Phys. Chem. C*, 2009, **113**, 4008.
84. B. Dam, S. Nandi, and A. K. Pal, *Tetrahedron Lett.*, 2014, **55**, 5236.
85. A. Goswami, R. N. Das, and N. Borthakur, *Ind. J. Chem., Sect. B: Org. Chem. Incl. Med. Chem.*, 2007, **46**, 1893.
86. T. Guntreddi, B. K. Allam, and K. N. Singh, *Synlett*, 2012, **23**, 2635.
87. F. Nemati and R. Saeedirad, *Chin. Chem. Lett.*, 2013, **24**, 370.
88. F. Nemati, M. M. Heravi, and R. Saeedirad, *Chin. J. Catal.*, 2012, **33**, 1825.

89. C. Y. Lin, C. F. Lo, L. Luo, H. P. Lu, C. S. Hung, and E. W. G. Diau, *J. Phys. Chem. C*, 2009, **113**, 755.

90. A. R. Kiasat and J. Davarpanah, *J. Mol. Catal. A: Chem.*, 2013, **373**, 46.

91. M. Z. Kassaee, H. Masrouri, and F. Movahedi, *Appl. Catal.*, *A*, 2011, **395**, 28.

92. H. R. Shaterian and F. Moradi, *Res. Chem. Intermed.*, 2015, **41**, 223.

93. H. R. Shaterian and M. Mohammadnia, *Res. Chem. Intermed.*, 2014, **40**, 371.

94. R. Ghahremanzadeh, G. I. Shakibaei, and A. Bazgir, *Synlett*, 2008, **8**, 1129.

95. M. R. Nabid, S. J. Tabatabaie, R. Gahremanzadeh, and A. Bazgir, *Ultrason. SonoChem.*, 2010, **17**, 159.

96. D. S. Raghuvanshi and K. N. Singh, *Tetrahedron Lett.*, 2011, **52**, 5702.

97. M. Z. Kassaee, H. Masrouri, and R. Massart *IEEE Trans. Magn.*, 1981, **17**, 1247.

98. F. Movahedi, *Appl. Catal., A*, 2011, **395**, 28.

99. J. Safari and Z. Zarnegar, *J. Chem. Sci.*, 2013, **125**, 835.

100. A. Rostami, B. Tahmasbi, and A. Yari, *Bull. Korean Chem. Soc.*, 2013, **34**, 1521.

101. W. Stöber, A. Fink, and E. J. Bohn, *J. Colloid Interface Sci.*, 1968, **26**, 62.

102. A. Chrobok, S. Baj, W. Pudło, and A. Jarzebski, *Appl. Catal.*, *A*, 2009, **366**, 22.

103. N. Azgomi and M. Mokhtary, *J. Mol. Catal. A: Chem.*, 2015, **398**, 58.

104. J. Safari and Z. Zarnegar, *Compt. Rend. Chim.*, 2013, **16**, 920.

105. Z. Zarnegar and J. Safari, *J. Nanopart. Res.*, 2014, **16**, 2509.

106. W. Cheng, X. Chen, J. Sun, J. Wang, and S. Zhang, *Catal. Today*, 2013, **200**, 117.

107. H. O. Bourbigou, L. Magna, and D. Morvan, *Appl. Catal.*, *A*, 2010, **373**, 1.

108. M. Tajbakhsh, M. Farhang, R. Hosseinzadeh, and Y. Sarrafi, *RSC Adv.*, 2014, **4**, 23116.

109. P. Liu, L. S. Fang, X. Lei, and G. Q. Lin, *Tetrahedron Lett.*, 2010, **51**, 4605.

110. H. Eshghi, A. Khojastehnezhad, F. Moeinpour, S. Rezaeian, M. Bakavolia, M. Teymouri, A. Rostami, and K. Haghbeen, *Tetrahedron*, 2015, **71**, 436.

111. H. Hashimoto, G. Kobayashi, R. Sakuma, T. Fujii, N. Hayashi, T. Suzuki, R. Kanno, M. Takano, and J. Takada, *ACS Appl. Mater. Interfaces*, 2014, **6**, 5374.

112. K. Mandai, M. Hanata, K. Mitsudo, H. Mandai, S. Suga, H. Hashimoto, and J. Takada, *Tetrahedron*, 2015, **71**, 9403.

Ahmed H. M. Elwahy was born in 1963 in Giza, Egypt. He graduated from Cairo University, Egypt in 1984 then he got his M.Sc. and Ph.D. degrees in 1988 and 1991, respectively, at Cairo University in the field of organic synthesis. He was awarded the Alexander von Humboldt research fellowship in 1998–2000 and in 2003, 2005, 2009, 2010 and 2012 with Prof. Klaus Hafner, at TU Darmstadt, Germany. In 2002 he was appointed as a full Professor of Organic chemistry at Cairo University. In 2001 he received the Cairo University Award in Chemistry and in the same year he received the State-Award in Chemistry. He published around 100 scientific papers in distinguished international journals.

Mohamed R. Shaaban was born in 1971 in Cairo, Egypt. He graduated from Cairo University, Egypt in 1992 then he joined Professor Ahmad M. Farag's research group. He received his Ph.D. in 2001 at Tokyo, Institute of Technology, Japan. In 2001 he was promoted to a Lecturer of Organic Chemistry at Cairo University and continued his research work on organic synthesis as well as on palladium catalyzed C–C cross-couplings. In 2009 he was promoted to Associate Professor of Organic chemistry, and in 2014 he was promoted to Professor of Organic Chemistry at Faculty of Science, Cairo University.